PDGFRβ SIGNALING IN MOUSE EPICARDIAL AND MURAL CELLS INFLUENCES BLOOD VESSEL REMODELING

APPROVED BY SUPERVISORY COMMITTEE

Michelle D. Tallquist, Ph.D.

Raymond MacDonald, Ph.D.

Joseph Hill, M.D./Ph.D.

David Russell, Ph.D.

DEDICATION

None of this work would have been possible without the support of my colleagues, friends, and family. In particular, I would like to thank my mentor, Michelle Tallquist. Over the past four years she has helped me grow both as a scientist and an individual. I will carry the lessons that I have learned with me throughout my life. I would also like to thank all current and former members of the Tallquist lab for their suggestions and discussions. They made the lab a good environment in which to work. Holly Mead and Haley Newton provided a lot of technical support. Chris Smith performed the flow cytometry analysis. In addition, I owe a huge debt of gratitude to Wendy French. Her scientific input was invaluable and the friendship we've developed will last long after we leave graduate school.

Many other individuals at UT Southwestern have helped my projects out along the way. My thesis committee has provided appreciated input on my project. Ray MacDonald and Joe Garcia have been great collaborators. John Shelton and James Richardson have provided valuable technical advice. Tom Januszewski taught me how to use the electron microscope. Alisha Tizenor helped me learn the ropes of Photoshop. Stephen Johnson was a lifesaver many times with my computer. The MST Program provided valuable support along the way.

Last, but not least, I want to thank my friends and my family for their support and patience as I worked through these projects. I couldn't have done this without them and I will cherish the memories that we formed during this time. I especially want to thank Chase, my brother and my parents. I can't think of any words that are adequate to describe how grateful I am to you. I just can't thank you enough for all you do for me.

PDGFRβ SIGNALING IN MOUSE EPICARDIAL AND MURAL CELLS INFLUENCES BLOOD VESSEL REMODELING

by

AMY MARIE MELLGREN

DISSERTATION

Presented to the Faculty of the Graduate School of Biomedical Sciences

The University of Texas Southwestern Medical Center at Dallas

In Partial Fulfillment of the Requirements

For the Degree of

DOCTOR OF PHILOSOPHY

The University of Texas Southwestern Medical Center at Dallas

Dallas, Texas

May 2009

PDGFRβ SIGNALING IN MOUSE EPICARDIAL AND MURAL CELLS INFLUENCES BLOOD VESSEL REMODELING

AMY MARIE MELLGREN, M.D./Ph.D.

The University of Texas Southwestern Medical Center at Dallas, 2009

SUPERVISING PROFESSOR: MICHELLE D. TALLQUIST, Ph.D.

Platelet derived growth factor receptor β (PDGFRβ) is a receptor tyrosine kinase expressed in vascular smooth muscle cells (VSMC), which promotes proliferation and migration. We provide evidence of additional roles for the PDGFRβ prior to the differentiation of VSMC. We show that PDGFRβ, as well as PDGFRα, is expressed in epicardial and subepicardial mesenchymal cells, which are precursors for coronary VSMC. We demonstrate that PDGFRβ$^{-/-}$ mice exhibit a lack of coronary VSMC and have disrupted endothelial vessels on the ventral surface of the heart; however, neither conditional ablation of the PDGFRβ

with an SM22 Cre Tg, which is expressed in differentiated VSMC, nor with a myocardin^{Cre}, which has an earlier expression profile and is believed to control VSMC differentiation, phenocopy the lack of coronary VSMC found in PDGFRβ$^{-/-}$ mice. Further investigations into PDGFRβ$^{-/-}$ mice revealed a defect in the function of the epicardium. The epicardium exhibited an altered cellular morphology and a decreased ability to migrate into the myocardium both in vivo and ex vivo. The decreased motility was associated with a nonpolarized distribution of actin and a lack of localization of Arp2/3 to the cell periphery. Moreover, these defects appeared to be dependent on the Src signaling pathway. This work thus establishes a novel in vivo role for the PDGFRβ at a stage of coronary VSMC development during which the epicardium undergoes cytoskeletal rearrangement in order to efficiently migrate into the myocardium and form the mesenchymal precursors of coronary VSMC.

In addition to this role in vasculogenesis, we demonstrate a role for the PDGFRβ in angiogenesis. Using point mutations in PDGFRβ we generated mice that possessed variations in the number of pericytes that were present in tissues, including the trachea and retina. We then utilized these mutant mouse lines to show that a decrease in pericytes affects the ability of the vasculature to respond to an angiogenic agent, Ang1. Moreover, this response is not secondary to hypoxia. This work emphasizes the value of targeting both VSMC and endothelial cells in therapies targeting vessel regeneration.

TABLE OF CONTENTS

PUBLICATIONS

Mellgren AM, Smith CL, Olsen GS, Eskiocak B, Zhou B, Kazi MN, Ruiz FR, Pu WT, Tallquist MD. Platelet-Derived Growth Factor Receptor β Signaling Is Required for Efficient Epicardial Cell Migration and Development of Two Distinct Coronary Vascular Smooth Muscle Cell Populations. Circulation Research 2008; 103(12):1393-401

Mellgren AM, Smith CL, Thurston G, Garcia J, Tallquist MD. (2009) Pericytes Regulate the Angiogenic Potential of Ang1. (In preparation)

LIST OF FIGURES

LIST OF TABLES

LIST OF ABBREVIATIONS

VSMC: vascular smooth muscle cells

PDGF: platelet derived growth factor

PDGFRα: platelet derived growth factor receptor α

PDGFRβ: platelet derived growth factor receptor β

SRF: serum response factor

SMα-actin (αSMA): smooth muscle α-actin

SM myosin heavy chain (SMMHC): smooth muscle myosin heavy chain

SM22α: smooth muscle 22α

EMT: epithelial to mesenchymal transition

ZO1: zona occludins 1

Tcf-lef: T-cell factor/lymphoid enhancing factor

aPKC: atypical protein kinase C

Arp2/3: actin related proteins 2/3

PEO: proepicardial organ

VCAM: vascular cell adhesion molecule

EPDC: Epicardial-derived cell

Fog2: friend of gata 2

PECAM: platelet/ endothelial cell adhesion molecule

ICAM: intercellular adhesion molecule

Flk: fms like tyrosine kinase

WT1: Wilms tumor 1

Par3: partition defective 3

Ets1/2: E-Twenty-Six 1/2

RALDH: retinaldehyde dehydrogenase

RXR: retinoid X receptor

RA: retinoic acid

FGF: fibroblast growth factor

EGF: epidermal growth factor

TGFβ: transforming growth factor β

PI3K: phosphoinositide-3 kinase

HGF: hepatocyte growth factor

FAK: focal adhesion kinase

Tbx18: t-box gene 18

GFP: green fluorescent protein

YFP: yellow fluorescent protein

TEM: transmission electron microscopy

GAPDH: glyceraldehyde-3-phosphate dehydrogenase

DAPI: 4',6-Diamidino-2-Phenylindole

R26: Rosa26

MKO: myocardin cre knock out

SKO: Sm22 cre knockout

RTK: receptor tyrosine kinase

FBS: fetal bovine serum

BHLH: basic helix loop helix

BrdU: bromodeoxyuridine

TUNEL: terminal deoxynucleotidyl transferase Biotin-dUTP nick end labeling

Grb2: growth factor receptor bound protein

RasGAP: ras GTPase activating protein

Shp2: Src homology 2 (SH2) domain-containing protein tyrosine phosphatase

PLCy: phospholipase C gamma

CCFSE: 5-6-carboxy 2-7-dichlorofluorescein diacetate succinimidyl ester

Ang1: angiopoietin 1

eNOS: Endothelial Nitric Oxide Synthase

VEGF: vascular endothelial growth factor

Glut1: glucose transporter 1 protein

Hif: hypoxia inducible factor

Tsp: thrombospondin

CHAPTER ONE

INTRODUCTION

Pericytes and the Vasculature

Blood vessels are dynamic in the sense that they can respond to hypoxic or ischemic situations through increases in size or number. This adaptability is important, as vessels are necessary for cellular function. Furthermore, due to the reliance of embryonic tissues on oxygen, nutrients and growth factor exchange, blood vessels are crucial for development. Embryos that are unable to perform vasculogenesis or angiogenesis are not viable past embryonic day 10.5 (E10.5) (Carmeliet et al., 1996; Dumont et al., 1994; Ferrara et al., 1996; Fong et al., 1995; Sato et al., 1995; Shalaby et al., 1995; Suri et al., 1996).

Blood vessels are composed of two primary cell types: an inner tube of endothelial cells and an outer covering of mural cells (reviewed in (Hungerford and Little, 1999)). Although the characteristics of blood vessels can vary depending on the needs of that particular tissue, all vessels form by either vasculogenesis or angiogenesis (reviewed in (Carmeliet, 2003; Jain, 2003; Risau, 1997)). Vasculogenesis involves the de novo generation of vessels. Blood islands develop from angioblasts and subsequently reorganize to form endothelial tubes. These tubes then undergo a remodeling process to form vessels. It is believed that when remodeling is complete, the vessel recruits mural cells to stabilize the

vessel. In general, if the mural cell component is one cell layer thick, then the cells are referred to as pericytes. Conversely, if there are multiple layers of mural cells, then they are termed vascular smooth muscle cells (VSMC). These terms are often used interchangeably. Once the mural cells coat the endothelial cells the vasculature is characterized as mature. The process of angiogenesis is different in that the vessels are generated from pre-existing vasculature. In this process, the endothelial cells proliferate and migrate in a directed manner to form a nascent vessel. Similar to vasculogenesis, the endothelial cells then recruit VSMC to complete vascular development (Hellstrom et al., 1999; Lindahl et al., 1997).

Both endothelial and mural cells are required for a functional vasculature. Several examples exist of communication between the two cell types. Platelet derived growth factor BB (PDGFBB) is secreted by endothelial cells and binds to a receptor, platelet derived growth factor receptor β (PDGFRβ), on VSMC to stimulate migration and proliferation (Hellstrom M, 1999; Lindahl et al., 1997). Conversely, Angiopoietin 1 (Ang1) is secreted by pericytes and binds to a receptor, Tie2, on endothelial cells to stimulate blood vessel remodeling (Davis et al., 1996; Suri et al., 1996). A defect in either signaling system affects both cell types; loss of PDGFBB results in the formation of aneurysms, whereas loss of Ang1 is associated with a reduction in perivascular cell number (Lindahl et al., 1997; Suri et al., 1996).

The importance of endothelial cells is reviewed in several articles (Carmeliet, 2003; Cleaver and Melton, 2003); however, for the purpose of this report we will focus on the development and role of mural cells. Mural cells are derived from several different cell populations: neural crest, lateral plate mesoderm, somites, splanchnic mesoderm, gut mesothelium, and proepicardium (Hungerford et al., 1996; Pouget et al., 2006; Viragh and Challice, 1981; Wilm et al., 2005). As these cells differentiate they express a spectrum of transcription factors, contractile proteins, cytoskeletal proteins, and cell surface molecules that define their lineage. The transcription factors, myocardin and SRF, are early regulators of VSMC differentiation (Du et al., 2003; Li et al., 2003; Manabe and Owens, 2001; Strobeck et al., 2001; Yoshida et al., 2003). SMα-actin and SM myosin heavy chain are contractile proteins typically expressed in differentiated cells, but can also be found in embryonic skeletal and cardiac muscle, mesothelial cells, activated fibroblasts, and myofibroblasts. SM22α is a cytosolic protein that is considered a late stage marker for VSMC (reviewed in (Owens, 1995)). NG2 and the PDGFRβ are transmembrane proteins expressed by mural cells, as well as many other cell types (Grako and Stallcup, 1995; Shinbrot et al., 1994). Overall, VSMC are a heterogeneous cell type and their differential protein expression is likely a reflection of their various developmental origins and cellular niches. The diversity of this cell type demonstrates that more information is required to

understand the signals that direct the differentiation and determination of the various subpopulations that exist among tissues and within a given tissue.

Coronary VSMC: A Special Case

One of the VSMC lineages that derive from an unusual source is the coronary VSMC. Unlike other VSMC, these cells arise from the proepicardium in mice and the proepicardial organ (PEO) in chick. This precursor population consists of a grape-like cluster of epithelial cells that forms on the septum transversum around E9.0 (Viragh and Challice, 1981). In the mouse, epithelial cysts detach from the proepicardium and travel through the pericardial cavity to reattach to the atrioventricular groove of the myocardium (Sengbusch et al., 2002). Aggregates of cells then spread toward the lateral and ventral surfaces of the heart, eventually encompassing the organ by E11 and flattening to form the outer layer of the heart, the epicardium (Komiyama et al., 1987; Viragh and Challice, 1981).

A subpopulation of the epicardial cells is then believed to undergo an epithelial to mesenchymal transition (EMT) to form the subepicardial mesenchyme. This transition involves both transcriptional and non-transcriptional changes that transform a stationary epithelial cell to a motile mesenchymal cell. The process of EMT has been characterized extensively in other developmental systems, in the progression of fibrosis, as well as cancer models, and involves the

interaction of several signaling pathways (reviewed in (Savagner, 2001; Thiery, 2003; Thiery and Sleeman, 2006; Zeisberg and Kalluri, 2004)).

There are multiple steps in the transition between a stationary epithelial cell and a motile mesenchymal cell. There is an upregulation of transcription factors such as twist, slug, and snail, which can repress expression of E-cadherin. The latter protein is a component of the adherens junctions, which are present in epithelial cells. Downregulation of E-cadherin in combination with tight junction proteins such as ZO1, is thus important for dissociating epithelial cells from one another. The down regulation of E-cadherin is also associated with a relocalization of β-catenin from adherens junctions to the nucleus. β-catenin then activates tcf-lef, which further controls the transcriptional induction of EMT. In addition, the loss of adheren junctions is associated with a loss of apical basal polarity that can be monitored by disruptions in the apical localization of proteins such as aPKC and ezrin.

While junctional proteins are being downregulated, expression of mesenchymal proteins, such as vimentin and vinculin, is upregulated. There is also an up regulation of matrix metalloproteinases that degrade the basement membrane and provide an avenue for cell migration. However, to complete the process of migration the cells reorganize their cytoskeleton. The actin localization changes from a subcortical distribution to a filamentous pattern. In addition, there is activation of the cytoskeletal machinery that concentrates in

lamellipodia and/or fillopodia and allows the cell to move. For example, several signaling pathways converge on Arp2/3 to nucleate actin filaments.

Although these cellular processes illustrate some of the standard components of EMT, many of these mechanisms have been characterized only in vitro. Investigations in vivo reveal that the specific nature of the EMT process can be tissue-dependent. Studies in both chicks and mice have afforded insight into the epicardial EMT.

Utilization of the chick as a model system has provided the ability to trace and isolate cells populations. To trace the cells either a dye can be injected into the cell population of interest or there is a surgical replacement of a cell population with the equivalent quail cell population, which possesses histologically distinct nuclei. Utilizing these techniques, epicardial derived cells (EPDCs) were shown to invade the myocardium, subendocardial space, and the atrioventricular cushion (Gittenberger-de Groot et al., 1998). The ability to dissect out the proepicardial organ (PEO) also lent itself as a tool to characterize the EMT process. The chick PEO is the equivalent of a mouse epicaridium. When the PEO was explanted, epithelial cells migrated out and exhibited cobblestone morphology and cytokeratin expression. These cells had the ability to transform into mesenchymal cells when cultured for 3-5 days in 10% serum. This transformation was observed in collagen gels where spindle shaped cells that had reorganized their actin could be observed at the edges of the culture

(Landerholm et al., 1999). Moreover, if the explants were plated on a collagen gel, the mesenchymal cells could be quantified by examining the number of cells that had invaded the gel (Dettman et al., 1998).

In addition characterizing the epicardial EMT process, lineage tracing in the chick has provided a means of analyzing the cell populations that arose from the subsequent differentiation of the subepicardial mesenchyme. Fibroblasts and coronary VSMCs were shown to originate from the epicardium based on morphology, location, and marker analysis (Mikawa and Gourdie, 1996; Vrancken Peeters et al., 1999). Moreover, in support of these lineage tracing experiments, mutation of genes important for epicardial function caused a corresponding disruption in VSMC. For example, α4 integrin is an adhesion molecule that is expressed in the proepicardial cells and binds to a cognate receptor, VCAM, on the surface of the myocardium. When α4 integrin expression was knocked down in the chick, the epicardium was not maintained and an in vitro analysis demonstrated a corresponding decrease in the formation of VSMC (Dettman et al., 2003). Connexin 43 is another protein that is expressed in the epicardium and that exhibited a decrease in vascular smooth muscle myosin staining in the heart when knock out analysis was performed (Li et al., 2002).

Nonetheless, there still exists a paucity of information regarding when different lineages are specified and controversy concerning which lineages derive from the epicardium versus simply interact with the tissue and its derivates during

development. Endothelial cells have been suggested to have an epicardial origin; however, it is a matter of debate whether they are EPDCs or are derived from the liver (Gittenberger-de Groot et al., 1998; Lie-Venema et al., 2005). In fact, coronary artery defects are a consistent phenotype in studies with epicardial disruption. For example, the p300 acetyltransferase knockout exhibits a delay in the epicardial formation, a decrease in subepicardial mesenchyme, and a disruption of endothelial cell remodeling (Shikama et al., 2003). Fog2 null mice fail to form endothelial vessels as determined by PECAM, ICAM, and Flk staining and have a thin myocardium (Tevosian et al., 2000).

The epicardium was found to not only be important for the derivation of multiple cell lineages, but also for the ability of the compact zone of the myocardium to proliferate properly. Without an effective epicardium the compact myocardium does not expand to a normal size. This outcome is demonstrated in the knockout phenotypes of several lines of mutant mice that have a primary defect in epicardial function, including the WT1 knockout, the par3 knockout, and the ets1 and ets2 knockdown (Hirose et al., 2006; Lie-Venema et al., 2003; Moore et al., 1999).

Retinoic acid (RA) also has an important role in these interactions between the epicardium and myocardium. The expression of retinaldehyde dehydrogenase (RALDH), which converts retinol to RA, can also be used as a marker of both the PEO and the epicardium. In addition, the 9-cis retinoic acid

receptor, RXR, is an important contributor to cardiomyocyte proliferation (Chen et al., 2002; Xavier-Neto et al., 2000). The increase in proliferation that was induced by epicardial cell conditioned media could be abolished using RXR null cells. Additional studies revealed that RA induced fibroblast growth factor (FGF) expression in the epicardium, which then mediated cardiomyocyte proliferation (Lavine et al., 2005). Moreover, specific ablation of RXR in the epicardium revealed additional defects in coronary vasculogenesis. This included abnormal branching of the vessels and downregulation of Wnt9b, which regulates epicardial EMT in a β-catenin-dependent manner (Merki et al., 2005).

Growth Factors in Epicardial Development

The ability to culture epicardial cells has implicated several growth factors as potential modulators of the epicardial EMT. Stimulation of both chick and mouse epicardial cells with EGF or bFGF caused the cells to transform into a spindle shaped, mesenchymal-like morphology and/or to invade a collagen gel (Dettman et al., 1998; Wada et al., 2003). Morabito evaluated the ability of several growth factors to induce EMT by quantitating the number of mesenchymal cells that had migrated into the collagen gel. In this system FGF1, 2, and 7 produced maximal EMT, while TGFβ1, EGF and VEGF stimulated EMT to a lesser extent (Morabito et al., 2001). Utilization of these cultures and an assessment of a more distal endpoint, VSMC formation, suggested that TGFβ1,

EGF, PDGFAA, PDGFAB, and PDGFBB had the ability to affect epicardial differentiation. This interpretation was based on expression of calponin, caldesmon, and αSMA (Compton et al., 2006; Lu et al., 2001; Wada et al., 2003).

Although these studies suggest that these growth factors can influence epicardial development in vitro, they do not demonstrate that they do so in vivo. Expression analysis reveals that TGFβ1 is expressed in the PEO, and that all three TGFβ isoforms are expressed in the epicardium (Molin et al., 2003). In addition, the Tgfβ2 and TGFβ3 null mice exhibit reduced myocardial thickness, which is consistent with other epicardial defects (Azhar et al., 2003).

PDGFRβ

A combination of in vitro studies and expression analyses suggested that the PDGFRβ could influence epicardial development in vivo. PDGFRβ is expressed in the chick proepicardium as well as the mouse epicardium (Guadix et al., 2006; Ponten et al., 2005). In addition, PDGFDD, a ligand specific for PDGFRβ, is expressed in the epicardium (Ponten et al., 2005). PDGFRβ is also expressed in a cell population that is derived from the epicardium, the coronary VSMC (Ponten et al., 2005).

PDGFRβ is a receptor tyrosine kinase that has an established role in VSMC function. Endothelial cells express one of this receptor's ligands, PDGFBB. Secretion of this signal stimulates the recruitment of differentiated

VSMC to the blood vessel and promotes proliferation of these cells (Hellstrom et al., 1999). The importance of PDGFRβ in this cell population was suggested when the loss of either the receptor or the PDGFBB ligand resulted in embryonic lethality with severe hemorrhaging and edema (Leveen et al., 1994; Soriano, 1994a). When chimeric analysis was performed to determine whether there was a competitive advantage for wild-type cells over PDGFRβ$^{-/-}$ cells in vascular development, wild-type cells preferentially localized to pericytes and vascular smooth muscle cells (Crosby et al., 1998; Tallquist et al., 2000). Further analyses of PDGFRβ$^{-/-}$ and the PDGFB$^{-/-}$ mice revealed a substantial reduction in the numbers of pericytes and VSMC based on morphology and marker analyses (Hellstrom et al., 1999; Lindahl et al., 1997). A severe reduction occurred in several tissues including the brain, heart, lung, adipose tissue, and GI villi. Moreover, the absence of mural cells was associated with enlarged vessels, aneurysms, and endothelial hyperplasia (Hellstrom et al., 2001; Lindahl et al., 1997).

In terms of a potential role in epicardial development, PDGFRβ activates several signaling pathways that have a role in EMT or its constituent's processes. This activity involves the PI3K and Src signaling pathways. PI3K is often implicated in cell migration and cytoskeletal rearrangement (reviewed in (Sasaki and Firtel, 2006), and can activate multiple downstream factors that are important in these processes. For example, PI3K activates Rac1, which is upstream of the

WAVE proteins. WAVE proteins are able to promote the nucleation of actin by Arp2/3 at the migrating edge of cells (Miki et al., 1998; Miki et al., 2000; Sossey-Alaoui et al., 2005; Yan et al., 2003). Src signaling has been suggested to play a specific role in EMT as well as a general role in cytoskeletal rearrangements. In an epithelial cancer cell line Src was found to initiate EMT through a pathway involving Abl, p68RNA helicase, and β-catenin (Yang et al., 2006). Moreover, Src has been shown to signal to many proteins that are important for cytoskeletal rearrangements, a necessary process of EMT. Src can directly and indirectly stimulate cortactin to induce actin reorganization and lamellipodial protrusion (Boyle et al., 2007). The activation of cortactin by Src enhances the ability of Arp2/3 to nucleate actin filaments (Tehrani et al., 2007). In vivo, the stabilization and activation of actin filament nucleation by cortactin is important for germ cell migration in *Drosophila* (Somogyi and Rorth, 2004). Src can also activate paxillin, which is a scaffolding protein that has been shown to mediate HGF-induced epithelial morphogenesis (Ishibe et al., 2003). Additionally, Src can mediate the activation of FAK. In a colon cancer cell line, this activation was important for the disassembly of focal adhesions, which is necessary for the cell to migrate to a new location (Brunton et al., 2005). Thus, one signaling pathway can influence cytoskeletal rearrangement and motility through multiple mechanisms.

Our studies focus on exploring a role for the PDGFRβ and its signaling pathways in the epicardial EMT in vivo. We utilize mice with a conditional deletion of PDGFRβ, PDGFRβ null mice, and a series of mice with tyrosine to phenylalanine point mutations at different locations in the cytoplasmic domain of the PDGFRβ. These point mutations provide an opportunity to link specific signaling pathways downstream of PDGFRβ to function. The point mutations prevent phosphorylation at residues that serve as docking sites for downstream signaling molecules, and therefore mutation of these sites leads to an inhibition of individual pathways (Figure 1.1). These point mutations not only help delineate the function of PDGFRβ in the development of coronary vasculature, but also can be used to assess a later role for the differentiated mural cell in angiogenic processes.

Figures

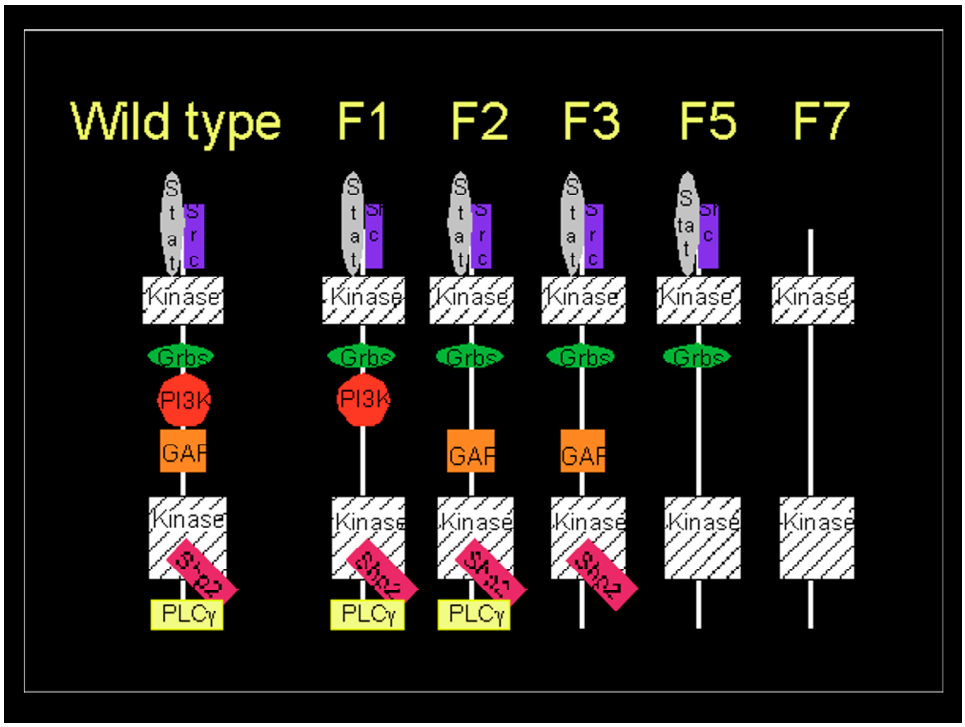

Figure 1.1 The PDGFRβ F Series
A schematic representation of the cytoplasmic domain of the PDGFRβ. The receptor has a split kinase activation domain and several tyrosines that become phosphorylated upon receptor activation. This modification provides docking sites for several downstream signaling molecules: Stat, Src, Grb2, PI3K, RasGAP (GAP), Shp2, and PLCy. In the F series (F1, F2, F3, F5, and F7), tyrosine to phenylalanine point mutations are made at specific residues to block the binding and activation of individual signaling molecules. The diagram above reveals the pathways that are not disrupted in each mouse.

CHAPTER TWO

PDGFR EXPRESSION AND EPICARDIAL CHARACTERIZATION

Introduction

In vitro studies of epicardial cells suggest that several growth factors are important for the ability of the epicardium to undergo EMT and subsequently differentiate into coronary VSMC. One of these growth factors is PDGF. In PEO explant studies, stimulation of epithelial outgrowth with PDGFBB increases the rate at which the cells rearrange their actin to a filamentous pattern characteristic of mesenchymal cells. PDGFBB increases the expression of several markers of VSMC, including calponin and SM22 (Landerholm et al., 1999). Stimulation of a rat epicardial cell line with PDGFAA, which is specific for the PDGFRα, and PDGFAB also induce the expression of VSMC markers (Wada et al., 2003).

The in vitro induction of VSMC through either the PDGFRα or PDGFRβ is consistent with their ability to stimulate several overlapping downstream signaling pathways (Figure 2.1). In vivo, these signaling pathways cooperatively regulate cellular function (Richarte et al., 2007). The signaling capabilities are also partially redundant. When chimeric receptors were generated by attaching the extracellular domain of the PDGFRα with the intracellular domain of the PDGFRβ, the signaling cascades activated by PDGFRβ cytoplasmic domain

resulted in the normal development of most PDGFRα dependent cells. In contrast, PDGFRα did not entirely rescue the development of cells dependent on the PDGFRβ. Hemizygous mice exhibited several phenotypes that were consistent with partial loss of PDGFRβ function (Klinghoffer RA, 2001).

Therefore, when the receptors are coexpressed, any phenotypes resulting from the deletion of one receptor may be masked by the presence of the other receptor. In vivo studies suggest that the PDGFRα may play a less significant role in coronary VSMC development than the PDGFRβ. The PDGFRβ specific ligand, PDGFDD, is expressed exquisitely in the epicardium (Ponten et al., 2005). The PDGFRβ null lacks coronary VSMC (chapter 3). Finally, unlike the PDGFRβ, the PDGFRα is not expressed in the coronary VSMC.

The PDGFRβ has the potential to exert an influence on coronary VSMC development at multiple time points. It is thus important to characterize the normal development of the epicardium in vivo during coronary VSMC development when the PDGFRs are expressed and can affect cellular function. It is also beneficial to evaluate the conditional deletion of the PDGFRβ at specific stages of coronary VSMC development to specifically assess the time(s) at which the PDGFRβ could exert its influence over coronary VSMC development. As previously discussed, the expression profile of VSMC proteins changes as the VSMC differentiates. Two Cre lines that exhibit differential expression during

the development of VSMC are the SM22 Cre Tg and myocardin^{Cre}. SM22 is a protein associated with a differentiated VSMC and could therefore provide a means of deleting the PDGFRβ after differentiation has occurred (Boucher et al., 2003; Li et al., 1997). In contrast, myocardin is transcription factor that is considered a master regulator of VSMC differentiation and is expressed early in the development of VSMC (Li et al., 2003; Yoshida et al., 2003) (Du et al., 2003; Manabe and Owens, 2001; Strobeck et al., 2001). Although there is Cre expression in additional cell populations, including the myocardium, the restricted expression of the PDGFRβ suggests that the two Cre lines can provide insight into the role of the PDGFRβ in coronary VSMC development.

Materials and Methods

Experimental animals

Wild type, PDGFRα$^{GFP/+}$, PDGFRβ$^{fl/+}$, PDGFRβ$^{+/-}$, Myocardin^{Cre}, SM22 Cre Tg, R26^{YFP} mice were maintained on a mixed C57Bl/6 X 129SV background. We utilized MKO to signify the deletion of the PDGFR with the myocardin cre. SKO is used to delineatedSM22 deletion of the PDGFR. We used mice that were heterozygous for the *XlacZ4* transgene to visualize pericyte populations (Tidhar et al., 2001). All animal experiments were approved by the Institutional Animal Care and Use Committee (IACUC) at the University of Texas Southwestern

Medical Center and performed according to the Guide for the Care and Use of Laboratory Animals published by the NIH.

Epicardial Culture

Primary epicardial cells were isolated from E11.5 hearts as previously described (Morabito et al., 2001). Hearts were removed at day 2. Cultures were allowed to grow for ten days for immunocytochemistry. For western analysis, day 5 cultures were starved in 1%FBS for 2 days and then stimulated for the times indicated.

Immunohistochemistry

Whole Mount

E9.5 embryos were fixed in 4%PFA. A 1:200 dilution of the PDGFRβ (eBioscience) was used. For the E17.5 hearts, the protocol was adapted from Manipulating the Mouse Embryo for PECAM staining. Hearts were fixed overnight in 4:1 Methanol:DMSO at 4°C. This was followed by 5-10 hours in 4:1:1 Methanol:DMSO:H202 at 4°C and three 20min washes in 1:1 Methanol:PBS were performed prior to placing hearts in PBS. Hearts were blocked for 2 hours in PBSMT (2% milk, 0.5% TritonX in PBS) and then incubated with 1:200 PECAM (BD Biosciences) overnight. Samples were washed 5 times for a total of 8 hours followed by 2 hours in 1:200 biotinylated anti-rat (Vector Labs). An overnight wash and 5 additional washes in PBT

(0.5%TritonX in PBS) for at least 1 hour were followed by use of a Vectastain ABC kit and developed with DAB (Vector Labs).

Frozen Sections

Hearts were isolated from the embryo and then samples were fixed for 2 hours in 4% PFA, put in 30% sucrose overnight at 4°C and embedded in Tissue Tek O.C.T. compound. 0.5% Triton was used to remove OCT. The following dilutions were used: PDGFRβ (1:200 eBiosciences), ZO1 (1:300), vimentin (1:500 Sigma), twist (1:200, Santa Cruz), slug (1:400 gift R.MacDonald), YFP (1:500 AbCAM), PECAM (1:200 BD Biosciences) and α4integrin (1:200 Chemicon).

Immunocytochemistry

Cells were fixed in 4%PFA. Calponin (Sigma) was used at a 1:200 dilution. Phalloidin488 (Molecular Probes) used at 1:200 dilution.

β–galactosidase staining

Frozen sections were placed in PBT for 15 minutes, which was followed by three 5-minute washes. Sections were incubated overnight at room temperature in 25μl of x-gal in N,N-Dimethyl Formamide per ml of staining stock (5mM $KFe(CN_2)_2$), 2mM $MgCl_2$, 0.3% Detergent, in PBS). Slides were dehydrated and mounted with Cytoseal.

Western Analysis

Cell lysates were prepared in EB lysis buffer supplemented with aprotonin, sodium orthovanadate, and PMSF. Western was performed as previously described using the following antibodies: PDGFRβ: (Upstate 1:1000) and cytoskeletal actin: (1:5000 Novus) (Tallquist et al., 2003).

RT-PCR

RNA was isolated from 3 PEOs using Qiagen RNEasy Kit. cDNA was synthesized utilizing standard Clontech Protocols. Primer sequences available upon request.

Flow Cytometry

11 proepicardiums were isolated and pooled together. Cells were processed per standard flow cytometry protocols.

TEM

Hearts were isolated from the embryo and fixed in 2.5% glutaraldehyde in 0.1M Cacodylate buffer. Hearts were routinely processed for TEM.

Imaging

Fluorescent imaging utilized the Zeis Axiovert 200 with the Hamamatsu ORCA-ER camera and Open Lab. Color imaging of slides performed with the Zeis Axiovert 200 with the Olympus DP71 camera and DP software. Whole mount imaging used the Nikon SMZ1000 with either the Olympus DP71 camera or a Nikon digital camera. TEM images were taken on JEOL 1200 EX Electron Microscope.

Results

PDGFR Expression

Several in vitro studies have suggested a possible role for the PDGFRs early in the development of coronary VSMC, specifically in the function of the proepicardium or the epicardium. We examined their expression at each stage of coronary VSMC development to determine when the receptors are present. Consistent with studies that were performed in the chick, we demonstrated expression of the PDGFRβ in the proepicardium (Guadix et al., 2006) (Figure 2.2). Immunohistochemical analysis was performed on E9.5 embryos and showed that the PDGFRβ was localized to a vesicular outcropping of cells dorsal to the heart tube, which is morphologically characteristic of the proepicardium (Figure 2.2A). To further substantiate our findings, we performed RT-PCR on microdissected proepicardiums (Figure 2.2B). The RT-PCR showed the expression of the PDGFRβ with several proepicardium markers, including WT1 and Tbx18. However, the microdissection may have had some myocardial contamination since the expression of ehand was detected. Our flow cytometry results were also consistent with the presence of the PDGFRβ in the microdissected proepicardium. These dissections included a slightly larger area of cells due to the cell number requirements for flow cytometry. Nonetheless, the

PDGFRβ was present in 24% of the dissected cell population (Chris Smith, unpublished observations).

We then investigated the possible expression of PDGFRα in the PEO. We utilized the PDGFRα^{GFP} mouse line, which has a nuclear localized GFP inserted into the PDGFRα locus. Sections through the E9.5 PDGFRα^{GFP} embryo were analyzed for expression of the PDGFRα (Figure 2.2 D,F) and α4 integrin, a proepicardium marker (Yang et al., 1995) (Figure 2.2 E,F). The localization of the PDGFRα did not coincide with that of α4 integrin. This suggested that either the PDGFRα was not expressed in the proepicardium or it was expressed in a subset of proepicardial cells that either do not express α4 integrin or have not yet turned on expression of α4 integrin.

As we were interested in the role of the PDGFRs throughout coronary VSMC development, and because the published in vitro data was performed on both primary cultures of epicardial cells from chick PEO explants and a rat epicardial cell line, we continued our expression analysis at later time points (Figure 2.3). The proepicardial cells encompass the heart by E11.5 and form the epicardium. At E12.5 we observed coexpression of the PDGFRβ with the PDGFRα in the epicardium (Figure 2.3A-D). This coexpression in the epicardium was still prevalent at E14.5 (Figure 2.3E-H). In addition, when the epicardially-derived subepicardial mesenchyme was examined, there was a population of cells

expressing both receptors and a smaller proportion of cells that expressed only the individual receptors. These studies suggested that not only were both receptors present to influence epicardial function, but they likely have overlapping as well as distinct roles in this developmental process.

Because both receptors were present in the epicardium, we continued our initial characterization by isolating primary epicardial cells from E11.5 heart explants and investigating the expression of the receptors in vitro. To derive primary epicardial cultures hearts are plated on collagen-coated dishes. The epicardial cells then migrate out from the heart as a sheet and after two days the heart is removed. Although epicardial cells can be generated from E11 to E13.5 hearts, the E11.5 hearts maintain the epicardial cobblestone morphology to a greater extent than the E13.5 hearts, which were found to have a higher rate of spontaneous mesenchymal transformation at the edges of the culture. To ensure that the expression of our receptors was maintained in vitro we performed western blot analysis for PDGFRβ (Figure 2.4A) and fluorescent imaging of PDGFRα^{GFP} to assess the PDGFRα (Figure 2.4B). Both analyses confirmed the existence of both PDGFRs in vitro.

To further compare the in vitro expression pattern to that in vivo we examined the expression of PDGFRα in epicardial cells that had time to differentiate. PDGFRα was utilized since we could monitor its expression on an individual cell basis with the PDGFRα^{GFP}. When we examined the cells for

PDGFRα^{GFP} and the F-actin binding protein, phalloidin, the PDGFRα was expressed in epicardial cells that displayed the typical subcortical distribution of actin, but was not present in cells that had a filamentous actin arrangement that is characteristic of mesenchymal cells. Moreover, when we stained the cultures for calponin, a VSMC protein, we noticed that PDGFRα was turned off when calponin was distributed throughout the cytoplasm, which is typical for a differentiated VSMC. This suggested that the PDGFRα was down regulated upon VSMC differentiation. Assuming that the PDGFR expression in the subepicardial mesenchyme represented epicardial-derived cells, these results suggest that the differentiation of the cells to VSMC may be the point of divergence in the PDGFR expression pattern.

In Vivo Characterization of Epicardial EMT

Because the PDGFRα wasn't expressed in a single VSMC and given the exquisite expression of the PDGFDD ligand, we focused our analysis on the PDGFRβ. To carefully evaluate if the PDGFRβ was essential for coronary vessel formation, we performed phenotypic analysis of coronary vessels in the PDGFRβ null embryos. We found that coronary vessel development and VSMC recruitment were severely affected. This analysis will be described further in Chapter 3. Although we had the tools to investigate the role of the PDGFRβ in vivo, careful examination of the literature suggested that little analyses had been

accomplished on epicardial EMT in vivo. The majority of epicardial studies in vivo have looked at endpoints such as formation of vasculature or myocardial thickness. In addition, most studies have been carried out in vitro. Therefore it was necessary to characterize the wild type murine epicardial EMT process in vivo prior to assessing a potential role for the PDGFRβ.

EMT is a multistep process that involves the loss of cellular contacts, the down regulation of epithelial genes, up regulation of mesenchymal genes, cytoskeletal reorganization, degradation of the basement membrane and subsequent migration to a new location. To determine whether the epicardial cells had traditional junctions we examined the epicardium by transmission electron microscopy (TEM) (Figure 2.5AB). Our results suggest that the epicardium does not exhibit the typical tripartite junctions of epithelial cells. There not did appear to be any tight junctions or desmosomes present in the epicardium. There were also no typical adherens junctions displaying symmetric densities or defined intercellular cross bridges. In contrast, the epicardial junctions that were present were more like intermediate junctions with irregular shaped electron densities and less defined intercellular bridges. Despite the lack of typical epithelial junction structures, our complementary immunohistochemical analysis revealed that a majority of the junctional proteins are expressed by the murine epicardium. ZO1, a component of tight junctions, was expressed in the epicardium throughout the time of our analysis (E12.5 to E14.5) (Figure 2.5). β-catenin, which is associated

with adherens junctions, was also expressed at E14.5 (Sfigure 3.3). This suggests that the epicardium maintains some characteristics of a traditional epithelium.

In vitro, the reorganization of actin is utilized to follow the EMT process because there is a change in its subcortical distribution in epithelial cells to a filamentous pattern in mesenchymal cells. We therefore evaluated the localization and expression of actin using phalloidin (Figure 2.5). In vivo, the immature epicardial cells (E12.5) display a subcortical actin distribution. This actin localization pattern changes over time and by E14.5, the majority of cells concentrated the actin to their basolateral surface. It is possible that the cells with subcortical actin may be undergoing the EMT process. This interpretation is consistent with the belief that epicardial cells can undergo EMT while they migrate over the surface of the heart. As the number of cells with the subcortical actin decrease, the epicardium becomes covered in flattened epicardial cells that distribute actin to their basolateral surface. Interestingly, the squamous appearance of these epicardial cells is distinct from the traditional cuboidal cells associated with an epithelium. This provides an additional feature that distinguishes the epicardium from other epitheliums.

Another traditional marker for EMT is vimentin. Vimentin is an intermediate filament protein whose expression is up regulated in vitro upon the transition to a mesenchymal phenotype. However, its expression has been noted in the epicardium (Perez-Pomares et al., 2003). We examined its in vivo

expression from E12.5 to E15.5 in the ventricles (Figure 2.6). Although the expression is not limited to the epicardium or subepicardial mesenchyme, we were initially able to see vimentin expression in the epicardium and then follow the time dependent appearance of vimentin positive cells in the subepicardial mesenchyme. As cells migrate into the myocardium there is a concomitant decrease of vimentin expression in the epicardium. However, it is important to note that with this analysis we are not able to differentiate whether the vimentin positive cells in the myocardium arose from the epicardium, as we believe, or whether cells that were already present in the myocardium began expressing the protein.

Finally, we examined the expression of transcription factors that have been shown to be important in EMT. Twist is a bHLH factor that can induce EMT and is up regulated in several metastatic cancers (Kang and Massague, 2004). We examined its expression at E12.5 and E14.5 using an antibody that recognized both twist1 and twist2 (Figure 2.7). At E12.5 the majority of epicardial cells were positive for twist along with a large number of myocardial cells. To determine whether there were differences in expression of the two isoforms at this time we utilized a twist2 Cre mouse that turned on the Rosa 26 β−galactosidase reporter in all cells that expressed twist2. When β−galactosidase positive cells are incubated with an exogenous β−galactosidase substrate, the cells turn blue and can be distinguished from the surrounding cells. Although a large

number of cells within the myocardium were twist2 positive, no epicardial cells were positive (Figure 2.7). Therefore, the epicardial cells appear to widely express twist1 at E12.5. This expression is diminished at E14.5 when a small number of subepicardial cells are twist positive. The zing finger protein slug is another transcription factor that is up regulated during EMT. We examined its expression at E12.5 and observed a marked difference from twist (Figure 2.7G). Slug was expressed in a small number of subepicardial cells as opposed to epithelial cells. This is consistent with other slug expression analyses in which it was localized to the mesenchyme and where it was suggested that the in vivo role of slug is to maintain the undifferentiated mesenchymal state (Savagner et al., 1998).

Conditional Ablation of the PDGFRβ

We have shown that the PDGFRβ is present at each step in the development of coronary VSMC, defined the cell types and steps involved in the development of coronary VSMC and in data to be discussed in chapter 3 we have demonstrated that loss of PDGFRβ signaling disrupts the formation of coronary VSMC. To characterize the cell population that the PDGFRβ is affecting which impacts coronary VSMC development, we then performed conditional deletions of the PDGFRβ. We utilized two different Cre systems: SM22, which is expressed in differentiated VSMC, and myocardin, which is responsible for

transcriptionally regulating VSMC differentiation. The first step in the conditional analysis was to assess whether the Cre was expressed in the expected cell populations. The Rosa26^{YFP} provided a means to tag cells that expressed Cre. We analyzed E17.5 Rosa26^{YFP} PDGFRβ$^{fl/+}$ hearts that had either the SM22 Cre Tg or the myocardin^{Cre} (Figure 2.8). We performed costaining with either PECAM, to identify endothelial cells, or the PDGFRβ. The utilization of the PDGFRβ not only provided a means of identifying VSMC but also directly showed the coexpression of the Cre and the protein it would be deleting. Consistent with previous expression reports SM22 and myocardin were present in both the myocardium and the coronary VSMC.

We continued our analysis by determining the presence of coronary VSMC and endothelial vessels at E17.5 in the conditional deletions. However, it is important to note that the complete deletion of the PDGFRβ would need to be established before drawing definitive conclusions. The SM22 induced deletion of the PDGFRβ was examined first since it is a late stage marker (Figure 2.9). The presence of coronary VSMC and endothelial vessels in this conditional knockout suggested that while the PDGFRβ is important for VSMC proliferation and migration, deletion of the receptor in differentiated VSMC does not substantially affect the initial development of the coronary VSMC. Moreover, the phenotype suggests that the defects observed in the PDGFRβ nulls were likely due to a role for the PDGFRβ prior to the differentiation of the coronary VSMC. To evaluate

an earlier time in coronary VSMC development we utilized the myocardin^{Cre}. When the VSMC and endothelial cell populations were examined with the myocardin induced deletion of the PDGFRβ there was also not a substantial change in the coronary VSMC population or the endothelial vessels (Figure 2.10). This suggested that if the PDGFRβ had a role in coronary VSMC formation it either preceded the expression of myocardin, it was in a distinct cell population, or its function was redundant with another growth factor.

Discussion

VSMC comprise a heterogeneous cell population that arises from multiple origins. The coronary VSMC come from a unique population of cells whose developmental importance is of recent interest. Our studies reveal that both of the PDGFRs are present in the correct location to exert an early influence over coronary VSMC development. We characterized several of the steps that occur in the evolution of an epicardial cell to a coronary VSMC in vivo. In addition, we suggest that the PDGFRβ has an important role within these cell populations, but it is prior to the differentiation of the VSMC.

As part of our characterization we assessed how the in vitro system models in vivo development. As the markers that are typically used for in vitro assessment have not been fully characterized in vivo, we investigated the expression of several of these markers. We found that although the morphology

of the epicardium is different from that of a typical epithelium, several of the same markers can be utilized to follow the EMT progression in vivo. In addition, consistent with our in vitro characterization of the presence of both the PDGFRα and the PDGFRβ in epicardial cultures, the PDGFRs exhibit overlapping expression in the epicardium in vivo. Moreover, the presence of subepicardial mesenchyme, which expresses only one of the receptors or the other, is consistent with the down regulation of the PDGFRα in cultured cells that have differentiated into VSMC.

The overlapping and yet distinct expression profiles of the receptors suggest that their expression patterns could be used to delineate subpopulations of cells that develop during coronary VSMC formation. It would be interesting to sort for the cell populations that express either or both receptors to examine the relative functions of each population in vitro. Additionally, the cell populations could also be examined for differential regulation of transcription factors that may promote the cell to follow its particular lineage. It would also be interesting to investigate the effects of RA signaling on the ability of the isolated cell populations to regulate transcription in vitro. RALDH, which synthesizes RA, is expressed in the epicardium and is downregulated upon differentiation. Moreover, in other systems RA has been shown to inhibit PDGFR induced gene expression. Thus it could act to restrict some of the functions of the PDGFR until a cell is ready to differentiate.

To assess the potential times at which the PDGFRβ could influence coronary VSMC development we performed conditional analysis. While we focused on the PDGFRβ, future studies looking at the conditional ablation of the PDGFRα, as well as the double conditional knockout will yield important insights in the redundant and unique functions of the receptors. Our analysis of the SM22 Cre Tg and myocardin^{Cre} suggest that the PDGFRβ has a role in coronary VSMC development prior to the differentiation of coronary VSMC and outside of its canonical role in inducing proliferation and migration of differentiated cells. However, it is also possible that the PDGFRα signaling is masking a phenotype or that there is incomplete deletion of the receptor. In the future it will be necessary to catalogue the expression of these Cres at earlier time points as well as their effectiveness in deleting the PDGFRβ. Moreover, it will be interesting to use additional Cre lines to remove expression of the PDGFR at earlier timepoints during this developmental process.

Figures

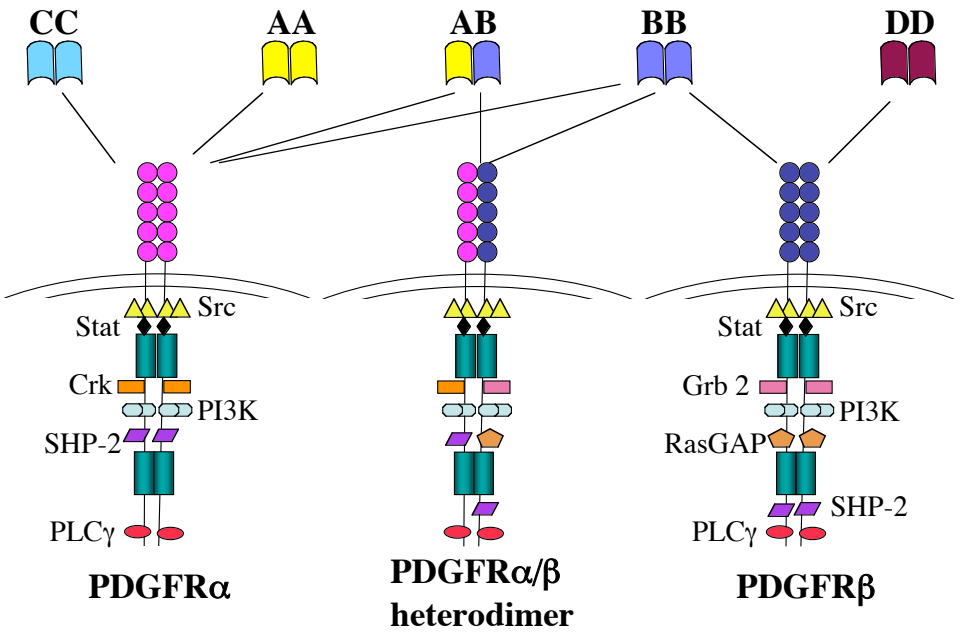

Figure 2.1 PDGFR Signaling Pathways
The schematic above illustrates the ability of the PDGFRα and the PDGFRβ to homo or heterodimerize upon ligand binding and receptor activation. This activation results in the docking and activation of several of the same downstream signaling molecules. The docking of RasGAP to the PDGFRβ is one distinguishing characteristic between the receptors.

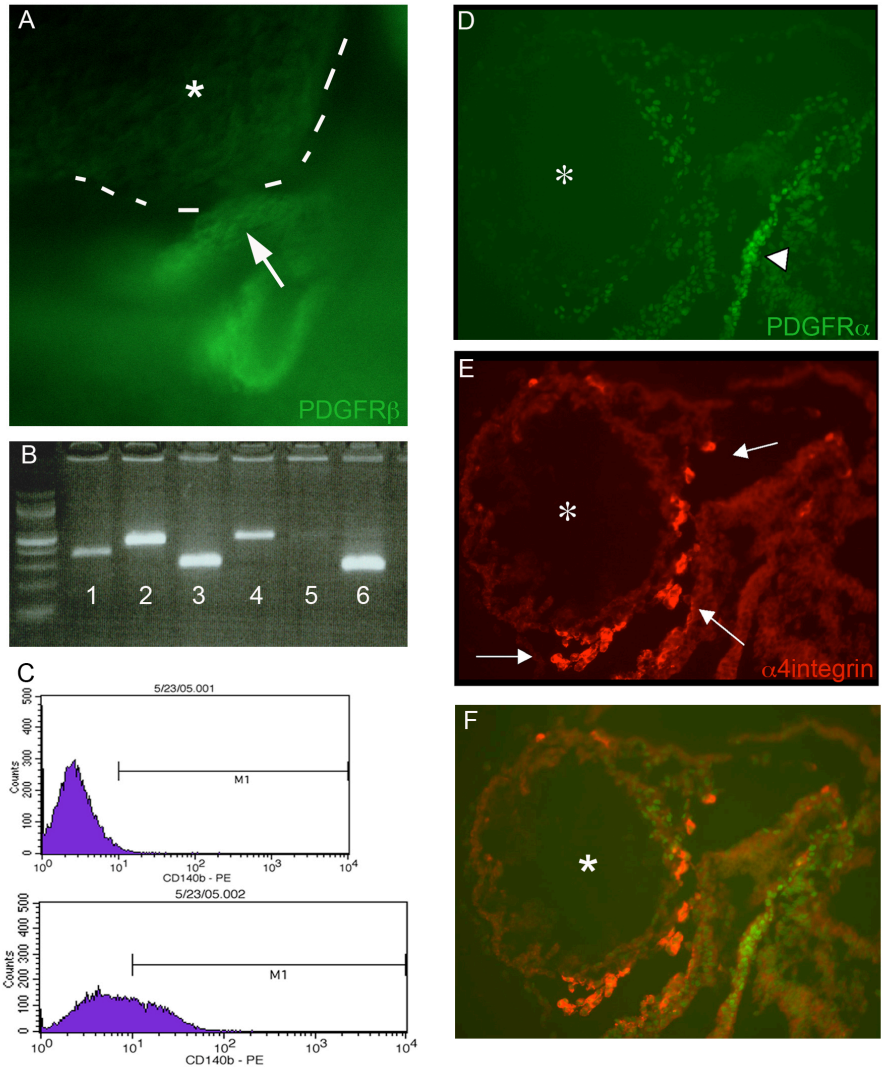

Figure 2.2 PDGFRs in the Proepicardium
The PDGFRβ is expressed in the proepicardium. (A) Whole mount immunofluorescence analysis of E9.5 embryo shows the expression of the PDGFRβ in the grape-like cluster of cells dorsal to the outlined heart tube. (B) RT-PCR analysis of dissected proepicardiums examines the expression of (1) the PDGFRβ, (2) Tbx18, (3) WT1, (4) ehand, (5) dhand, and (6) GAPDH. (C) Flow cytometry was also performed by Chris Smith on the dissected proepicardiums. There is a shift in the signal when the PDGFRβ (lower panel) antibody is compared to a negative control (upper panel). (D) PDGFRα expression is analyzed with the PDGFRα^{GFP} mouse and compared to the expression of (E) α4 integrin, a PEO marker. (F) The expression patterns are overlaid. Astericks show the location of the heart. Arrows marks the proepicardium. Arrowhead delineates PDGFRα^{GFP} positive cells.

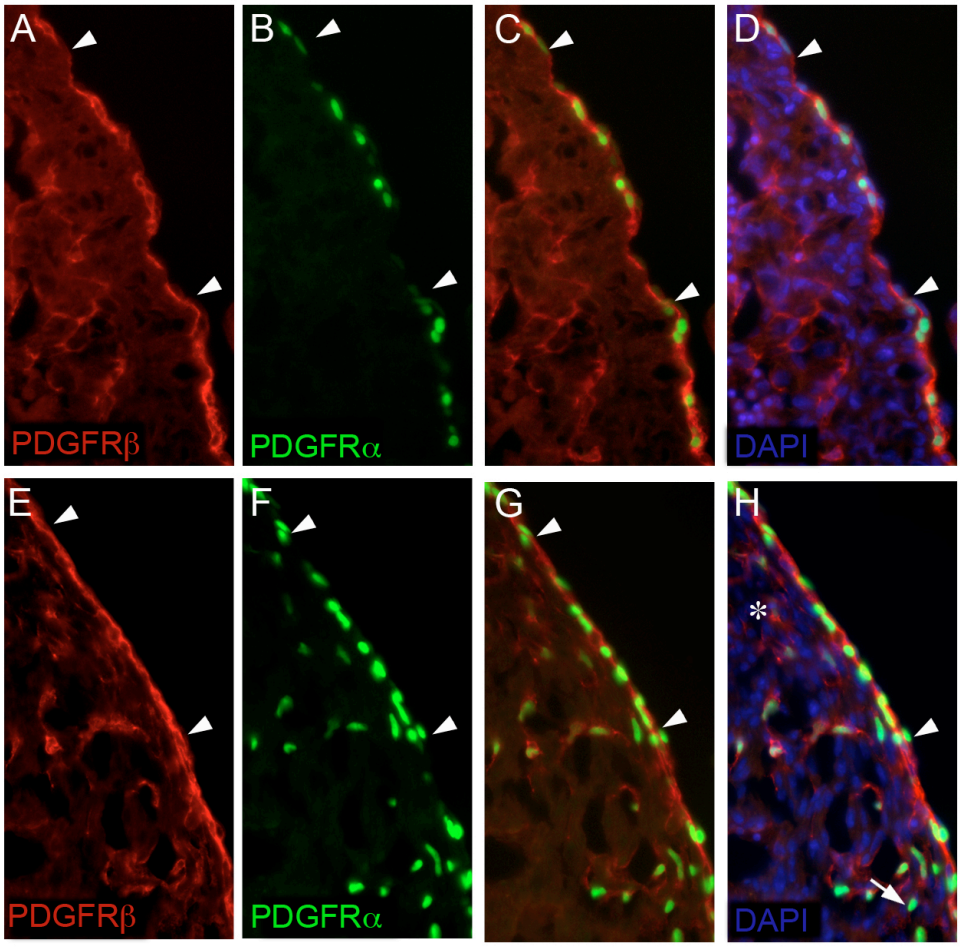

Figure 2.3 PDGFRα and PDGFRβ in the Epicardium and Subepicardial Mesenchyme
(A-D)E12.5 and (E-H)E14.5 hearts were examined for the expression of the PDGFRs. PDGFRα was identified with a nuclear knockin GFP (green). PDGFRβ was identified with immunohistochemistry(red). Merged images are shown (D,H) with and (C,G) without DAPI (blue). Although there is strong overlap between the PDGFRα and the PDGFRβ in the epicardium, in the subepicardial mesenchyme there are cells that only express (arrow) PDGFRα or (asterick) PDGFRβ. Arrowheads mark the edge of the epicardium.

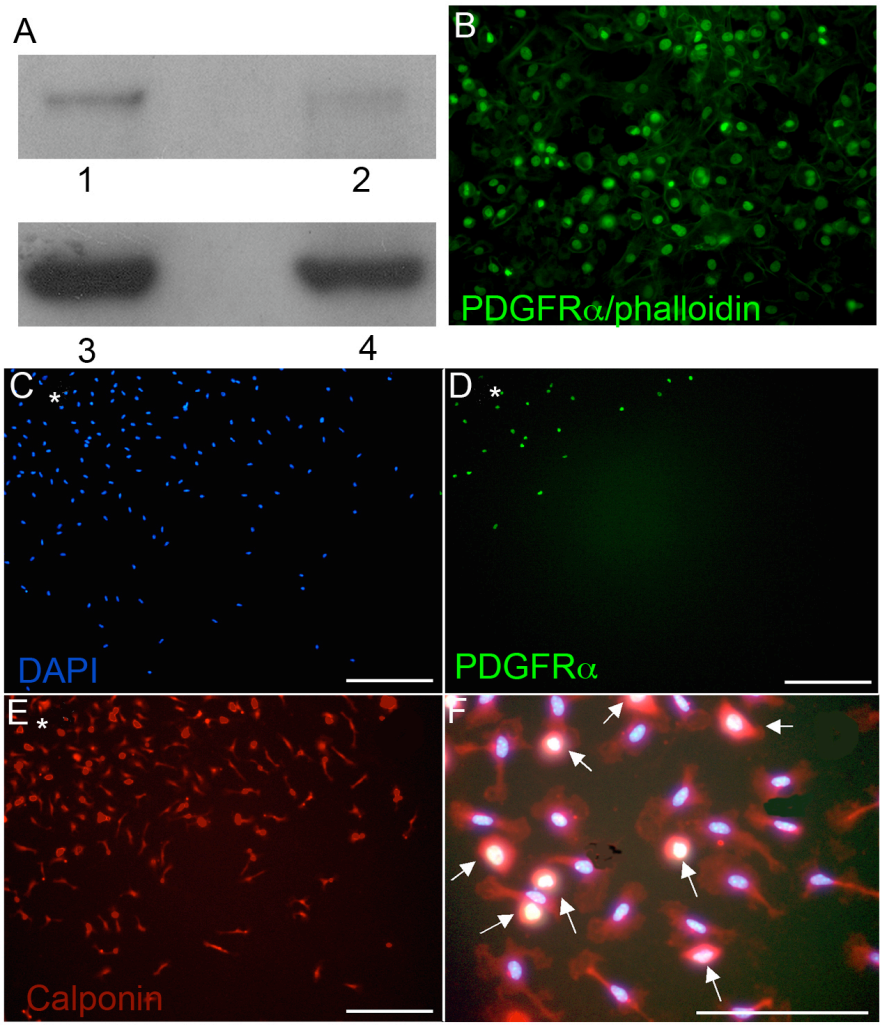

Figure 2.4 Characterization of the Epicardial Culture System
(A) (1) PDGFRβ was found to be present in the epicardial cell protein lysate. (2) 3T3 cells were used a positive control. (3,4) Actin was used as a loading control. (B) The PDGFRα^{GFP} was utilized to show expression of the PDGFRα in primary epicardial cultures. (C-F) D10 epicardial cultures are stained for (C) DAPI, (D) PDGFRα, and (E) calponin, a VSMC marker. (F) Merged images of the cells at a higher magnification. Astericks show the original placement of the heart for epicardial outgrowth. Arrows point to PDGFRα positive cells. Studies in B-F were performed by MD Tallquist.

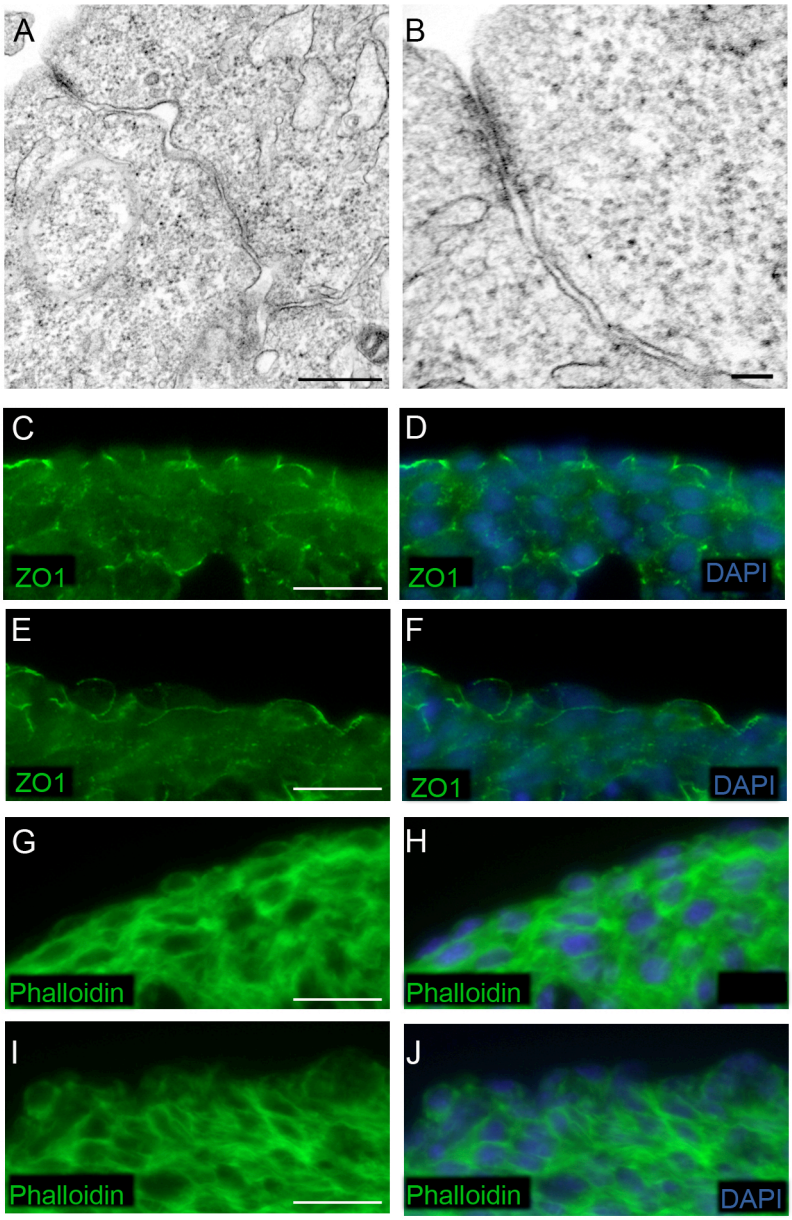

Figure 2.5 Epicardial Junctions and the Cytoskeleton
(A,B) TEM images of E13.5 epicardial junctions are shown at two magnifications. (A) Scale = 500nm. (B) Scale = 100nm. (C-F) Tight junctions are delineated with the ZO1 marker at (C,D) E12.5 and (E,F) E13.5. (G-J) Actin organization is shown with phalloidin at (G,H) E12.5 and (I,J) E13.5. Images are illustrated (D,F,H,J) with and (C,E,G,I) without DAPI. (C-J) Scale = 0.025mm.

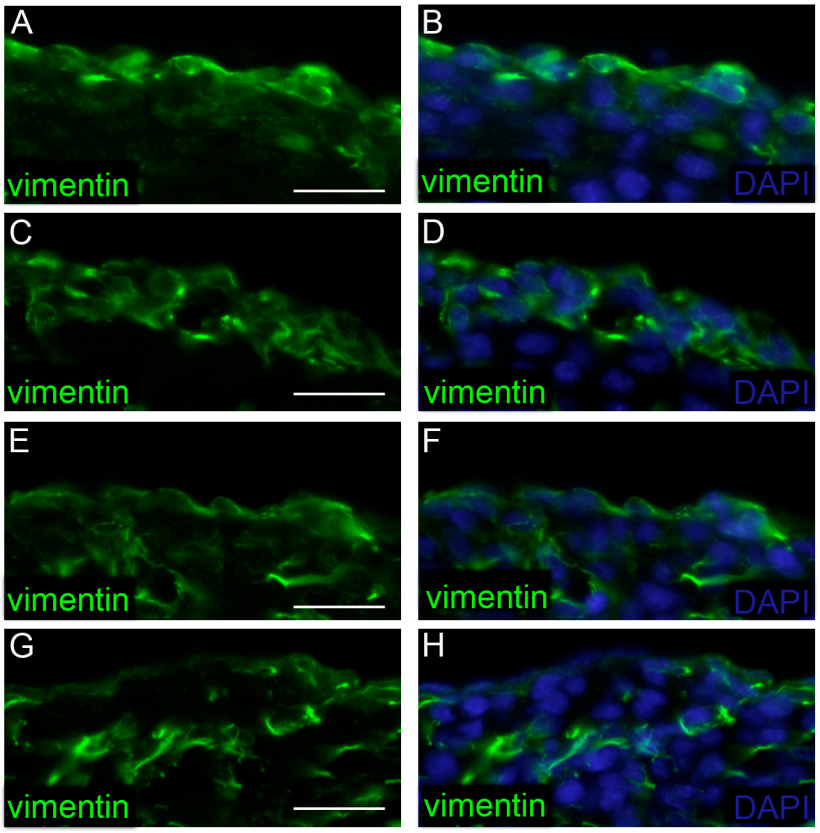

Figure 2.6 In Vivo Analysis of Vimentin Expression
(A-H) The localization of vimentin (green) is illustrated at (A,B) E12.5, (C,D) E13.5, (E,F) E14.5 and (G,H) E15.5 heart sections. Vimentin is shown (B,D,F,H) with and (A,C,E,G) without DAPI. Scale= 0.025mm.

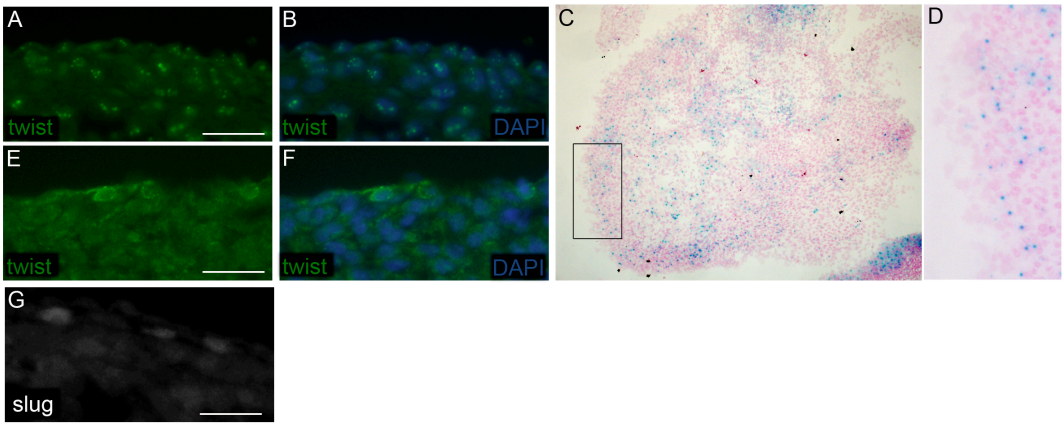

Figure 2.7 EMT Associated Transcription Factors in the Epicardium
(A,B,E,F) Twist 1 and Twist 2 expression (green) is examined in the (A,B) E12.5 and (E,F) E14.5 heart (B,F) with and (A,E) without DAPI. (C,D) The twist2 Cre mouse is used in combination with R26 βgalactosidase reporter (blue) to show cells that have expressed twist2. Sections are processed for nuclear fast red. The box delineates the area of magnification. This study was performed by MD Tallquist. (G) Slug expression is illustrated in the subepicardial layer of the E12.5 heart. Scale=0.025mm.

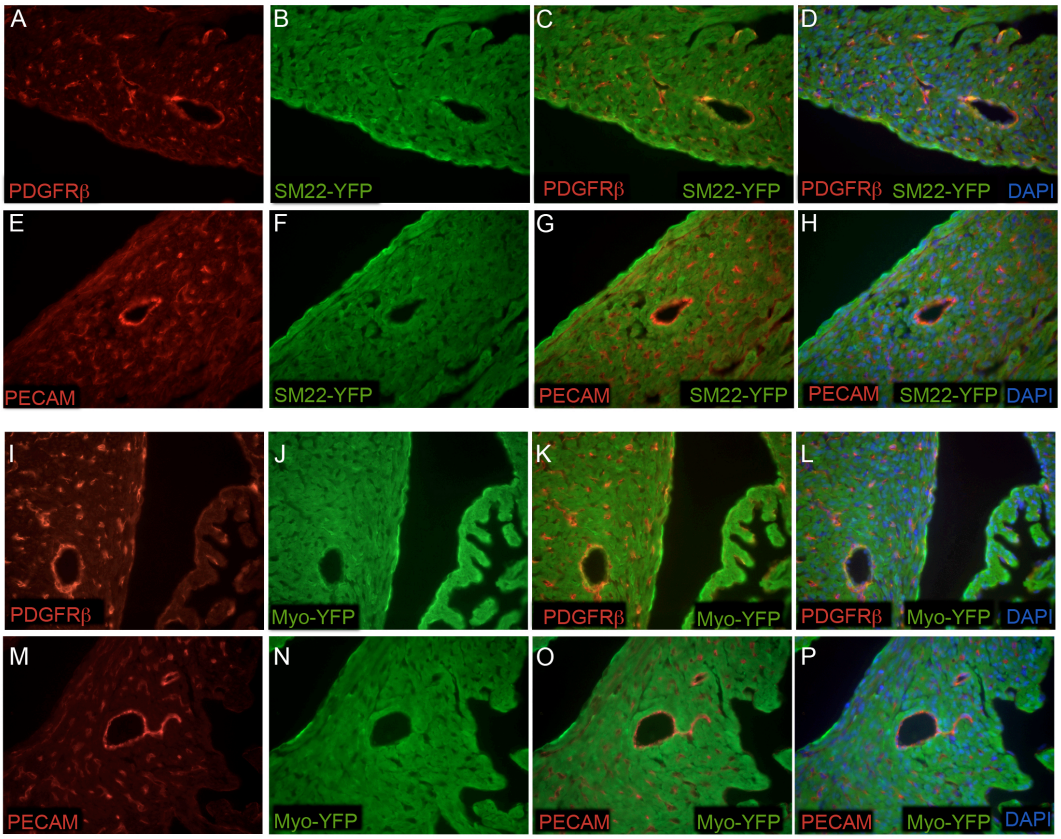

Figure 2.8 SM22 and Myocardin Cre Expression Patterns
(A-H) Expression of the SM22 Cre Tg was determined by colocalization analysis of a (B-D, F-H) $R26^{YFP}$ reporter with (A,C,D) a smooth muscle cell marker, PDGFRβ, or (E,G,H) an endothelial cell marker, PECAM at E17.5. (I-P) Expression of the $Myocardin^{Cre}$ (Myo) was determined by colocalization analysis of (J-L, N-P) a $R26^{YFP}$ reporter with a (I,K,L) smooth muscle cell marker, PDGFRβ, or (M,O.P) an endothelial cell marker, PECAM at E17.5. (D,H,L,P) DAPI (blue) used to identify cell nuclei.

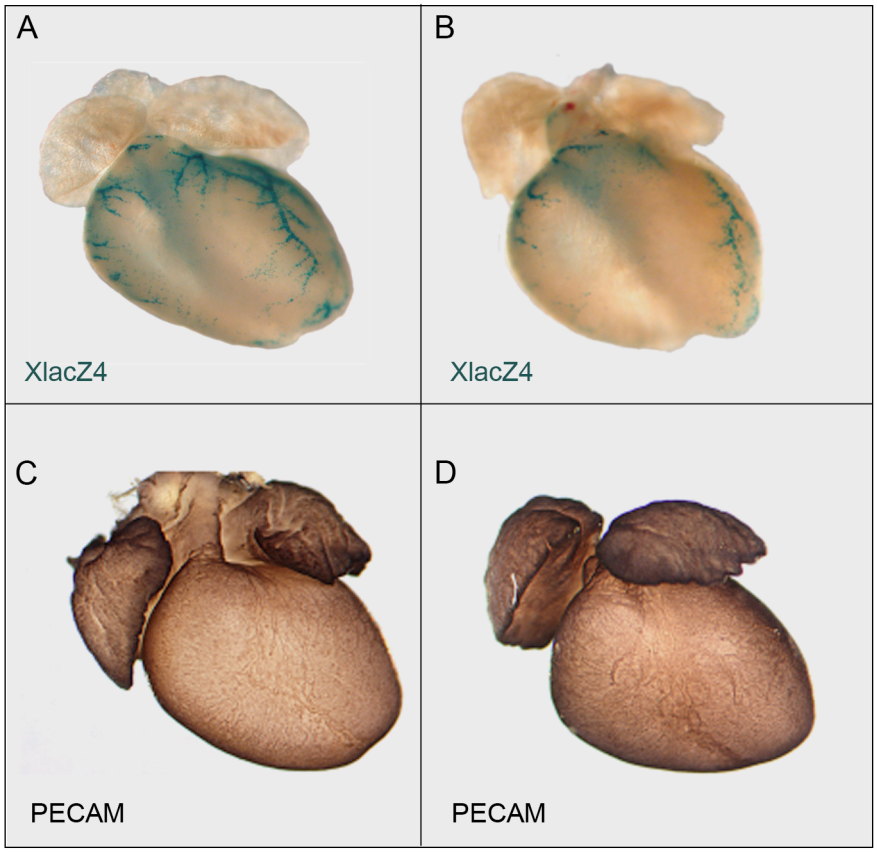

Figure 2.9 Coronary Vasculature in the SM22 Cre Tg
(A-B) At E17.5 coronary VSMC were examined using the *XlacZ4* (blue) in (A) PDGFRβ$^{fl/-}$ and (B)PDGFRβ$^{SMO/-}$ mice. (C-D) Endothelial vessels were also examined at E17.5 using PECAM staining on (C) PDGFRβ$^{+/+}$ and (D) PDGFRβ$^{SMO/-}$ mice.

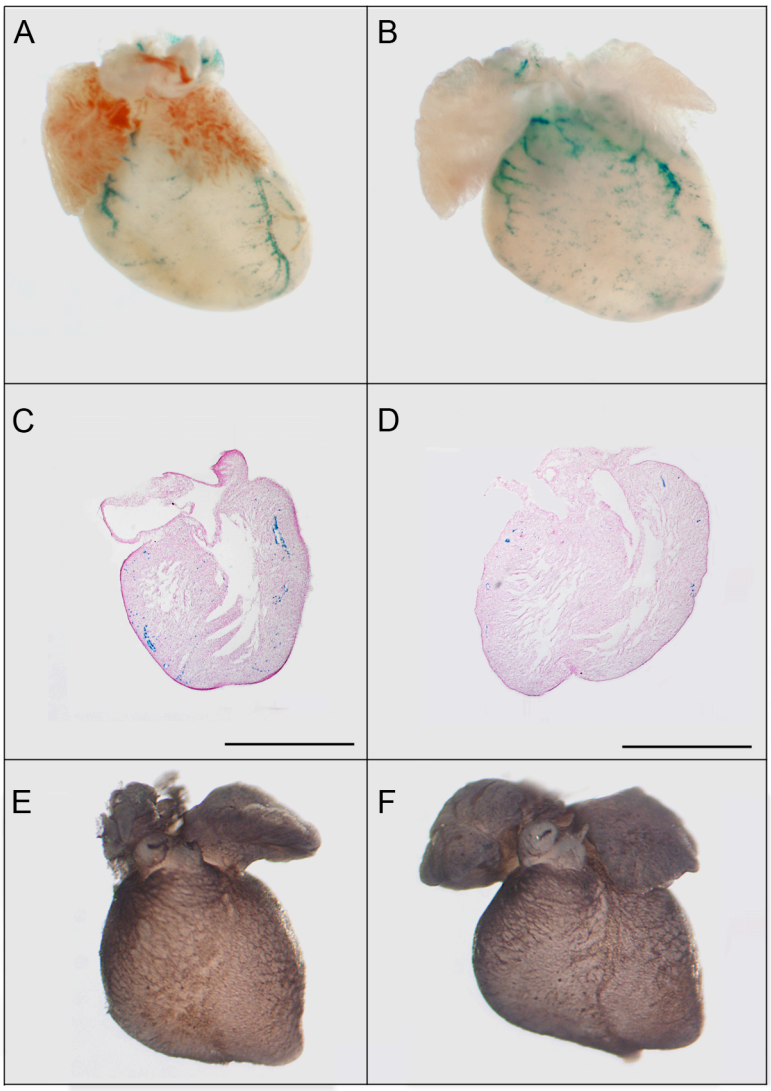

Figure 2.10 Coronary Vasculature in the Myocardin^{Cre}
(A-D) Coronary VSMC were examined using the *XlacZ4* (blue) in (A,B) whole mount and (C,D) sections of E17.5 (A) PDGFRβ$^{fl/+}$, (B) PDGFRβ$^{MKO/-}$, (C) PDGFRβ$^{MKO/+}$, and (D) PDGFRβ$^{MKO/-}$mice. (E,F) PECAM staining was used to identify vessels in the E17.5 (E) PDGFRβ$^{fl/+}$ and (F) PDGFRβ$^{MKO/-}$.

CHAPTER 3

A ROLE FOR THE PDGFRβ IN EFFICIENT EPICARDIAL TO MESENCHYMAL TRANSFORMATION

Introduction

The transition from an epithelial cell type to a mesenchymal cell type involves changes in cell morphology, motility, and transcription. This process, known as epithelial to mesenchymal transition (EMT), is important during development and has been implicated during pathological conditions such as fibrosis and metastasis (Batlle et al., 2000; Cano et al., 2000; Iwano et al., 2002). A complex configuration of signaling molecules including receptor tyrosine kinases (RTK), TGFβ receptors, and Wnt receptors, cooperate to reorganize the actin cytoskeleton, downregulate epithelial junctional proteins, and upregulate mesenchymal proteins. Although these EMT pathways have been studied in some developmental systems, including neural crest cell and somite delamination, relatively little is known about the EMT that occurs during the development of coronary blood vessels.

The formation of the coronary vasculature is essential for the development and function of the heart. Unlike other vascular structures that form from the differentiation of mesoderm derivatives, the coronary vessels originate from cells that bud off the septum transversum. These cells are identified as the proepicardium. In the mouse the proepicardial cells attach to the developing heart

tube initially as clusters, but then converge to form the epicardium, an epithelial sheet covering the entire myocardium, (Viragh and Challice, 1981). Some of these epicardial cells undergo the process of EMT to form the endothelial, smooth muscle, and fibroblasts of the heart (Dettman et al., 1998; Mikawa and Gourdie, 1996; Perez-Pomares et al., 1997; Poelmann et al., 1993). While disruption of genes essential for the formation of the epicardium leads to severe defects in coronary artery formation, few genes have been identified that are required during the process of EMT.

The role of the PDGFRβ in differentiated vascular smooth muscle cells (VSMC) is well established, and *PDGFRβ* and *PDGFB* null animals exhibit severe deficiencies in multiple vascular beds including the brain, eye, kidney, skin, and heart (Hellstrom et al., 1999; Leveen et al., 1994; Lindahl et al., 1998; Lindahl et al., 1997; Soriano, 1994b). Recent reports have suggested that in the avian system PDGFRβ expression occurs before VSMC differentiation (Van Den Akker et al., 2005) and that PDGFRβ signal transduction can induce the process of EMT (Yang et al., 2006). To investigate the function of the PDGFRβ in epicardial development, we have examined PDGFRβ null embryos and discovered that the receptor is not only required for formation of coronary VSMC but also at an earlier stage for efficient migration of epicardial cells into the subepicardial mesenchyme.

Material and Methods

Experimental animals

Wild type, PDGFRβ$^{+/-}$, PDGFRβ$^{F1/F1}$, PDGFRβ$^{F5/F5}$ and PDGFRβ$^{F7/F7}$ mice were maintained on a mixed C57Bl/6 X 129SV background. We used mice that were heterozygous for the XlacZ4 transgene to visualize pericyte populations (Tidhar et al., 2001). All animal experiments were approved by the Institutional Animal Care and Use Committee (IACUC) at the University of Texas Southwestern Medical Center and performed according to the Guide for the Care and Use of Laboratory Animals published by the NIH.

Cell culture

Primary epicardial cells were isolated from E11.5 hearts. Briefly, hearts were plated on rat-tail collagen in 15% FBS on glass bottom dishes. Hearts were removed at day 2. Scratch was made with P10 tip on day 4 after changing media to 5% FBS. Imaging was performed at 0 hours and 17 hours.

CCFSE

E13.5 hearts were isolated from the indicated strains. Hearts were incubated with 24μM CCFSE (Molecular Probes) in starvation media for 1 hour. Hearts were fixed in 4% PFA and embedded in OCT for frozen sections. Autofluorescence was quenched with 50mM NH_3Cl in TBS for 1 hour. DAPI was utilized for nuclear localization and slides were mounted in 1:1 glycerol:PBS.

β-galactosidase staining

Hearts were fixed in 2% formaldehyde 0.2% glutaraldehyde, washed with PBS and then incubated overnight at room temperature in 25µl of x-gal in N,N-Dimethyl Formamide per ml of staining stock (5mM $KFe(CN_2)_2$), 2mM $MgCl_2$, 0.3% Detergent, in PBS). For sections, hearts were embedded in paraffin. After sectioning hearts were counterstained with nuclear fast red and mounted with cytoseal.

Whole Mount Immunohistochemistry

Protocol adapted from Manipulating the Mouse Embryo for PECAM staining (Hogan, 1994). Hearts were fixed overnight in 4:1 Methanol:DMSO at 4°C. This was followed by 5-10 hours in 4:1:1 Methanol:DMSO;H_20_2 at 4°C and three 20 min washes in 1:1 Methanol:PBS were performed prior to placing hearts in PBS. Tissues were blocked for 2 hours in PBSMT (2% milk, 0.5% TritonX in PBS) and then incubated with 1:200 PECAM (BD Biosciences) overnight. Samples were washed 5 times for a total of 8 hours followed by 2 hours in 1:200 biotinylated anti rat (Vectashield anti rat kit). Overnight wash and 5 additional washes in PBT (0.5% TritonX in PBS) for at least 1 hour were followed by use of Vectastain ABC kit and developed with DAB (Vector Labs).

For phalloidin staining, samples were fixed 2 hr in 4% PFA. Hearts were permeabilized in 0.5% TritonX for 1.5 hours, then blocked with 1% BSA 0.5% TritonX for 1 hour and finally incubated with 1:200 dilution of Phalloidin488

(Molecular Probes). DAPI used for nuclear localization. Hearts were squash mounted.

Frozen Section Immunohistochemistry

Hearts were isolated from the embryo and then samples were fixed for 2 hours in 4% PFA, put in 30% sucrose overnight at 4°C and embedded in OCT. 0.5% TritonX was used to remove OCT. The following conditions were utilized for antigen retrieval, block and primary antibodies. For PDGFRβ staining: 1 hour block 3% NDS 0.5% TritonX, and 1:200 PDGFRβ (eBioscience) overnight. For BrdU: 30min 2N HCl in PBT at 37°C, 5 min 0.1M NaBorate pH8.5, 45 min block 3% NDS in 0.5% TritonX, 2 hours 1:50 BrdU (Becton Dickinson). For αSMA: 1hour block 3% BSA in 0.5% Tween, 2 hours 1:250 αSMA FITC (Sigma). For SMMHC: 1 hour block 3% BSA in 0.5% Tween, 2 hours 1:250 SMMHC (BTI). For PECAM: 1 hour block 3% BSA in 0.5% Tween, overnight 1:200 PECAM (BD Pharmingen). For collagen IV: 3% NGS 0.5% Tween 30min, 2 hours 1:500 collagen IV (Chemicon). For fibronectin: 3% NGS 0.5% Tween 30min, 2 hours 1:1000 (Sigma). For laminin: 3% NGS 0.5% Tween 30min, 2 hours 1:1000 (Sigma). For aPKC: 30 min block 5% FBS 0.1% TritonX, 1hour 1:300 aPKC (Santa Cruz) For phalloidin 488 (1:200, Molecular Probes). For β−catenin: 15min Tris EDTA 98°C, 30 min block 5% FBS 0.1% TritonX, 1 hour 1:500 β−catenin (BD Transduction). For ZO1: 1hour 5% FBS 0.1% TritonX, overnight 1:300 ZO1 (Zymed). For α4 integrin: 1hour 1% BSA 2% NDS,

overnight 1:200 α4integrin (Chemicon). For twist: 1 hour 5% FBS .1%TritonX, overnight 1:200 twist (Santa Cruz). For vimentin: 30 min block 5% FBS 0.1% TritonX, 1 hour 1:500 vimentin (Sigma). For Arp2/3: 30 min block 5% FBS 0.1% Triton, 1 hour 1:100 Arp2/3 (Upstate).

Proliferation Index

40x fields of view were used to quantitate the proliferation index. A box of a defined size was drawn in ImageJ and the number of BrdU positive cells and the number of DAPI stained nuclei was determined. 9 fields of view were used per sample. The index for each field of view was determined and then the average of the indexes was calculated.

Paraffin Sections

Hearts were isolated from the embryo and samples were fixed overnight in 4%PFA and embedded in paraffin. After sectioning slides were deparaffinized. For WT1 stain: 15 min at 97°C in Tris EDTA pH9, block 1%BSA 0.05%Tween, and 1:100 WT1 (DAKO) for 2 hours.

H&E staining was performed with standard protocol.

TEM

Hearts were isolated from the embryo and fixed in 2.5% glutaraldehyde in 0.1M Cacodylate buffer. Hearts were routinely processed for TEM.

Imaging

Confocal imaging was performed on the LSM510META (grant NIH 1-S10-RR019406-01). Fluorescent imaging utilized the Zeis Axiovert 200 with the Hamamatsu ORCA-ER camera and Open Lab. Color imaging of slides performed with the Zeis Axiovert 200 with the Olympus DP71 camera and DP software. Whole mount imaging used the Nikon SMZ1000 with either the Olympus DP71 camera or a Nikon digital camera. TEM images were taken on 1200 EX Electron Microscope.

Results

A role for PDGFRβ in coronary VSMC, endothelial vessel and myocardial development

Although PDGFRβ signaling is an established requirement for VSMC proliferation in multiple tissues, it is not understood why only some VSMC populations are affected in the *PDGFRβ* and *PDGFB* null animals. Coronary VSMC are of particular interest because of their unique origin in comparison to other VSMC. Previously, it has been reported that the α smooth muscle actin (αSMA) positive VMSC of the coronary arteries were reduced in the *PDGFB* and *PDGFRβ* null embryos (Hellstrom et al., 1999). To obtain quantitative data for this reduction, we crossed mice bearing the *PDGFRβ* null allele to the *XlacZ4* mouse line. *XlacZ4* mice express a nuclear localized β-galactosidase protein in VSMC (Tidhar et al., 2001), including those derived from the epicardium. In

wild type hearts, a few XlacZ4-positive cells were observed as early as E14.5 (data not shown), and by E15.5 numerous cells were identified on the heart surface (Figure 3.1A). A majority of cells were present in close proximity to the nascent coronary vessels, while single cells were found scattered on the surface as well as within the ventricles of the heart (Figure 3.1A and data not shown). In comparison, PDGFRβ null hearts contained no XlacZ4-positive cells (Figure 3.1B). Remarkably, even at E17.5 PDGFRβ$^{-/-}$ hearts did not possess a single β-galactosidase positive cell along the heart surface or within the ventricles (Figure 3.1D and data not shown). In contrast, abundant VSMC were present in wild type hearts both along the major coronary arteries as well as scattered along vessels within the ventricles (Figure 3.1C and data not shown). In the mutant hearts a few β-galactosidase positive cells were observed in the aortic arch, but these cells may have been neural crest in origin based on their location (Jiang et al., 2000). The complete loss of a population of VSMC in the heart suggested a more global requirement for PDGFRβ signaling in the coronary vasculature than a failure in VSMC proliferation.

During development, coronary VSMC and endothelial cells arise from an extracardiac source, although it is currently a matter of debate in the avian heart whether both cell types arise directly from the proepicardium (Perez-Pomares et al., 2002; Poelmann et al., 1993). Nonetheless, several models of epicardial disruption have an associated disruption of the endothelial vessels (Shikama et al.,

2003; Tevosian et al., 2000). The defects in the coronary VSMC in the PDGFRβ$^{-/-}$ caused us to examine the formation of the coronary arteries in more detail. One potential explanation for a failure of coronary vascular remodeling is lack of coronary vessel attachment to the aorta. This process occurs around E13.5 and disruption leads to aberrant coronary vessels. The examination of sections through a PDGFRβ$^{-/-}$ heart at E15.5 was consistent with the presence of coronary vessels that invaginate into the aorta and at E17.5 coronary vessels could still be discerned (Sfig 3.1). However, when whole mount PECAM staining was performed to identify the endothelial cells of hearts, the staining demonstrated that mutant hearts failed to form a mature vascular network on the ventral surface compared to wild type controls from E14.5 to E17.5 (Figure 3.1 E and F and data not shown). In wild type hearts the left coronary artery could be identified as the major vessel on the ventral surface, while in the PDGFRβ null heart clusters of endothelial cells and a primitive endothelial plexus were present. No dominant coronary vessel formation was observed on the ventral surface. The punctate pattern of PECAM staining was similar to epicardial defects observed in a thymosin β4 deficient hearts (Smart et al., 2007), and QH-1 staining observed in immature, quail coronary vasculature (Kattan et al., 2004). An additional characteristic that has been described with defective epicardial formation and/or function is a reduction in the thickness of the myocardial wall. Though not as severe as the defects that have been observed in other epicardial mutants (Moore

et al., 1999; Tevosian et al., 2000; Yang et al., 1995), the compact zone of the myocardium in the PDGFRβ null hearts was thinner than the wild type myocardium at several developmental stages (Figure 3.1G-J, Figure 3.2 and data not shown). This defect was consistent with previous observations in the *PDGFB* null hearts (Leveen et al., 1994).

To evaluate both the endothelial and VSMC populations more closely, we analyzed sections through E17.5 hearts by immunohistochemistry for PECAM and two other VSMC markers, smooth muscle myosin heavy chain (SM-MHC) and αSMA. SM-MHC is a marker exclusive to smooth muscle and stains small arterioles in the heart (Miano et al., 1994) while αSMA is expressed in VSMC, skeletal, and cardiac myocytes prior to birth (Woodcock-Mitchell et al., 1988). Although endothelial vessels were present throughout the PDGFRβ null myocardium, most were increased in diameter compared to that observed in the wild type hearts (Figure 3.1K-N). This result was consistent with previous results observed in brain vasculature in PDGFB and PDGFRβ null embryos (Hellstrom et al., 2001). Similar to the results that we obtained with XlacZ4 marker, we found no αSMA-positive cells in close association with endothelial vessels, although some αSMA expression remained in the cardiomyocytes (Figure 3.1 K and L). Results from SM-MHC demonstrated that a few SM-MHC-expressing cells were present in the mutant heart but the quantity of cells was greatly reduced compared to that present in the wild type (Figure 3.1M and N). These data

demonstrate that while PDGFRβ signaling did affect the overall formation of coronary VSMC and endothelial vessel patterning, endothelial cell differentiation was not disrupted.

Expression of PDGFRβ during coronary VSMC development

To identify when PDGFRβ expression begins in the development of the heart, we examined wild type embryos at various stages of development. Unlike many other VSMC that form from the dorsal aorta, lateral plate mesoderm or splanchnic mesoderm (Esner et al., 2006; Gerhardt and Betsholtz, 2003; Wilm et al., 2005) the VSMC that form in the heart are derived from a cell population that buds off the septum transversum. The population is referred to as the proepicardium. The proepicardium attaches to the dorsal aspect of the heart tube at E9.5 and in the mouse spreads as clusters of cells in a radial pattern, towards the lateral and ventral surface of the heart (Viragh and Challice, 1981) (Barnett 2004). As the cells cover the myocardium, they flatten and become the epicardium. Simultaneously, some of the epicardial cells undergo an epithelial to mesenchymal transition and migrate into the space between the epicardium and the myocardium. These cells comprise the subepicardial mesenchyme. Finally, this undifferentiated mesenchyme can differentiate into endothelial cells, VSMC or fibroblasts. We examined PDGFRβ expression throughout coronary vascular development and found that the PDGFRβ was expressed at each developmental

stage. Consistent with chick expression studies, the PDGFRβ was present in the proepicardium (data not shown). At E12.5, when the epicardium is formed we observe PDGFRβ in all cells of the epicardium (Figure 3.1 O). At E15.5 we also found PDGFRβ expression in the epicardium as well as the subepicardial mesenchyme and cells surrounding endothelial vessels (Figure 3.1 P). By E17.5 the PDGFRβ expression was reduced in the epicardium and the majority of positive cells appear near vessels (Figure 3.1 Q). These data support the possibility that PDGFRβ signaling may have an early role in coronary VSMC development and be involved during the establishment, maintenance, or the transition of the epithelium to a mesenchymal cell population.

Epicardial and subepicardial formation in the PDGFRβ$^{-/-}$

Because PDGFRβ expression was detected in the proepicardium we examined the formation and attachment of the proepicardium to the heart tube in wild type and mutant animals. To aid in the visualization of the proepicardium and the epicardium, we crossed the PDGFRβ null animals to mice that possessed a targeted insertion of the lacZ gene at the capsulin locus. Capsulin (Pod1, epicardin) is a bHLH transcription factor expressed in the proepicardium, epicardium, podocytes and facial mesenchyme (Hidai et al., 1998; Lu et al., 1998; Robb et al., 1998). In Figure 3.2 A and B we demonstrate, using the capsulin^{LacZ} tag for proepicardial derived cells, that proepicardial formation, attachment and

spreading over the myocardium occurred normally in PDGFRβ mutant embryos. At 9.5 in both mutant and wild type embryos, cells are budding off of the septum transversum and can be seen attaching to the surface of the heart tube. After proepicardial cells attach they begin spreading over the surface of the heart. This process continues until the heart is covered at around E13.5 (data not shown). In both mutant and wild type hearts at E13.5 the heart was covered by capsulin positive cells except for some patchy areas on the ventral surface of the right ventricle. Thus we did not observe any differences between the mutant and wild type hearts with regards to spreading of the epicardium. This suggests that both the migration and proliferation of the proepicardium occur normally in the absence of PDGFRβ signaling.

Although PDGFRβ null epicardial cells covered the entire surface of the heart, at E14.5 we observed irregular clusters of cells in the mutant heart compared to that observed in the wild type (Figure 3.2 C and D). To further evaluate potential irregularities in the epicardium, we compared mutant and wild type capsulin^{LacZ} tagged hearts in cross section and demonstrated a reduction in the number of flattened epicardial cells along the surface of the myocardium as well as a decrease in cells entering the subepicardial mesenchyme (Figure 3.2 E-L). Interestingly, using the capsulin^{LacZ} marker capsulin positive cells can be seen migrating as waves further into the ventricles of the heart. At both E14.5 and E15.5 fewer β-galactosidase positive cells were present in the mutant than in the

wild type. In addition, the cells that were present were distributed more sparsely than that observed in the wild type.

To verify the decreased number of cells entering the subepicardial space, we used an additional marker, WT-1 (Figure 3.2 M-T). WT-1 is a winged helix transcription factor that is expressed by the cells of the epicardium and subepicardial mesenchyme and is down regulated as these cells begin to differentiate (Moore et al., 1999). We observed a marked decrease in WT-1 positive cells in the subepicardial space of the PDGFRβ null hearts compared to that observed in the wild type control. These data demonstrate that loss of PDGFRβ signaling leads to a reduction in cells entering the subepicardial space. This reduction is consistent with an early role for PDGFRβ during the population or expansion of the subepicardial mesenchyme, in addition to its established role of inducing proliferation and migration of differentiated VSMC.

Proliferation and apoptosis of the subepicardial mesenchyme

To investigate if loss of PDGFRβ signaling leads to a reduction in the proliferation of the subepicardial mesenchyme we performed BrdU staining on mutant and wild type hearts at E14.5. In mutant and wild type hearts we observed similar numbers of proliferating cells in both the myocardial and the subepicardial space (Sfigure 3.2 A,B). Specifically, the wild type had 0.24 +/- 0.05 BrdU positive cells/ total nuclei and the PDGFRβ$^{-/-}$ exhibited a comparable 0.24 +/-

0.04 BrdU positive cells/total nuclei. These data demonstrate that there was no overt defect in proliferation. Because increased apoptosis could also explain the loss of mesenchymal cells in the subepicardial space, we performed TUNEL analysis on both whole mount and sections of PDGFRβ$^{-/-}$ and wild type hearts and observed very little apoptotic cells in the hearts at E13.5 and E14.5 (Sfigure 3.2 C,D and data not shown). Taken together these results indicate that the defect we observed in the formation of the subepicardial space was not caused by a reduction in proliferation or an increase in the apoptosis.

A role for PDGFRβ in EMT

Several recent papers have suggested that PDGFRβ may play an important role in the EMT process. Recent reports demonstrate that PDGFRβ signaling can induce β-catenin nuclear localization (Theisen et al., 2007; Yang et al., 2006). Others have shown that PDGFRβ signaling is involved in tumor EMT and metastasis (Fischer et al., 2007; Jechlinger et al., 2006). We stimulated E13.5 hearts ex vivo to determine if PDGF treatment would accelerate epicardial EMT.

Carboxyfluorescein (CCFSE) was used to follow the epicardial cell migration into the subepicardial space. CCFSE is a vital, lipophilic dye that incorporates into the cell membrane. When hearts are cultured in CCFSE, the epicardial cell surface is specifically labeled, the dye does not pass through the basement membrane, and the fluorescence can be used to follow the epicardial

cells as they undergo EMT ((Morabito et al., 2001) and Figure 3.3 A-D). We cultured hearts from PDGFRβ null and wild type embryos in media containing either PDGFBB or serum. Figure 3.3 A-D shows the results from these experiments. When wild type hearts were cultured in 10% FBS, an abundant number of dye-labeled cells were observed in the subepicardial mesenchyme (Figure 3.3 A). In contrast, when PDGFRβ null hearts were cultured under the same conditions few cells were observed entering the subepicardial space (Figure 3.3 B). These data suggested that in the absence of PDGFRβ signaling growth factors in the serum were not able to stimulate movement into the myocardium. Conversely, we tested whether PDGFBB stimulation was sufficient to induce epicardial migration. PDGFBB stimulation (Figure 3.3D) resulted in epicardial migration in wild type hearts over vehicle (Figure 3.3C). These results demonstrated that signals through the PDGFRβ could result in increased epicardial migration and that loss of the PDGFRβ lead to a reduced efficiency of epicardial derived cells entering the subepicardial space.

To further evaluate the efficiency of epicardial cell movements in vitro, we evaluated the ability of the PDGFRβ to induce migration of cultured epicardial with a scratch assay (Figure 3.3 E-H). Consistent with our results ex vivo we saw an increase in the distance that the epicardial cells traveled from time 0 (Figure 3.3 E,G) to 17 hours (Figure 3.3 F,H) when stimulated with PDGFBB (Figure 3.3 H) as opposed to vehicle (Figure 3.3 F). These results substantiate a role for the

PDGFRβ in promoting the cellular processes involved in the migration of epicardial cells.

Cellular morphology in the PDGFRβ$^{-/-}$

To further investigate the nature of the role of PDGFRβ in the epicardium we examined its ultrastructure at E13.5 and E14.5 (Figure 3.4 and data not shown). Similar to what we observed with normal histology TEM confirmed that the epicardial cells in the PDGFRβ null embryos (Figure 3.4 B,D,F,H) had abnormal morphology compared to wild type (Figure 3.4 A,C,E,G). Along both the right and left ventricle surfaces null epicardial cells frequently failed to flatten and extend along the myocardium. In contrast, wild type epicardial cells were aligned as a sheet along the myocardial surface. Occasionally, rounded cells were observed in wild type hearts but these were rare in occurrence compared to the number of rounded cells that were observed in the PDGFRβ null hearts. Taken together these data suggested that signals through the PDGFRβ may be required for cytoskeletal rearrangement of cells that have received an EMT signal and loss of this signal caused a failure in directed migration and these cells remain at the surface.

Cellular Adhesion and ECM

The data is suggestive of a failure of cytoskeletal rearrangements resulting in a failed migration; however, it is also possible that the abnormal ultrastructure

of the epicardial cells in the PDGFRβ$^{-/-}$ is due to a lack of extracellular matrix to which the cells can adhere or from the inability of the epicardial cells to form intercellular junctions. The epicardium is separated from the myocardium by a layer consisting of several matrix molecules, including fibronectin, laminin and type IV collagen (Kalman et al., 1995). Thus we compared the expression profiles of these matrix proteins in wild type (Sfigure 3.3 A,B,E,F, I, J) and PDGFRβ$^{-/-}$ (Sfigure 3.3 C,D,G,H, K,L) hearts. Fibronectin, laminin and collagen IV were all present in the PDGFRβ$^{-/-}$. This suggested that there was not a loss of extracellular matrix. To assess the adhesion of the epicardium to the underlying myocardium we examined α4 integrin expression since it is expressed by the proepicardium and binds to a receptor, VCAM, which is expressed by the myocardium. Our results showed that the loss of PDGFRβ did not result in a decrease in α4 integrin expression and was therefore not the likely source of our phenotype (Sfigure 3.3 M-P). We also examined the expression of β−catenin (Sfigure 3.3 Q-T) and ZO1 (Sfigure 3.3 U-X) to confirm our TEM results, which had suggested that intercellular junctions were present in the PDGFRβ$^{-/-}$ (Figure 3,4 and data not shown). These proteins are associated with epithelial junctions and in both the wild type (Sfigure 3.3 Q,R,U,V) and the PDGFRβ$^{-/-}$ (Sfigure 3.3 S,T,W,X) epicardium, ZO1 and β-catenin appeared to be present at the point of cellular contact. Therefore the components appear to be present for the proper

adhesion of the epicardial cells to the myocardium and to each other despite slight differences in staining patterns.

Cytoskeletal rearrangements and polarized migration

To further investigate how the loss of PDGFRβ signaling resulted in inefficient EMT we examined PDGFRβ$^{-/-}$ hearts for the ability of the epicardium to induce the necessary transcriptional changes. We investigated whether there was appropriate transcriptional upregulation of mesenchyal proteins by evaluation of vimentin expression. The presence of vimentin staining in the PDGFRβ$^{-/-}$ suggested that these cells were able to turn on mesenchymal proteins (Sfigure 3.4 E-H). Moreover, the persistent expression of vimentin in the epicardium of PDGFRβ$^{-/-}$ compared to wild type was consistent with an inefficient epicardial migration.

We also examined the ability of the cytoskeleton to reorganize and form a polarized epithelium. Phalloidin was utilized to visualize actin organization at E14.5 in both whole mount hearts and sections (Figure 3.5 A-D). In wild type hearts actin was localized to the basal surface of the epicardial cells (Figure 3.5 A,C,E). However, in PDGFRβ$^{-/-}$ hearts there was a large increase in the number of rounded epicardial cells with a subcortical actin distribution, which is characteristic of the immature epicardial cells that have not flattened over the myocardium nor migrated into the subepicardial mesenchyme (Figure 3.5 B,D,F).

In addition, the PDGFRβ$^{-/-}$ epicardium had a slightly greater proportion of cells in which aPKC was distributed in a uniform pattern around the circumference of the cell (Sfigure 3.4 A-D). The lack of either cytoskeletal rearrangement or polarization of these cells combined with the decreased formation of subepicardial mesenchyme, suggested that the EMT process was not completed and that a subpopulation of epicardial cells were caught at the surface of the heart.

To continue this line of anaylsis, we examined the expression of Arp2/3, which is responsible for nucleated atin filaments. Arp2/3 is thus the downstream target of several signaling pathways that are involved in cytoskeletal rearrangements. Interestingly, in the wild type mice there is an induction of Arp2/3 localization to the cell membrane beginning at E13.5 (Sfigure 3.5). This subcortical distribution becomes more prevelant in the wild type subepicardial mesenchyme at E14.5 (Figure 3.5 G,I). The localization of Arp2/3 to the membrane would allow it to initiate the formation of new actin filaments, which are important for cytoskeletal rearrangements. However, in the PDGFRβ$^{-/-}$ at E13.5 the Arp2/3 does not appear to localize to the membrane and is only present in epicardium as opposed to the subepicardial mesenchyme (Sfigure 3.5). Furthermore, PDGFRβ$^{-/-}$ hearts at E14.5 (Figure 3.5 H,J) have very few cells with the membrane localized Arp2/3. This, in combination with the rest of our data, suggests that the PDGFRβ is important in the mediating the cytoskeletal

rearrangements that are necessary for epicardial cells to efficiently migrate into the myocardium.

Responsible signaling pathways downstream of PDGFRβ

Several signaling pathways downstream of PDGFRβ have been linked to cytoskeletal rearrangements and cell migration. To understand which signals are important in our system we utilized a series of mice that have tyrosine to phenylalanine point mutations in the cytoplasmic tail of PDGFRβ (Tallquist et al., 2003). These point mutations ablate the ability of the receptor to signal through the PI3K pathway (PDGFRβ$^{F2/F2}$), the PI3K, RasGAP, Shp2, and PLCy pathways (PDGFRβ$^{F5/F5}$), or the Src, Grb2, PI3K, RasGAP, Shp2 and PLCy pathways (PDGFRβ$^{F7/F7}$). Thus these mice allow us to dissect out the relevant signaling pathways in vivo.

We initially focused on the formation of the subepicardial mesenchyme through examination of WT1 staining in the PDGFRβ$^{F2/F2}$, the PDGFRβ$^{F5/F5}$, and the PDGFRβ$^{F7/F7}$ at E15.5 (Figure 3.6). The PDGFRβ$^{F7/F7}$ exhibited a large decrease in WT1 staining that was comparable to that observed in the PDGFRβ$^{-/-}$ (Figure 3.6 and Figure 3.2). Therefore we compared the PDGFRβ$^{F2/F2}$ and the PDGFRβ$^{F5/F5}$ to the PDGFRβ$^{F7/F7}$ to evaluate the role of the PI3K and Src pathways. These two pathways have been implicated in EMT or more broadly with cytoskeletal rearrangement and migration. When the PI3K site was mutated

in the PDGFRβ$^{F2/F2}$ there was only a small decrease in the number of WT1 cells in the subepicardial mesenchyme compared to wild type. This did not recaptitulate the results of the PDGFRβ$^{F7/F7}$. Therefore, the PI3K pathway did not appear to be the primary pathway responsible for the PDGFRβ$^{F7/F7}$ phenotype. We then compared the PDGFRβ$^{F5/F5}$ to the PDGFRβ$^{F7/F7}$ to assess whether allowing the receptor to signal through the Src and Grb2 pathways would rescue the PDGFRβ$^{F7/F7}$ phenotype. Interestingly, since the formation of the subepicardial mesenchyme in the PDGFRβ$^{F5/F5}$ was comparable to the wild type heart, the Src and Grb2 pathways appear to be essential for proper formation of the subepicardial mesenchyme.

To further assess the role of PDGFRβ signaling pathways in epicardial cytoskeletal rearrangement and migration we evaluated phalloidin and Arp2/3 localization in PDGFRβ$^{F2/F2}$, PDGFRβ$^{F5/F5}$ and PDGFRβ$^{F7/F7}$ hearts (Figure 3.7). Consistent with our WT1 findings, the PDGFRβ$^{F7/F7}$ resembled a slightly less severe PDGFRβ$^{-/-}$ with an increased incidence of epicardial cells containing a subcortical distribution of actin. However, cells with this actin distribution were not present in PDGFRβ$^{F2/F2}$ or PDGFRβ$^{F5/F5}$ hearts. Moreover, although PDGFRβ$^{F2/F2}$ had the most prominent Arp2/3 staining, there was a greater prevalence of cells containing membrane localized Arp2/3 in the subepicardial mesenchyme of the PDGFRβ$^{F5/F5}$ compared to the PDGFRβ$^{F7/F7}$. Therefore the

Src pathway appears to be important in allowing PDGFRβ to mediating the majority of its function in the epicardium.

Discussion

Several studies have highlighted the emerging importance of the epicardium. The epicardium is essential for the formation of the coronary vasculature since the VSMC, fibroblasts and potentially endothelial cells originate from this cell population. Various mouse models have illustrated that the inability of the epicardium to form and/or function properly results in the loss or aberrant development of these cell lineages. In addition, the communication between the epicardium and myocardium is essential for the proper development of the myocardium. Moreover, recent studies in zebrafish have further demonstrated that the epicardium has a role in heart regeneration following injury (Lepilina et al., 2006).

Previous reports have suggested a possible role for the PDGFRβ in the epicardium based on localization. Expression analysis in chick revealed that the PDGFRβ was expressed in the proepicardial organ (Van Den Akker et al., 2005). Studies in the mouse revealed that the receptor and its ligand were present in the epicardium (Ponten et al., 2005). Our results confirmed that the PDGFRβ was in the proper location to affect epicardial function and further established a role for

the PDGFRβ in the ability of the epicardium to efficiently form the subepicardial mesenchyme.

There are several steps for the epicardial cells to undertake to complete the EMT that is necessary for the formation of the subepicardial mesenchyme. There are transcriptional changes, loss of junctions, cytoskeletal rearrangements, and the migration of the cells into the myocardium. A recent analysis in an epithelial cancer cell line demonstrated that PDGF signaling could induce EMT through the stimulation of β−catenin nuclear localization (Yang et al., 2006). Our results do not exclude this possibility in the epicardium, but point to an additional role for PDGF signaling in EMT. More specifically, in our system it appears that in the absence of the PDGFRβ a proportion of cells are poised to undergo EMT, but are unable to complete the cytoskeletal rearrangements that are involved in the migration of the epicardial cells into the subepicardial region.

It is well established that PDGF signaling has an important role in cytoskeletal rearrangements and migration in several cell types. We do not believe that this is a failure of chemotaxis. The exquisite expression of the ligand in the epicardium (Ponten et al., 2005) is more consistent with the activation of the cytoskeletal changes rather than a chemoattractant. Additionally, in the CCFSE experiment the epicardial cells migrated into the myocardium although the ligand was localized outside of the heart. In fact, the altered cellular structure and the subcortical actin distribution are consistent with a lack of cytoskeletal

rearrangements necessary for migration. Moreover, the defect in cytoskeletal rearrangements appears to be the result of an inability to properly localize Arp2/3. The membrane localization potentially represents an activation of Arp2/3 in vivo Arp2/3 is a complex that promotes actin nucleation at sites of cytoskeletal rearrangement and therefore is the direct target of several signaling molecules, including WASP, WAVE and cortactin.

Several of the pathways downstream of the PDGFRβ can potentially converge on the activation of Arp2/3. The tyrosine to phenylalanine point mutants provided a unique opportunity to delineate which signaling pathway(s) are important for PDGFRβ signaling in the epicardium in vivo. The apparent rescue of the phenotype when the PDGFRβ is able to signal through only the Src and Grb2 sites suggest that these pathways are of particular importance and are in line with recent studies showing the activation of Arp2/3 mediated by Src's activation of cortactin.

Although our results reveal the importance of the PDGFRβ in the cytoskeletal rearrangements of the epicardium, it is important to note that there was a reduction of the subepicardial mesenchyme rather than a complete loss of this cell population as we observe with the coronary VSMC. One potential reason is that the PDGFRβ is affecting a subpopulation of the epicardium. The differential staining pattern of two subepicardial mesenchyme markers, capsulin and WT1, is consistent with the presence of multiple cell populations. It is

possible that the PDGFRβ is uniquely affecting the population that becomes the VSMC and not altering the fibroblast population, which highlights the importance of assessing multiple markers in the evaluation of the subepicardial mesenchyme. It is also possible that PDGFRβ affects all the epicardial cells equally, but a subpopulation of the cells receives additional signals that can circumvent the loss of PDGFRβ. Finally, PDGFRβ could be exerting its effect at multiple time points along the development of the coronary VSMC. The compounded diminishment of the subepicardial mesenchyme with another defect at a later developmental stage could result in the loss of the VSMC with only a reduction in subepicardial mesenchyme.

In conclusion, we have demonstrated a novel role for the PDGFRβ in vivo and identified associated signaling pathways. In addition, our studies provide a framework for future epicardial work through its in vivo assessment of multiple markers that have previously been utilized in vitro. These findings are important for understanding the process of epicardial EMT, but may also have wider applicability to potential cancer models in which cells express PDGFRβ and undergo EMT.

Figures

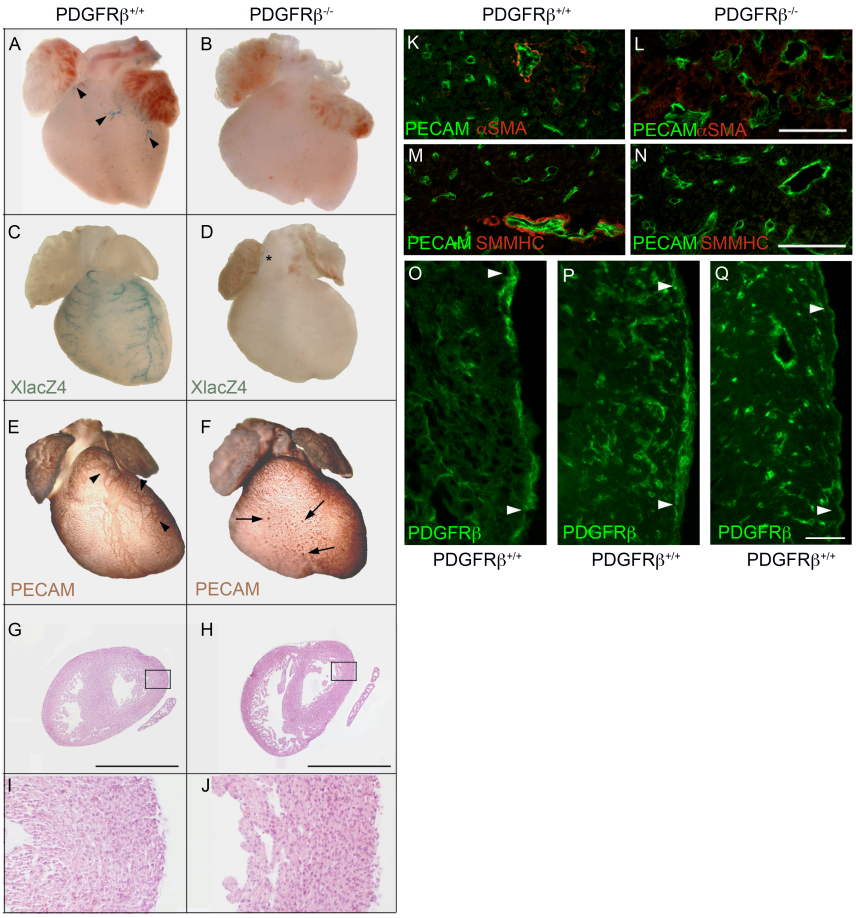

Figure 3.1 Early Role for the PDGFRβ in CVSMC Development
The number of pericytes present in the heart at (A,B) E15.5 and (C,D) E17.5 were examined in the (A,C) PDGFRβ$^{+/+}$ and the (B,D) PDGFRβ$^{-/-}$ using the *XlacZ4* mice, which express β-galactosidase in pericytes (blue). (E,F) Whole mount PECAM immunohistochemistry was utilized to examine endothelial vessel formation in the E17.5 (E) PDGFRβ$^{+/+}$ and (F) PDGFRβ$^{-/-}$ heart. Black arrowheads demarcate the remodeled vessels. Black arrows highlight the punctate PECAM staining. (G-J) H&E staining of a (G,I) PDGFRβ$^{+/-}$ and (H,J) PDGFRβ$^{-/-}$heart. Boxed areas indicate the area of magnification (I,J). (K-N) Sections through E17.5 (K,M) PDGFRβ$^{+/+}$ and (L,N) PDGFRβ$^{-/-}$ hearts stained for (K-N) PECAM (green) and either (K,L) αSM actin (red) or (M,N) SM myosin heavy chain (SMMHC)(red). (O) E12.5, (P) E15.5 and (Q) E17.5 heart sections stained with PDGFRβ (green). White arrowheads discern the edge of the epicardium.

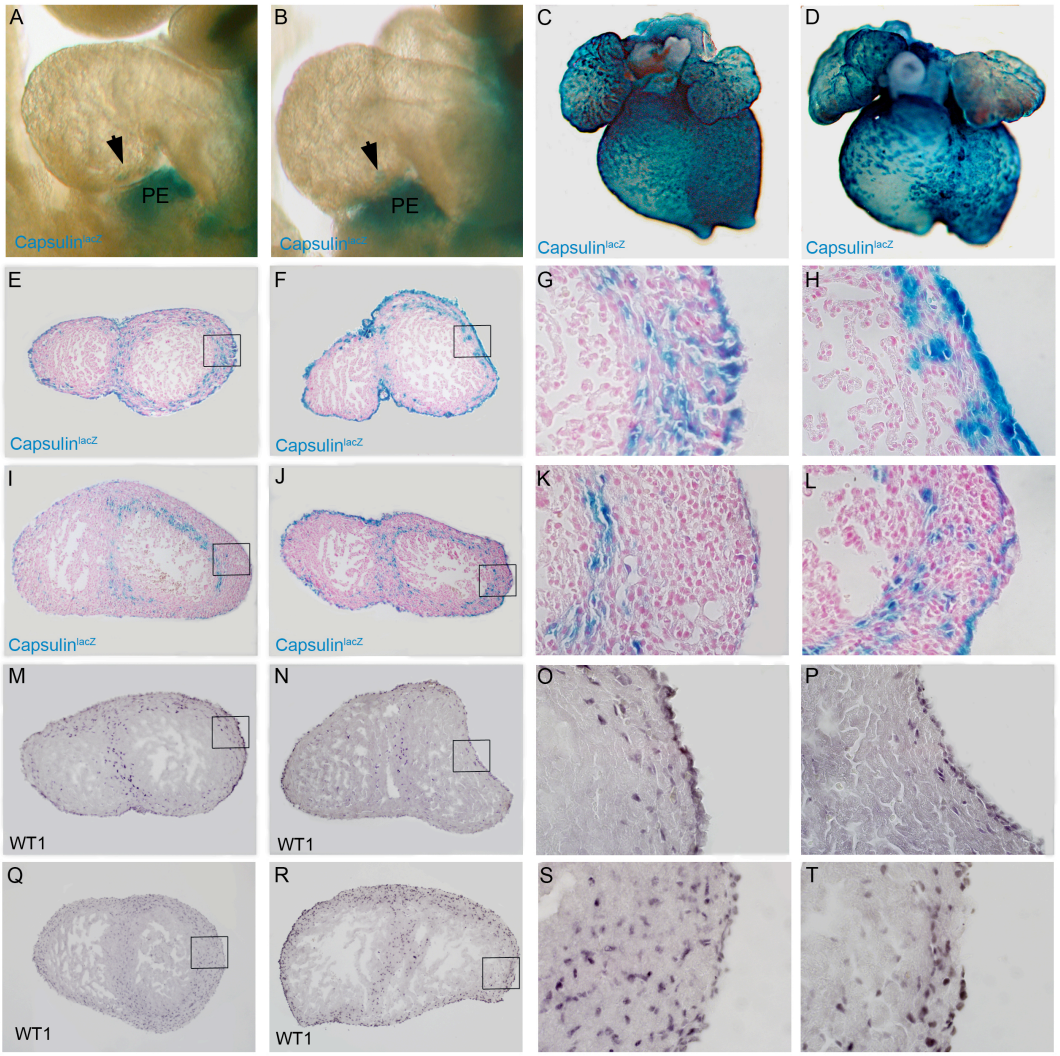

Figure 3.2 Decreased Formation of Subepicardial Mesenchyme in the PDGFRβ$^{-/-}$

(A,B) The proepicardium (PE) of E9.5 (A) PDGFRβ$^{+/+}$ and (B) PDGFRβ$^{-/-}$ embryos was identified with the capsulin^{lacZ} tag (blue). Arrowheads point to proepicardial cells that have attached to the dorsal surface of the heart. At later stages (C,D) epicardial cells on the surface of the E14.5 (C) PDGFRβ$^{+/+}$ and (D) PDGFRβ$^{-/-}$ heart are also identified with the capsulin^{lacZ} (blue). (E-H) Sections through a (E-H) E14.5 and (I-L) E15.5 (E,G,I,K) PDGFRβ$^{+/+}$ and (F,H,J,L) PDGFRβ$^{-/-}$ capsulin^{lacZ} (blue) hearts were counterstained with nuclear fast red. (M-T) WT1 staining (black) of (M-P) E14.5 and (Q-T) E15.5 (M,O,Q,S) PDGFRβ$^{+/+}$ and (N,P,R,T) PDGFRβ$^{-/-}$ heart sections. Boxes define the areas of magnification for the corresponding sections.

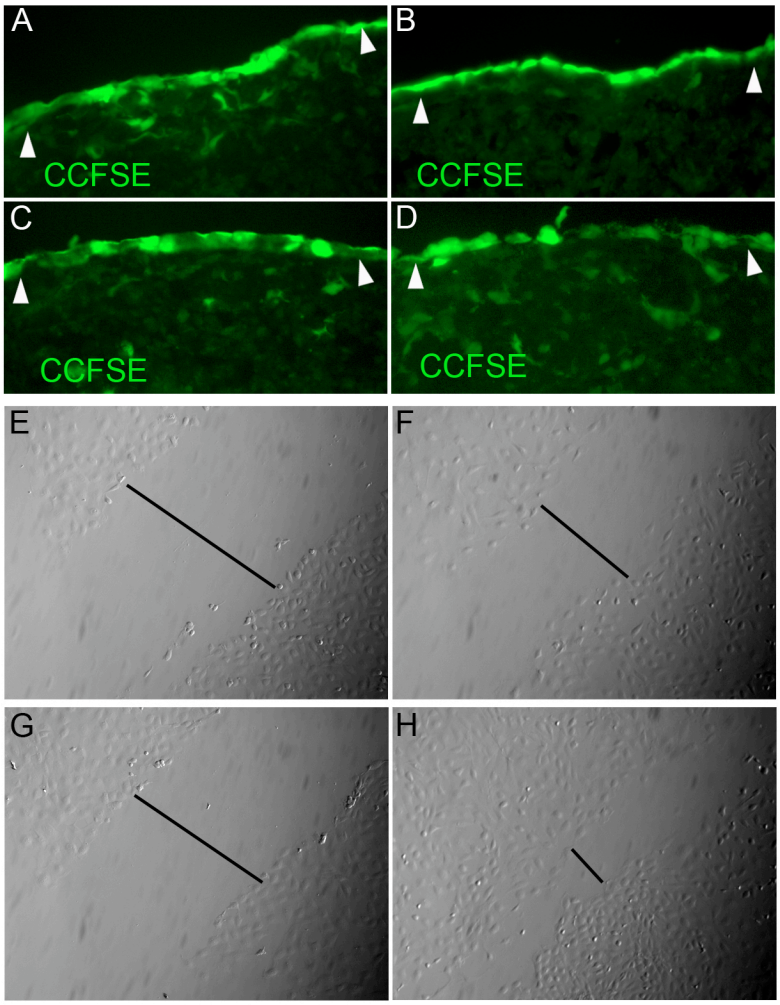

Figure 3.3 Importance of PDGFRβ in the Migration of Epicardial Cells
(A-D) EMT was monitored ex vivo using CCFSE (green) to trace epicardial cells as they undergo EMT and migrate into the myocardium. E13.5 (A) wild type and (B) PDGFRβ$^{-/-}$ hearts were cultured ex vivo in the presence of 10%FBS for two days. E13.5 (C,D) wild type hearts were also cultured for two days in (C) the absence and (D) presence of PDGFBB. Arrowheads mark the epicardial boundary. (E-H) Cultures of primary epicardial cells were monitored for their ability to migrate in the absence (F) and presence of (H) PDGFBB. Cell location was assessed at (E,G) time 0 and at (F,H) 17 hours. Black lines run between the edges of the scratch in each epicardial culture.

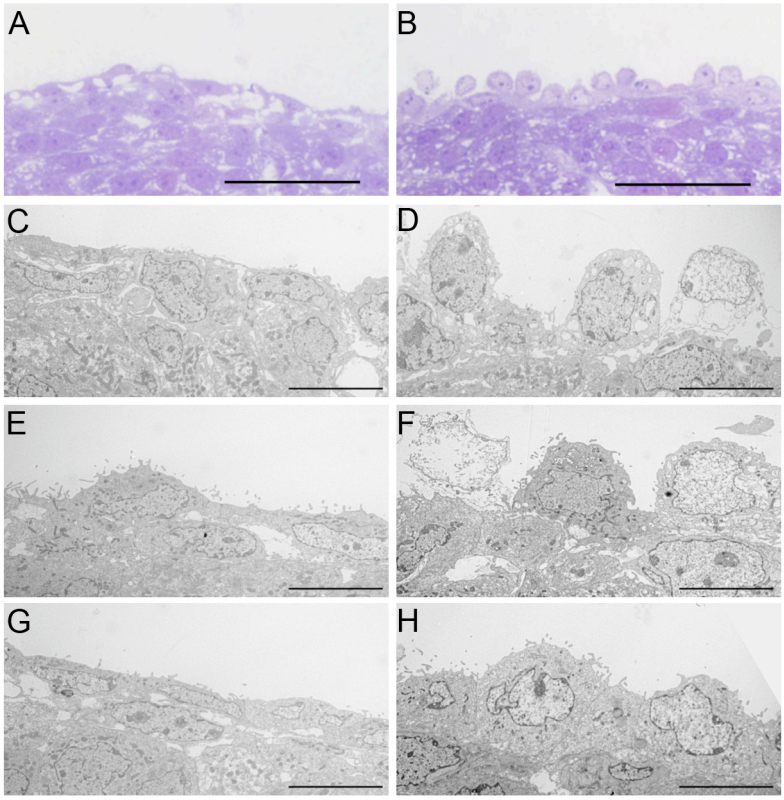

Figure 3.4 Altered Ultrastucture of the Epicardium in the PDGFRβ$^{-/-}$
(A,B) Thick sections of E13.5 (A) wild type and (B) PDGFRβ$^{-/-}$ hearts were processed for TEM and then imaged on a light microscope. Scale = 0.025mm. (C-H) Subsequent thin sections from the same samples were imaged with TEM. Three fields of view of (C,E,G) wild type and (D,F,H) PDGFRβ$^{-/-}$ hearts are shown. TEM Scale = 10 microns.

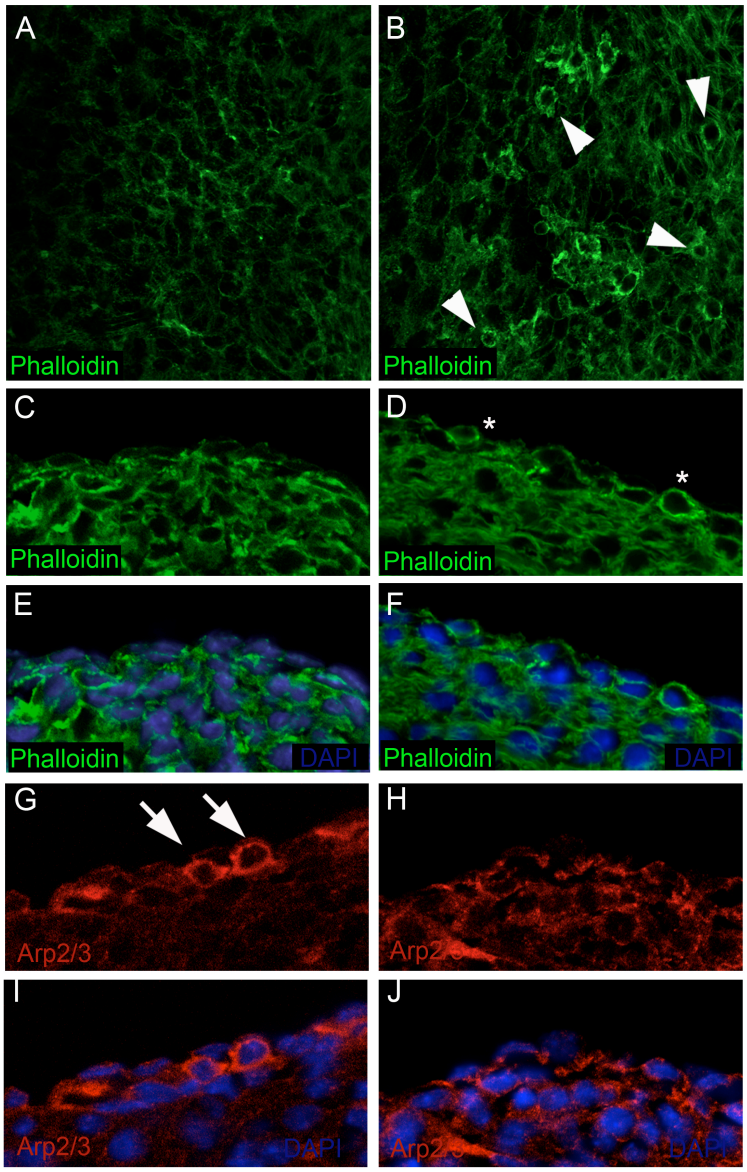

Figure 3.5 Inability of Cells to Complete EMT
(A,B) Whole mount labeling of actin on the (A) PDGFRβ$^{+/+}$ and (B) PDGFRβ$^{-/-}$ ventral heart surface at E14.5 was performed with phalloidin (green). Arrowheads highlight some of the cells on the surface of the heart that display a subcortical actin distribution. (C-F) Sections through an E14.5 heart were also utilized to evaluate phalloidin (green) in the epicardium of (C,E) PDGFRβ$^{+/+}$ and (D,F) PDGFRβ$^{-/-}$ hearts. The astericks point to rounded epicardial cells containing a subcortical actin distribution. (G-J) Arp2/3 staining (red) was performed on E14.5 (G,I) PDGFRβ$^{+/+}$ and (H,J) PDGFRβ$^{-/-}$ heart sections. Arrows mark Arp2/3 positive cells. All sections are shown (E,F,I,J) with and (C,D,G,H) without DAPI overlay.

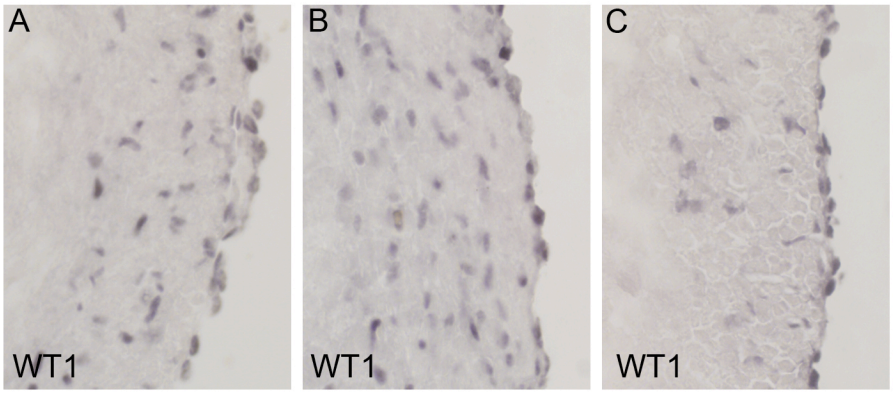

Figure 3.6 WT1 Expression in PDGFRβ Signaling Mutants
WT1 staining was performed at E15.5. Heart sections through the left ventricle of (A) PDGFRβ$^{F2/F2}$, (B) PDGFRβ$^{F5/F5}$ and (C) PDGFRβ$^{F7/F7}$ were examined.

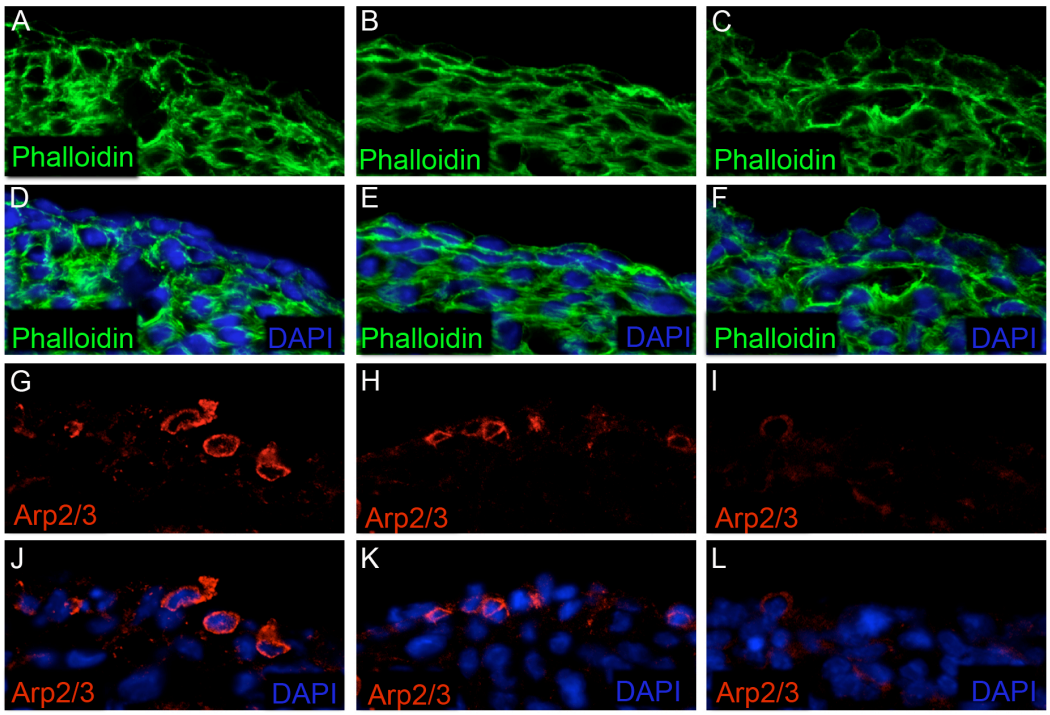

Figure 3.7 Importance of Src in Completing EMT
(A-F) Phalloidin (green) is utilized to image actin organization in sections through an E14.5 (A,D) PDGFRβ$^{F2/F2}$, (B,E) PDGFRβ$^{F5/F5}$, and (C,F) PDGFRβ$^{F7/F7}$ heart. Phalloidin is shown (A-C) in isolation and (D-F) with a corresponding DAPI (blue) overlay. (G-L) Arp2/3 staining (red) is also shown on E14.5 (G,J) PDGFRβ$^{F2/F2}$, (H,K) PDGFRβ$^{F5/F5}$, and (I,L) PDGFRβ$^{F7/F7}$ heart sections (J-L) with and (G-I) without a DAPI overlay(blue).

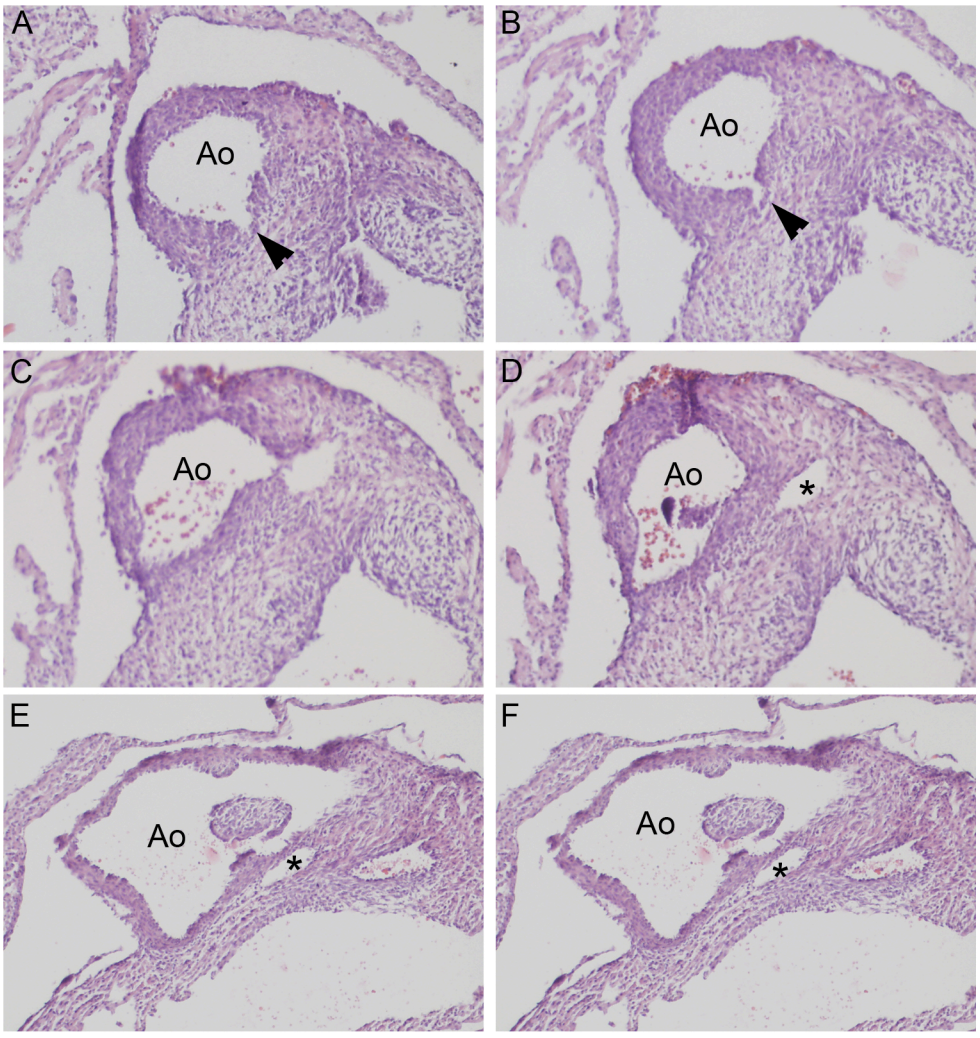

Sfigure 3.1 Coronary Arteries are Present in the PDGFRβ$^{-/-}$
Serial H&E sections through an (A,B) E15.5 and two (C-F) E17.5 PDGFRβ$^{-/-}$ hearts. Arrowheads mark the origin of the coronary artery. Astericks show the presence of coronary arteries. Ao= aorta.

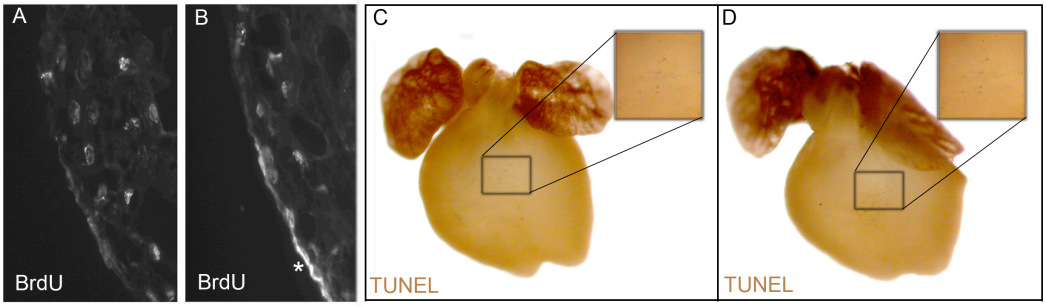

Sfigure 3.2 No Proliferative or Apoptotic Defect or Enhancement in the PDGFR $\beta^{-/-}$

(A,B) Proliferation was assessed in sections through E14.5 (A) PDGFR$\beta^{+/+}$ and (B) PDGFR$\beta^{-/-}$ hearts with BrdU incorporation (white). Astericks indicates background staining that was not nuclear localized. (C,D) Apoptosis was examined by performing whole mount TUNEL on E14.5 (C) PDGFR$\beta^{+/+}$ and (D) PDGFR$\beta^{-/-}$ hearts. Magnified regions in the box reveal the area with the largest number of TUNEL positive cells.

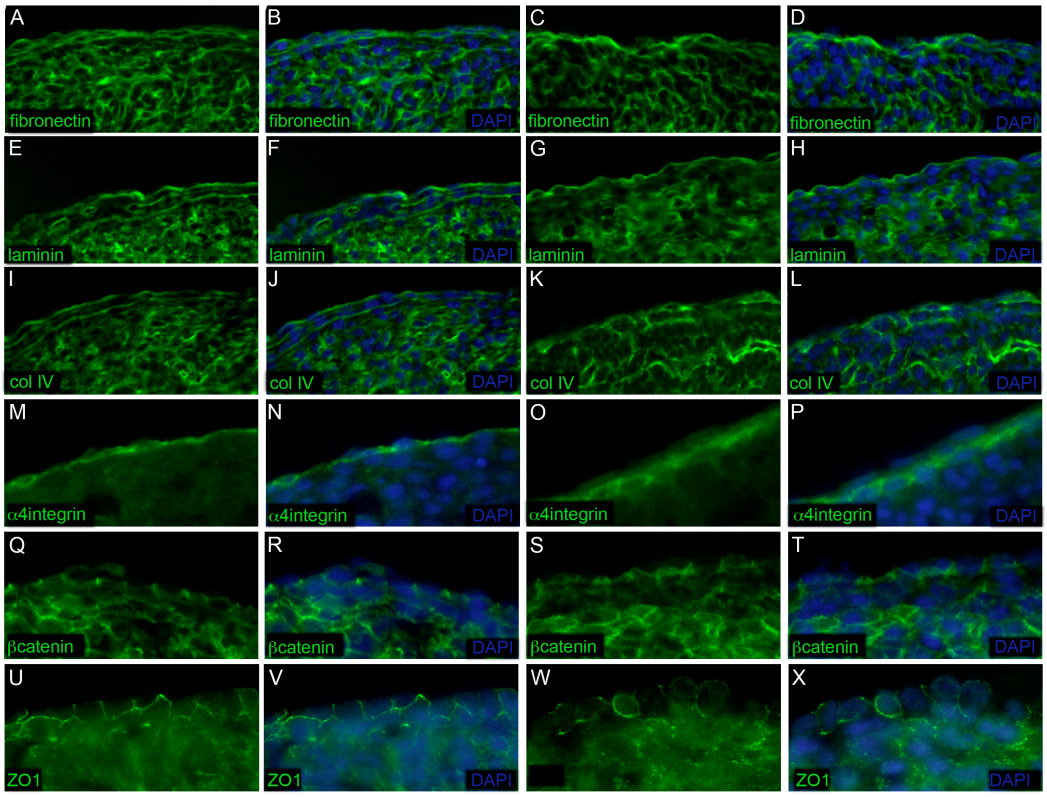

Sfigure 3.3 Presence of ECM Adhesion and Junctional Proteins
The presence of extracellular matrix, adhesion proteins and junctional markers were assessed at E14.5 in (A,B,E,F,I,J,M,N,Q,R,U,V) wild type and (C,D,G,H,K,L,O,P,S,T,W,X) PDGFRβ$^{-/-}$ hearts. Staining for (A-D) fibronectin, (E-H) laminin, (I-L) col IV, (M-P) α4 integrin, (Q-T) β–catenin and (U-X) ZO1 are shown in isolation (green) and overlaid with the corresponding DAPI image (blue).

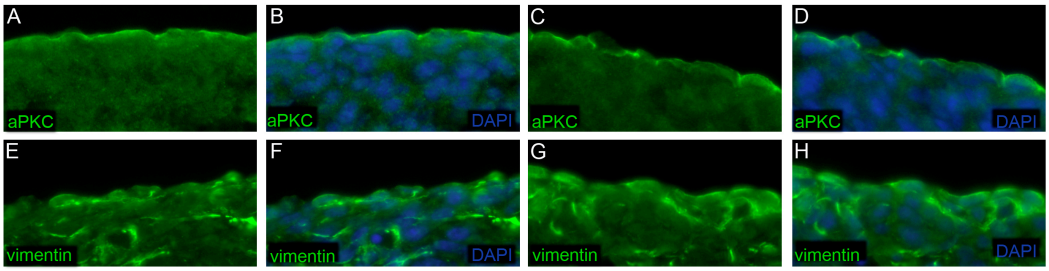

Sfigure 3.4 Assessment of Mesenchymal Markers and Polarity of the Epicardium
The localization of (A-D) aPKC (green) and (E-H) vimentin (green) were assessed at E14.5 in (A,B,E,F) wild type and (C,D,G,H) PDGFRβ$^{-/-}$ mice. Staining is illustrated (A,C,E,G) alone and (B,D,F,H) with DAPI (blue).

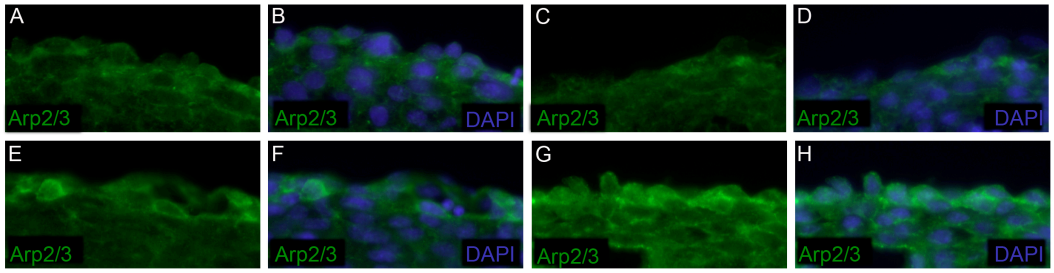

Sfigure 3.5 Developmental Time Course for Arp2/3
(A-H) Arp2/3 staining was performed on (A-D) E12.5 and (E-H) E13.5 (A,B,E,F) PDGFRβ$^{+/+}$ and (C,D,G,H) PDGFRβ$^{-/-}$ heart sections. Arp2/3 is shown (A,C,E,G) in isolation and (B,D,F,H) with the corresponding DAPI overlay.

CHAPTER FOUR

PERICYTES REGULATE THE ANGIOGENIC POTENTIAL OF ANG1

Introduction

Angiopoietin-1 (Ang1) is an important angiogenic factor that directs many activities in lymphatic and vascular endothelial cells (Eklund and Olsen, 2006). Its receptor, Tie2, is expressed on endothelial cells and upon ligand binding initiates cellular responses, including migration, sprouting, and proliferation (Koblizek et al., 1998; Thurston et al., 2005; Witzenbichler et al., 1998). Mice that lack either Ang1 or Tie2 exhibit cardiovascular defects and die early in embryogenesis (Sato et al., 1995; Suri et al., 1996). Conversely, mice over-expressing Ang1 have increased blood vessel densities and diameters in the skin, retina, trachea and tongue (Kim et al., 2007; Suri et al., 1998; Thurston et al., 2005). The effects of Ang1 appear to be context dependent because when Ang1 is over-expressed in the heart, no change in blood vessel function is observed (Visconti et al., 2002).

One of the main sources of Ang1 is the pericyte (Sundberg et al., 2002; Suri et al., 1996). Pericytes are the contractile, mesenchymal cells that surround microvessels in many tissues. Recently, the importance of the interactions of endothelial cells and pericytes in vascular responses has been established. Mice that have reduced numbers of pericytes exhibit severe vascular defects including

endothelial cell hyperplasia, vessel leakage, microaneurysms, and edema ((Bjarnegard et al., 2004; Hellstrom et al., 2001; Lindblom et al., 2003; Nystrom et al., 2006). Studies focused on understanding the interactions of pericytes and endothelial cells in retinal vasculature have demonstrated that reciprocal signals by each cell type are necessary for proper endothelial remodeling and pericyte recruitment (Benjamin et al., 1998; Uemura et al., 2002). The role of pericytes in tumor angiogenesis is slightly more ambiguous and may depend on the tumor type. For example, some tumor models demonstrate vasculature that contains very few pericytes. However, these few pericytes are able to protect endothelial cells from apoptosis (Abramsson et al., 2002; Gee et al., 2003). In another model, the inhibition of kinases expressed on both endothelial cells and pericytes leads to regression of late-stage tumors, suggesting that tumor vessels without a pericyte coating may be more susceptible to anti-angiogenic therapies (Bergers et al., 2003). Thus, an enhanced understanding of pericyte influences on the endothelial cells could lead to novel strategies for regulating angiogenesis in a variety of clinical settings.

To examine pericyte influences on the vascular response to exogenous Ang1, we have utilized mice with point mutations in the platelet derived growth factor receptor β (PDGFRβ). These mice possess alterations in signal transduction downstream of the receptor that lead to differences in pericyte numbers compared to wild type mice (Tallquist et al., 2003). One mouse line,

PDGFRβ$^{F7/F7}$, exhibits a 42-77% decrease in pericyte number depending on the tissue. The other mouse line, PDGFRβ$^{F1/F1}$, has an increase in pericyte number. In contrast to the *PDGFRβ*$^{-/-}$ or the *PDGFB*$^{-/-}$ mice, these mice survive past birth and, therefore, are suitable for postnatal studies. They provide a tractable system for addressing how the number of pericytes influences the ability of blood vessels to respond to Ang1.

Our studies demonstrate that the number of pericytes influences the endothelial response to an angiogenic stimulus. This effect occurred only when the pericyte levels were reduced. When pericyte levels were above normal, endothelial responses were indistinguishable from those in wild type animals. These data support the idea that not only do pericytes provide support to vessels but that they also have an intrinsic role in controlling endothelial responses to angiogenic signals.

Materials and Methods

Experimental animals

PDGFRβ$^{+/+}$, PDGFRβ$^{F1/F1}$ and PDGFRβ$^{F7/F7}$ mice were maintained on a mixed C57Bl/6 X 129SV background. All mice were heterozygous for the XlacZ4 transgene to visualize pericyte populations (Tidhar et al., 2001). The number of mice utilized for each set of experiments is indicated in figures or figure legends. Overall, 16 PDGFRβ$^{+/+}$, 8 PDGFRβ$^{F1/F1}$ and 20

PDGFRβ$^{F7/F7}$ mice were used for injections. BowAng1 (Regeneron Pharmaceuticals; 25mg/kg) (Zhang et al., 2002) or vehicle (50mM Tris, 150mMNaCl, 1mM $CaCl_2$) was injected i.p. for three consecutive days beginning at postnatal day 4 (P4). BowAng1 will be referred to as Ang1. BrdU (Sigma; 100 μg/g) was injected i.p. for two consecutive days beginning at P5. Tissues were isolated at P7 following injection of avertin (0.02 ml/g of 2.5% avertin). All animal experiments were approved by the Institutional Animal Care and Use Committee at the University of Texas Southwestern Medical Center and performed according to the Guide for the Care and Use of Laboratory Animals published by the NIH.

β-galactosidase staining and immunohistochemistry

For β-galactosidase staining, tissues were processed as previously described (Tallquist and Soriano, 2003). For co-staining with PECAM, samples were subsequently incubated with PECAM overnight, a biotinylated anti-rat antibody and Cy5 Streptavidin secondary. All trachea and non-β-galactosidase retina immunohistochemistry was performed as previously described (Thurston and Jean-Guillaume, 2003) with the exception of the BrdU co-staining in which the permeabilization step was preceded by a 30 min HCl treatment at 37°C and 10 min in 0.1M NaBorate pH8.5. The following primary antibodies were used: PECAM (BD Bioscience, 1:200) and BrdU (Sigma, 1:50). The following secondary antibodies were used at a 1:500 dilution; Alexa 488 Dk anti-Rt, Alexa

488 Gt anti-Ms, Alexa 594 Dk anti-Rt (Molecular Probes), Cy5 Streptavidin (Jackson Immunoresearch) or a 1:200 dilution; biotinylated anti-rat (Molecular Probes).

Imaging

Confocal imaging was performed on the LSM510META (grant S10-RR01940601). Fluorescent and black and white imaging utilized the Zeis Axiovert 200 with the Hamamatsu ORCA-ER camera and Open Lab. Color imaging of slides was performed with the Zeis Axiovert 200 with the Olympus DP71 camera and DP software. Composites were compiled in photoshop. To aid in visualization some images were pseudocolored green.

RT-PCR

The Qiagen RNeasy kit was used to isolate RNA from retina and trachea samples that had been frozen in liquid nitrogen. RT-PCR was carried out as previously described (Ding et al., 2005). Gene expression is the relative expression level compared to β-actin. Primer sequences are available upon request (J Garcia).

Quantification

Trachea quantifications were performed at 40x at the rostral end of the trachea. For pericyte quantification we examined 6 fields of view for each sample except for the STable quantification where we examined 4 fields of view. The samples for calculating baseline changes in pericyte number for Figure 4.1

were P7 pups that were unique from the injected samples. Trachea vessel width and number was performed by drawing a line between two cartilage rings and measuring the width of the vessels crossing that line as well as the number of vessels that crossed that line using Open lab. The quantification was performed on 10 fields of view for each sample. Statistical analysis on vessel width was performed with Mann Whitney U test.

Retina quantifications were performed at 63x with the exception of the proliferation studies, which were performed at 20x. Retina width was calculated by measuring the width of 70 vessels from at least 2 fields of view from each sample using ImageJ. The units of vessel width are pixels. Statistical analysis on vessel width was performed with Mann Whitney U test. Branch points in the retina were counted in ImageJ with at least 5 63x fields of view of PECAM stained images for each sample. A vessel was considered to have a branch point when it split into two directions and neither direction lead to a terminal vessel. Endothelial cell proliferation was quantified on two images from each sample. Cells that were positive for both BrdU and PECAM staining were quantified.

Results

Pericyte quantities in the trachea

To test the hypothesis that pericytes can influence the response of endothelial cells to Ang1 treatment, we examined the heart, retina, and trachea of

control and PDGFRβ mutant animals. Previous analysis of pericyte quantities in the neural tube, internal thoracic wall, retina, and heart demonstrated that PDGFRβ$^{F7/F7}$ mice have a severe decrease in pericytes and that PDGFRβ$^{F1/F1}$ mice have a modest increase in pericytes in all vascular beds analyzed (Tallquist et al., 2003). Because the trachea was not analyzed previously, we evaluated the pericyte number in control and mutant tracheas using the XLacZ4 transgenic mouse line. The XlacZ4 mouse line contains an enhancer trap that expresses nuclear β-galactosidase in vascular smooth muscle cells and pericytes with the exception of elastic arteries (Tidhar et al., 2001). The PDGFRβ$^{F7/F7}$ animals demonstrated a 73% decrease in pericyte number, while the PDGFRβ$^{F1/F1}$ trachea had a 20% increase in pericytes in the trachea compared to controls (Figure 4.1A-D). Therefore, the severe decrease and modest increase in pericytes in the trachea was consistent with our previous analysis of the pericyte populations in the PDGFRβ$^{F7/F7}$ and PDGFRβ$^{F1/F1}$ mice, respectively.

PDGFRβ$^{F7/F7}$ mice had increased blood vessel width but no hypoxia

Prior studies with Ang1 revealed that there is a reduced ability of blood vessels to increase their width in response to Ang1 between P14 and P30 (Thurston et al., 2005). One reason why the vessels may become unresponsive is because the vessels have acquired a mature phenotype as determined by acquisition of pericytes. Therefore, to investigate if a decrease in pericytes

impacts the extent of endothelial cell responses to Ang1, we examined tracheas, retinas, and hearts of PDGFRβ$^{F7/F7}$ mice by PECAM staining at P7, before endothelial cells demonstrate unresponsiveness to Ang1. Even in the absence of Ang1 treatment, we found a baseline increase in blood vessel width in the PDGFRβ$^{F7/F7}$ mice compared to PDGFRβ$^{+/+}$ mice in the trachea and retina (Figure 4.2A, C, A', C', E, G, and Figure 4.3). This suggested that a reduction in pericytes could result in increased endothelial cell proliferation or vessel dilation during development.

Embryos that completely lack PDGFRβ signaling exhibit brain endothelial cell hyperplasia and capillary dilation (Hellstrom et al., 2001). This effect on endothelial cells has been attributed to an up-regulation of hypoxia responsive genes, VEGF-A and Glut-1. Although the reduction of pericytes in the PDGFRβ$^{F7/F7}$ mice was not as severe as that found in the PDGFRβ$^{-/-}$ (Tallquist et al., 2003), we next determined if the observed increase in vessel diameter in PDGFRβ$^{F7/F7}$ tissues was caused by hypoxic conditions. We examined the basal levels of hypoxia-inducible genes in the PDGFRβ$^{F7/F7}$ tracheas and retinas and compared these levels to those observed in PDGFRβ$^{+/+}$ tissues. In the trachea no increase in either hypoxia inducible factor (HIF) family-dependent genes (Flk1, eNOS, VEGF-A, and Glut1) (Hirota and Semenza, 2006) or a HIF-independent gene (Tsp1) (Brat et al., 2003) was observed (Figure 4.4A). In the retina, there

was also no significant increase in expression of two HIF-dependent genes (VEGF-A and Glut1) or the HIF-independent gene, Tsp1 (Figure 4.4B). Taken together these data suggested that the basal increase in endothelial vessel width is not directly induced by sustained hypoxia.

Exaggerated vessel width in Ang1 treated mice with fewer pericytes

To determine if the reduction in pericytes rendered vessels more responsive to angiogenic treatments, we administered Ang1 to PDGFRβ$^{+/+}$ and PDGFRβ mutant mice. Mice were injected with Ang1 on three consecutive days beginning at P4. On P7 tissues were harvested and analyzed for vascular responses. In both PDGFRβ$^{+/+}$ and PDGFRβ$^{F7/F7}$ retinas and tracheas, there was an increase in vessel width upon Ang1 administration (Figure 4.2). However, the increase in blood vessel width in the PDGFRβ$^{F7/F7}$ Ang1-treated tissues was substantially greater than that observed in PDGFRβ$^{+/+}$. Not only did we observe an increase in the average width, but we also observed a shift in the distribution of vessel size such that a greater percentage of vessels had increased width (Figure 4.2 A-H, Figure 4.3). Consistent with previous analyses of Ang1 function (Thurston et al., 2005), the vessel width was not accompanied by a consistent change in vessel number (STable 4.I). In the retina, the capillary plexus exhibited the greatest increase in vessel width, while changes in the arteries and veins were less pronounced. Ang1 administration also resulted in the formation of

microaneurysms in the retinal endothelial vessels in 3 out of 4 of the PDGFRβ$^{F7/F7}$ mice, but only 1 out of 4 of the PDGFRβ$^{+/+}$ mice (data not shown). Similarly, there was an increase in the number of sites from which filopodial protrusions were initiated in the PDGFRβ$^{F7/F7}$ mice compared to PDGFRβ$^{+/+}$ mice. The filopodial protrusions were not restricted to the sprouting plexus margin and could be found throughout the plexus (Figure 4.2 E-H). While an increase in filapodial extensions was prominent and suggested that at a later time point there may be an increase in vessel branching, there was no observed change in established vessel branch points between the PDGFRβ$^{F7/F7}$ mice and PDGFRβ$^{+/+}$ mice (STable 4.I). Unlike the trachea and the retina, the heart showed no overt change in vessel density or width (Figure 4.2 I-L). Therefore, the reduced pericyte number in the PDGFRβ$^{F7/F7}$ mice selectively augmented the ability of the vasculature in both the retina and the trachea to respond to Ang1 treatment.

An increase in pericytes did not change endothelial vessel responses

To test whether an increase in pericyte number would further restrict endothelial responses, we examined the endothelial vessels in the tracheas, retinas, and hearts of Ang1-treated PDGFRβ$^{F1/F1}$ mice. In all three tissues examined, endothelial responses (vessel number and width) to Ang1 treatment were similar in PDGFRβ$^{+/+}$ and PDGFRβ$^{F1/F1}$ vessels (Figure 4.3, Figure 4.5A-L,

STable 4.I). One difference observed between PDGFRβ$^{+/+}$ and PDGFRβ$^{F1/F1}$ mice was that the PDGFRβ$^{+/+}$ retinas had a few areas of PECAM staining that resembled aneurysms, whereas no aneurysms were observed in the PDGFRβ$^{F1/F1}$ (data not shown). Thus, a minor increase in pericytes did not alter the blood vessel response to Ang1.

Pericyte numbers did not change upon Ang1 treatment

Because the PDGFRβ$^{F7/F7}$ mice exhibited differences in vessel width when compared to controls and the response of the retina and trachea was more prominent, we focused further analysis on these tissues in the PDGFRβ$^{F7/F7}$ mice compared to PDGFRβ$^{+/+}$ mice. While our studies examined the role of the pericytes in influencing the endothelial cell response, endothelial cells also send signals to pericytes that influence their migration and proliferation (reviewed in (Betsholtz, 2004; Jain and Booth, 2003)). Therefore, to ascertain whether recruitment of pericytes was enhanced during Ang1 treatment, we quantified pericyte numbers in the trachea and retina after Ang1 treatment. We utilized the XlacZ4 mouse line to mark pericytes and compared PDGFRβ$^{+/+}$ and PDGFRβ$^{F7/F7}$ retinas and tracheas at baseline and with Ang1 treatment. We observed no substantial increase in the number of pericytes in retinal and tracheal vasculature upon Ang1 administration (Figure 4.6, STable 4.I). Thus, despite the dramatic

influence on endothelial vessel width, pericyte biology appeared unperturbed by the acute Ang1 treatment.

Increased endothelial proliferation in vessels with reduced pericytes

Previous Ang1 studies have shown that the increase in vessel width is due to an increase in endothelial cell proliferation (Thurston et al., 2005). To assess whether the mechanism of vessel enlargement in the PDGFRβ$^{F7/F7}$ mice was consistent with these findings, we analyzed the proliferation of endothelial cells in the retina with BrdU incorporation (Figure 4.7, Table 4.I). Our results showed an increase in the number of BrdU positive endothelial cells in PDGFRβ$^{+/+}$ retinal vessels with Ang1 treatment (Figure 4.7A,B, Table 4.I). In addition, the PDGFRβ$^{F7/F7}$ retinal vasculature consistently displayed a greater increase in BrdU incorporation compared to PDGFRβ$^{+/+}$ in three separate experiments (Figure 4.7, Table 4.I). The reduced pericyte numbers in PDGFRβ$^{F7/F7}$ mice resulted in a 2-3 fold increase in endothelial cell proliferation. These results supported the idea that the increase in vessel width observed in the PDGFRβ$^{F7/F7}$ retinas and tracheas was caused by an increase in endothelial cell proliferation due to loss of interaction with pericytes.

Discussion

Understanding the influence of pericytes on the response of endothelial cells to angiogenic factors is critical for the development and optimization of therapies to improve blood supply to ischemic tissues or to impair blood supply to tumors. Our results show that an increase in pericytes does not greatly affect the ability of endothelial cells to respond to Ang1 treatment. In contrast, a decrease in pericytes leads to increased endothelial cell proliferation. These findings are complementary to recent studies that have examined vessel regression in systems where pericyte recruitment has been affected. Taken together these results suggest that the presence and activities of pericytes should be considered when developing treatments for altering blood vessel formation and function.

Endothelial-pericyte interactions control endothelial cell behavior

Our findings suggest that pericytes do not play a passive role in endothelial cell responses in vivo. Our data, in combination with previous studies, demonstrate that endothelial cells exhibit a dynamic range of responses when pericyte quantities are manipulated. In the extreme situation when pericyte development is profoundly affected, blood vessels of many tissues including the eye, brain, and kidney are perturbed. Endothelial cells become hyperplastic, microvessels become leaky, and vessel organization is disrupted (Bjarnegard et

al., 2004; Enge et al., 2002; Hellstrom et al., 2001; Leveen et al., 1994; Lindahl et al., 1997; Soriano, 1994a).

In more established vessels, if pericyte dissociation is caused by blocking antibodies, ligands, or drug treatment, the results vary depending on the tissue being analyzed. In the retina, pericyte association is necessary for vessel maturation, and disruption of pericyte-endothelial interactions leads to abnormal vessel remodeling and vessel regression. Interestingly, injection of either VEGF or Ang1 is able to partially rescue these defects by either acceleration of new pericyte recruitment or stabilization of endothelial cell interactions, respectively (Benjamin et al., 1998; Uemura et al., 2002). In our system, where the development of pericytes is affected to a lesser extent, pericyte-endothelial interactions were maintained, and hypoxia was not observed. We did observe an increase in vessel width, a greater incidence of aneurysms, and an increased number of sites with filopodial protusions after Ang1 administration suggesting that pericytes can also influence endothelial cells in subtle ways.

Recently, multiple studies have addressed the importance of pericyte-endothelial interactions in vessel regression studies. In tumors, disruption of pericyte association renders endothelial vessels more susceptible to anti-angiogenic treatments (Baffert et al., 2006; Bergers et al., 2003; Erber et al., 2004; Ostman and Heldin, 2007). In retinal vascularization models, the disruption of PDGFRβ signaling in addition to VEGF signaling resulted in more effective

vessel regression than disruption of VEGF signaling alone (Jo et al., 2006). Our results complement these studies by demonstrating that, at least in some tissues, a reduction in pericyte-endothelial interactions directly influences the extent to which endothelial cells proliferate in response to an angiogenic stimulus. These data are consistent with previous reports in vitro that show pericytes can inhibit endothelial cell proliferation (McIlroy et al., 2006; Orlidge and D'Amore, 1987). We also investigated the converse situation, an increase in pericytes, and found that there was a limit to the effects that pericytes have on endothelial cell proliferation. In PDGFR$\beta^{F1/F1}$ mice endothelial vessel enlargement was indistinguishable from that observed in PDGFR$\beta^{+/+}$ mice. These data suggest that there may be a threshold for pericyte influence on endothelial cell responses and that once a certain level of pericytes is reached there is little additional regulation of endothelial cell behavior.

Potential mechanisms for pericyte influence on endothelial cells

There are several possibilities to explain how pericytes might be influencing endothelial cell responses. Accumulating evidence suggests that components of the extracellular matrix have both angiogenic and anti-angiogenic activities. Sparc, perlecan, and multiple collagen-derived peptide fragments have all been shown to affect angiogenic responses (Kalluri, 2003). Although it is still a matter of controversy, it is believed that pericytes are important contributors of

extracellular matrix molecules to the endothelial basement membrane (Bell et al., 2001; Davis and Senger, 2005). The ability of pericytes to modulate the matrix is supported by studies that demonstrate improper association of pericytes with endothelial cells leading to changes in expression of fibronectin, laminin, and collagen IV, all molecules that have been linked to angiogenesis (Xian et al., 2006). The matrix also provides a means for sequestering soluble growth factors. Therefore, if these growth factors are not retained properly, endothelial cells may demonstrate enhanced responses to other angiogenic stimuli.

A second means by which pericytes could be affecting endothelial cell behavior is by secretion of soluble factors that inhibit proliferation. For example, pericytes secrete many molecules that are anti-angiogenic, including tissue inhibitor of matrix metalloproteinases 2 and 3, transforming growth factor β (TGFβ), and thrombospondin 2 (Lau, 1999; Saunders et al., 2006; Seo et al., 2003; Streit et al., 1999; Wisdom et al., 2005). Although anti-angiogenic activities have been ascribed to many of the molecules that pericytes produce, others such as VEGF (Darland et al., 2003) and Ang1 (Stoeltzing et al., 2003) clearly have angiogenic effects. As has been suggested previously, it is possible that the maturation state of the endothelial cell dictates endothelial responses to such factors. In nascent vessels TGFβ, Ang1, and VEGF may induce proliferation in endothelial cells, but in a mature setting where endothelial cells are in contact

with pericytes, these factors may play a role in stabilizing the vessel (Ramsauer and D'Amore, 2007).

Finally, the pericyte could be influencing the endothelial cells through direct contact. Pericytes, unlike vascular smooth muscle cells, come in direct contact with endothelial cell membranes (Cuevas et al., 1984). Regions exist where basement membrane does not separate endothelial cells and pericytes. These gaps permit direct crosstalk between the two cell types. The establishment of junctional complexes and signaling by Eph receptors and Notch components are potential means for pericyte-endothelial cell interactions. Precedence for the coordination of pericyte and endothelial proliferation by direct contact has been demonstrated in vitro (Hirschi et al., 1999; Orlidge and D'Amore, 1987).

Differential tissue responses

Our data also suggested that there is a different response to loss of pericytes depending on the tissue that is being examined. A decrease of pericytes in the retina and the trachea enhanced the resulting increase in vessel width, but in the heart there was no dramatic change in the vascular response. This could be due to the heterogeneity of the pericytes, endothelial cells or the tissues (reviewed in Thorin et al. (Thorin and Shreeve, 1998)). When the vessel width of the retina and trachea are compared, the response of the PDGFR$\beta^{F7/F7}$ trachea was more dramatic. One possible explanation is the higher density of pericytes observed in

the retinal vessels compared to the tracheal vessels at the time points examined. It is also possible that signaling through the PDGFRβ is more important in the vasculature of these tissues. Although we use the mutant PDGFRβ mice for their altered pericyte levels, we must not forget that we also have impaired PDGFRβ signaling within the pericytes. Finally, in the heart, pericytes are derived from a unique developmental origin compared to other tissues (Viragh and Challice, 1981). Therefore, the signaling between pericytes and endothelial cells may be different in the heart. It is important to combine the lessons learned from both the stimulation, as well as the inhibition of angiogenesis to gain a deeper insight into the role of pericytes in vivo and evaluate potential therapeutic synergies that may result from targeting both the endothelial cell as well as the pericyte.

Figures

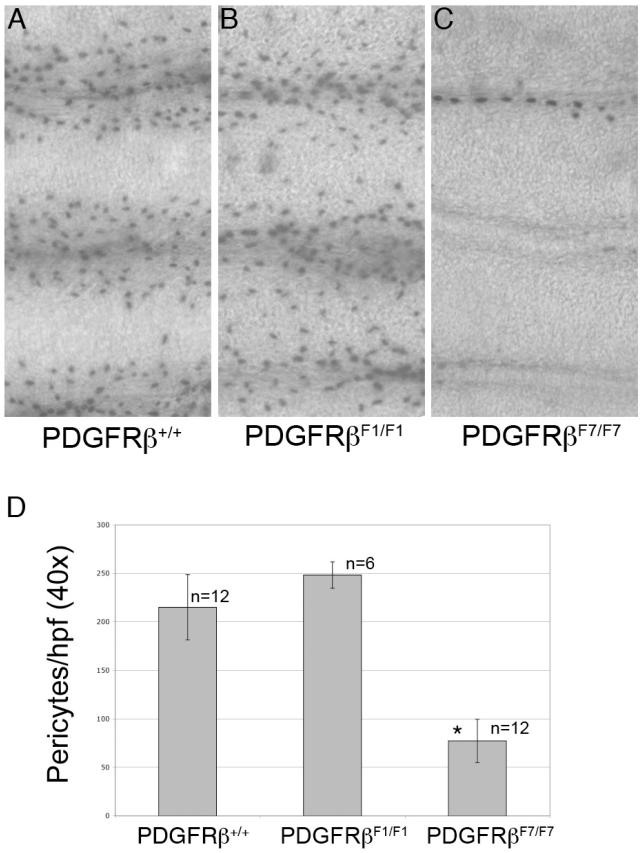

Figure 4.1 Pericyte Quantities in PDGFRβ Mutant Tracheas
P7 tracheas from (A) PDGFRβ$^{+/+}$, (B) PDGFRβ$^{F1/F1}$, and (C) PDGFRβ$^{F7/F7}$ mice were stained for pericytes (black) using the XlacZ4 reporter mouse. Images are taken at 10x. (D) Quantification of pericytes in the tracheas revealed a modest increase in pericytes in the PDGFRβ$^{F1/F1}$ animals and a substantial decrease in pericytes in the PDGFRβ$^{F7/F7}$ mice. Percent change was calculated using the average number of pericytes from PDGFRβ$^{+/+}$ controls as the baseline value of 100%. Pericyte numbers were averages of six fields of view from each trachea. Sample size is indicated with (n) for each genotype. Asterisk indicates significance of $p<0.001$ as determined by t-test.

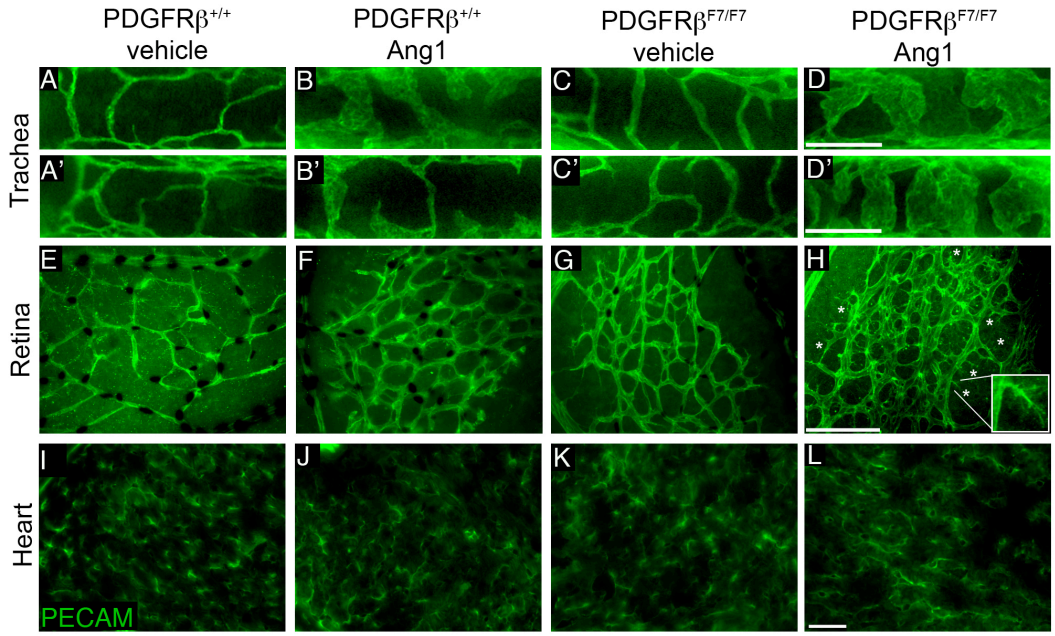

Figure 4.2 PDGFRβ$^{F7/F7}$ had Increased Vessel Width in Response to Ang1 Treatment

PECAM (green) stained tissues from (A,A',B,B',E,F,I,J) PDGFRβ$^{+/+}$ and (C,C',D,D',G,H,K,L) PDGFRβ$^{F7/F7}$ (A-D, A'-D') tracheas, (E-H) retinas, and (I-L) hearts. For tracheas, (A-D, A'-D') two separate intercartilage areas are shown. Images are representative of at least three independent experiments with Ang1 treatment for the trachea and retina and one independent experiment for the heart. Asterisks illustrate examples of the filopodial protrusions. Inset is an enlargement of indicated filopodia. Scale = 0.1mm.

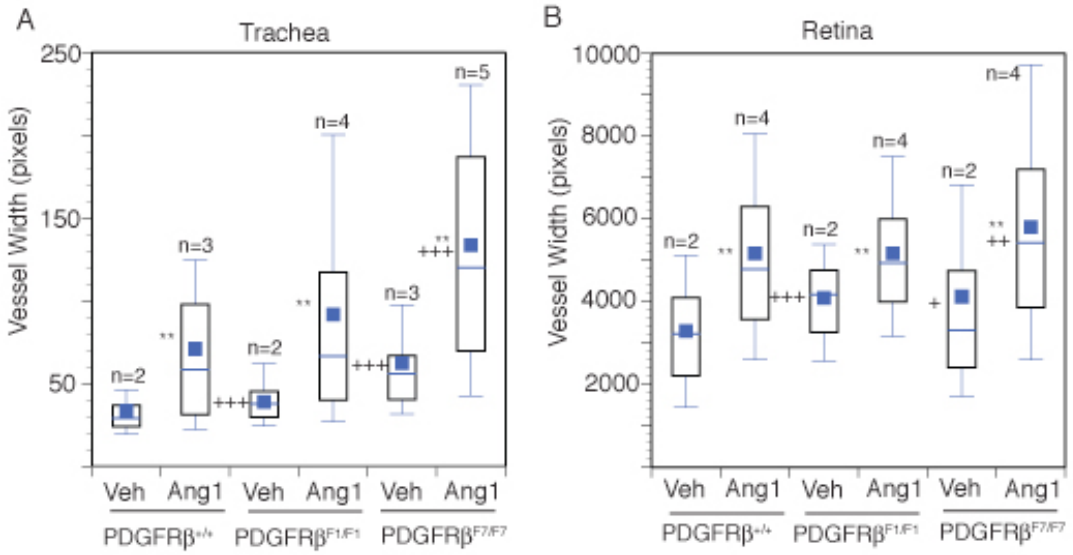

Figure 4.3 Pericytes Influence on Ang1 Induced Changes in Vessel Width
(A-B) Quantification of vessel width in the (A) trachea and (B) retina of PDGFRβ$^{+/+}$, PDGFRβ$^{F1/F1}$, and PDGFRβ$^{F7/F7}$ mice that were treated with vehicle (veh) or Ang1. Quantification performed as described in materials and methods. n indicates the number of animals used. Box plot diagram uses the top, middle, and bottom line of the box to represent the 75th, 50th and 25th percentile respectively. The square represents the mean. Whiskers extend from the 10th percentile on the bottom to the 90th percentile on the top. *designates statistical differences within a genotype between Ang1 treated and control. Specifically, *p<0.01, **p<0.001. +designates statistical differences between marked genotype and PDGFRβ$^{+/+}$ samples that received the same treatment. Specifically, +p<0.05, ++p<0.01, +++p<0.001. Statistics determined via Mann Whitney U Test.

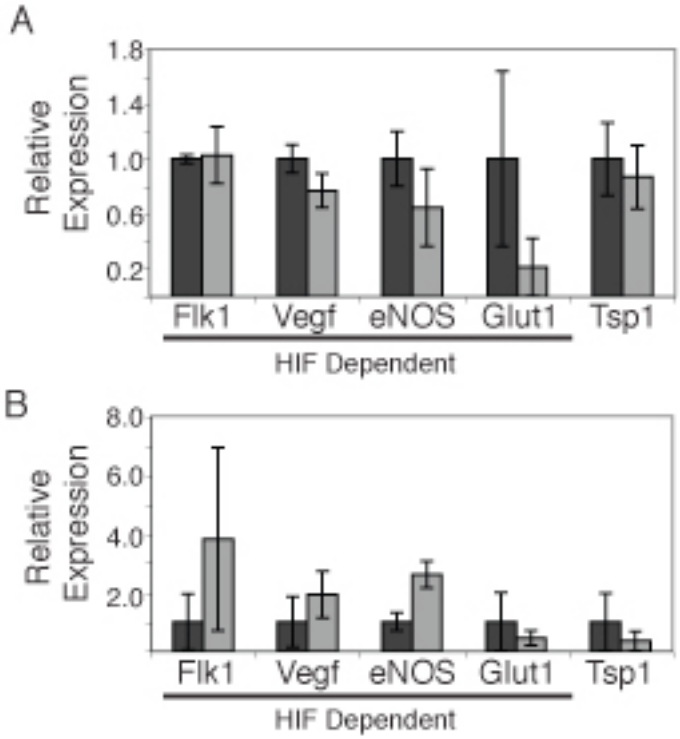

Figure 4.4 Hypoxia was not Observed in the PDGFRβ$^{F7/F7}$
(A-B) Real time PCR was performed on whole P7 (A) tracheas and (B) retinas from PDGFRβ$^{+/+}$ (dark grey) and PDGFRβ$^{F7/F7}$ (light grey) samples. β−actin was used to standardize the levels within each sample and samples were then normalized to the PDGFRβ$^{+/+}$ levels. PDGFRβ$^{+/+}$ trachea, PDGFRβ$^{F7/F7}$ trachea and PDGFRβ$^{F7/F7}$ retina samples were performed in triplicate. PDGFRβ$^{+/+}$ retina samples were performed in duplicate. Real time

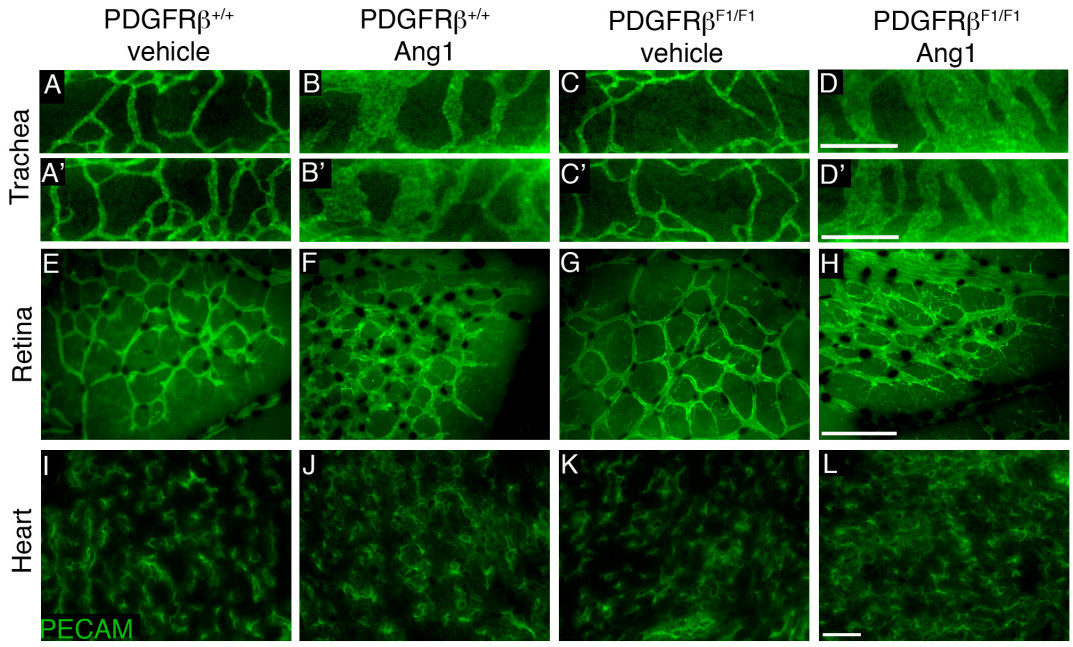

Figure 4.5 Vessels in PDGFRβ$^{F1/F1}$ and PDGFRβ$^{+/+}$ Respond Similarly to Ang1 Treatment

PECAM (green) stained tissues from (A,A',B,B',E,F,I,J) PDGFRβ$^{+/+}$ and (C,C',D,D',G,H,K,L) PDGFRβ$^{F1/F1}$, (A-D, A'-D') tracheas, (E-H) retinas, and (I-L) hearts. Trachea images are as indicated in Figure 2. Images are representative of at least two independent experiments with Ang1 injection for the trachea and retina and one independent experiment for the heart. Scale = 0.1mm.

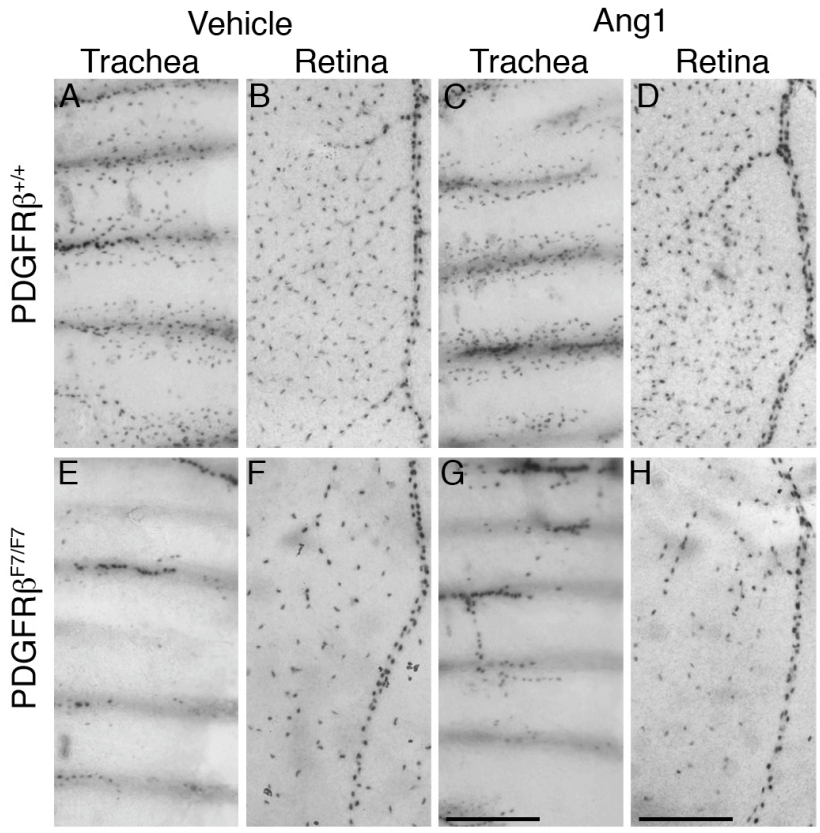

Figure 4.6 Pericyte Numbers Unaltered with Ang1 Treatment
Pericytes (black) in the (A,C,E,G) tracheal and (B,D,F,H) retinal vasculature were identified with the XlacZ4 reporter mouse in (A-D) PDGFRβ$^{+/+}$ and (E-H) PDGFRβ$^{F7/F7}$ mice. Scale = 0.1mm.

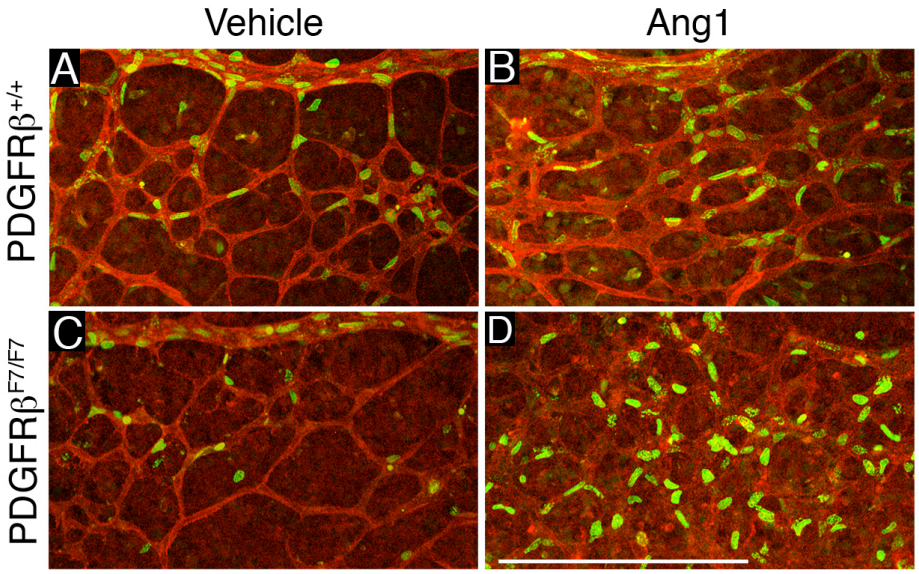

Figure 4.7 Increased Vessel Width Associated with Endothelial Cell Proliferation
(A-D) Confocal images of proliferation of endothelial cells in (A, B) PDGFRβ$^{+/+}$ and (C, D) PDGFRβ$^{F7/F7}$ retinas that were treated with (A, C) vehicle or (B, D) Ang1. Endothelial cells were identified by PECAM staining (red) and the proliferating cells were labeled with BrdU (green). These images are representative of three independent experiments, whose results are quantified in Table 1. Scale = 0.1mm.

		PDGFRβ$^{+/+}$		PDGFRβ$^{F7/F7}$	
		Vehicle	Ang1	Vehicle	Ang1
Experiment	1	109.5+/-6.4	118.5+/-2.1	81+/-4.2	187.5+/-2.1
	2	43.5+/-2.1	81.5+/-10.6	33+/-4.2	85.5+/-0.7
	3	45.5+/-10.6	87+/-9.9	31.5+/-13.4	107+/-12.7

Table 4.1 Quantification of Endothelial Cell Proliferation
Endothelial cell proliferation in the retina was calculated in three independent experiments. Experiments were performed with littermate controls with the exception of experiment 1, where the PDGFRβ$^{+/+}$ control was an age-matched control.

	PDGFRβ$^{+/+}$		PDGFRβ$^{F1/F1}$		PDGFRβ$^{F7/F7}$	
	Vehicle	Ang1	Vehicle	Ang1	Vehicle	Ang1
Trachea Vessel Number	3.1+/-1.7 (1)	1.5+/-1.4 (2)	3.6+/-1.5 (2)	2.7+/-1.6 (4)	2.0+/-1.8 (3)	2.5+/-1.3 (5)
Retinal Branch Points	35+/-13 (2)	44+/-17 (2)	33+/-9 (2)	43+/-10 (5)	32+/-13 (2)	36+/-12 (3)
Trachea Pericytes	154+/-23 (1)	162+/-14 (1)	n.d.	n.d.	44+/-18 (1)	57+/-13 (1)
Retina Pericytes	22+/-4.9 (4)	22+/-4.4 (1)	20+/-5.0 (5)	21+/-5.0 (4)	7.1+/-2.8 (3)	4.7+/-3.6 (4)

STable 1: Quantification of Pericytes, Branching and Vessel Number
Additional pericyte and endothelial vessel parameters were quantified in the trachea and retina as stated in the materials and methods. Pericytes were quantified using the XlacZ4 transgene as described in materials and methods. Values in parentheses indicate the number of samples utilized for that quantification. n.d. (not determined).

CHAPTER FIVE

DISCUSSION

Despite the fact that blood vessels are composed of two cell types, endothelial cells and VSMC, the majority of studies have focused on the role of endothelial cells in vascular development and disease states. The VSMC is often considered a secondary component that only participates in vessel dilation and stability. However, our work highlights the significance of the VSMC. Our studies examine PDGFRβ signaling in mesenchymal cells during both vasculogenic and angiogenic processes. The results characterize the developmental stages of VSMC and demonstrate how the functions of VSMC endothelial cells are closely intertwined.

As previously discussed our studies of coronary VSMC development have elucidated a novel role for the PDGFRβ in the efficient migration of epicardial cells. These results provide the first direct in vivo evidence of PDGFRβ function prior to coronary VSMC differentiation. Interestingly, these analyses also underscore several important points about coronary VSMC development. One of these is the idea of heterogeneity. In characterizing the migration of epicardial cells into the myocardium, we utilized WT1 and capsulin. Although both proteins are considered markers of the epicardium and epicardial derived

cells, they exhibit differential staining patterns over the examined time course. The WT1 positive cells are more homogenously dispersed upon entering the myocardium, whereas the capsulin positive cells appear to migrate waves. Nonetheless the loss of PDGFRβ appears to affect both cell populations. It is possible that the PDGFRβ affects a progenitor cell population prior to the division of the cell populations. It is also possible that lineages are predetermined and the PDGFRβ is affecting a population of cells in addition to coronary VSMC, such as fibroblasts, that we have not yet examined. More detailed co-expression studies would be beneficial to delineate the point at which these two sub populations diverge. It would also be interesting to see how the divergence relates to the expression of the PDGFRβ and PDGFRα.

Additional conditional analysis will also provide important insight into the development of these cell populations. There are several potential approaches. The first would be to examine an epicardial specific deletion of the PDGFRβ. I would expect that the defects in epicardial cell migration and coronary VSMC formation would be recapitulated. It could be interesting to knock out PDGFRβ in WT1 and capsulin positive cells. However, the expression of both of these proteins in the epicardium makes it less likely to have a phenotype that is different from the epicardial deletion. However, results have the potential of discerning if one of these populations is more representative of the coronary VSMC. A conditional timed deletion may be more beneficial, especially given the potential

role for the PDGFRβ at multiple time points during coronary VSMC development. However, prior to performing these studies it would be advantageous to validate a system for identifying fibroblasts in the event that one of the subpopulations preferentially develops into a fibroblast population. Our preliminary work with fsp was not conducive to studying fibroblasts in the heart.

It is also very important to evaluate the conditional deletion of PDGFRβ in combination with PDGFRα. PDGFRβ may be regulating the function of cells in which redundant signaling pathways mask its effect. PDGFRα is a likely candidate with its ability to stimulate similar signaling pathways, its presence in the epicardium and its partially overlapping expression in the subepicardial mesenchyme. The deletion of both receptors in the epicardium may result in a more dramatic phenotype in the subepicardial mesenchyme. This would be consistent with studies in our lab on the yolk sac, which show a slight phenotype with the PDGFRβ$^{-/-}$, but a failure in vascular remodeling when both receptors are deleted. Complimentary studies would involve a chimeric analysis with both receptors to analyze which cell populations wild type cells have a competitive advantage over those lacking one of the receptors. I would expect that wild type subepicardial mesenchymal cells would have an advantage over PDGFRβ$^{-/-}$ cells.

Another area of heterogeneity that our studies draw attention to is that concerning the genes in control of VSMC differentiation and function. I would have expected that the myocardin deletion of the PDGFRβ would have yielded a

more significant phenotype given the role of myocardin in VSMC differentiation. These results may be interpreted that PDGFRβ has a role prior to myocardin induction. However, it is also possible that myocardin has a lesser role in the coronary VSMC in comparison to other VSMC populations or that it has a lesser role in a subpopulation of coronary VSMC.

Our studies have also suggested that the src signaling pathway is important for PDGFRβ function. However, in line with the heterogeneity theme, this does not imply that other signaling pathways are not involved or do not predominate at another point in the developmental time course. For example, once in the subepicardial mesenchyme it may be more important for the PDGFRβ to signal through the PI3K pathway to move further into the myocardium, perhaps in a chemotaxic manner. The presence of the wave1 and wave2 in epicardial cultures suggests that these could be the mediators of PI3K function.

Besides elucidating the development of coronary VSMC, our studies also examined the relationship of the VSMC with the endothelial cells. Our Ang1 studies revealed that decreasing pericyte numbers potentiated the ability of endothelial cells to respond to Ang1. This provides substantial support for combination therapies that affect both VSMC and endothelial cells. According to our data this could be more effective in controlling blood vessel growth. However, our studies suggest that there must be a dramatic decrease in VSMC numbers to achieve this potentiation. Because VSMC provide essential support to

vessels throughout the body, these data also imply that it would be very important to have a localized reduction in VSMC in the treatment area.

Our results also underscore some important components for developing targeted treatments. First, it is necessary to understand both the direct and indirect effects generated by the treatment. The data from our Ang1 studies reveal that VSMCs can be targeted to have the desired, albeit secondary, effect on endothelial cells. In contrast, the epicardial studies provide an example of an unintended effect. These studies showed how disruption of coronary VSMC with the PDGFR$\beta^{-/-}$ also affected the remodeling of endothelial vessels. This could become an obstacle to treatment if a drug targeting VSMC unintentionally inhibited the vascularization of wounds or the blood supply to a fetus. Second, our results emphasize that it is important to characterize the cell population that is being targeted, as it may be a heterogeneous population that responds differently to therapies.

The results of our studies establish the importance of the PDGFRβ and pericytes in remodeling and angiogenesis. They reveal mechanisms of action that have the potential to be applied to other vascular beds, tissues that undergo EMT, cancers that are metastasizing, and tumors that need blood vessels to survive. They may also improve therapies involving vascular grafts or developing engineered tissues.

BIBLIOGRAPHY

Abramsson, A., Berlin, O., Papayan, H., Paulin, D., Shani, M., and Betsholtz, C. (2002). Analysis of mural cell recruitment to tumor vessels. Circulation *105*, 112-117.

Azhar, M., Schultz Jel, J., Grupp, I., Dorn, G.W., 2nd, Meneton, P., Molin, D.G., Gittenberger-de Groot, A.C., and Doetschman, T. (2003). Transforming growth factor beta in cardiovascular development and function. Cytokine & growth factor reviews *14*, 391-407.

Baffert, F., Le, T., Sennino, B., Thurston, G., Kuo, C.J., Hu-Lowe, D., and McDonald, D.M. (2006). Cellular changes in normal blood capillaries undergoing regression after inhibition of VEGF signaling. Am J Physiol Heart Circ Physiol *290*, H547-559.

Batlle, E., Sancho, E., Franci, C., Dominguez, D., Monfar, M., Baulida, J., and Garcia De Herreros, A. (2000). The transcription factor snail is a repressor of E-cadherin gene expression in epithelial tumour cells. Nat Cell Biol *2*, 84-89.

Bell, S.E., Mavila, A., Salazar, R., Bayless, K.J., Kanagala, S., Maxwell, S.A., and Davis, G.E. (2001). Differential gene expression during capillary morphogenesis in 3D collagen matrices: regulated expression of genes involved in basement membrane matrix assembly, cell cycle progression, cellular differentiation and G-protein signaling. J Cell Sci *114*, 2755-2773.

Benjamin, L.E., Hemo, I., and Keshet, E. (1998). A plasticity window for blood vessel remodelling is defined by pericyte coverage of the preformed endothelial network and is regulated by PDGF-B and VEGF. Development *125*, 1591-1598.

Bergers, G., Song, S., Meyer-Morse, N., Bergsland, E., and Hanahan, D. (2003). Benefits of targeting both pericytes and endothelial cells in the tumor vasculature with kinase inhibitors. J Clin Invest *111*, 1287-1295.

Betsholtz, C. (2004). Insight into the physiological functions of PDGF through genetic studies in mice. Cytokine Growth Factor Rev *15*, 215-228.

Bjarnegard, M., Enge, M., Norlin, J., Gustafsdottir, S., Fredriksson, S., Abramsson, A., Takemoto, M., Gustafsson, E., Fassler, R., and Betsholtz, C. (2004). Endothelium-specific ablation of PDGFB leads to pericyte loss and glomerular, cardiac and placental abnormalities. Development *131*, 1847-1857.

Boucher, P., Gotthardt, M., Li, W.P., Anderson, R.G., and Herz, J. (2003). LRP: role in vascular wall integrity and protection from atherosclerosis. Science (New York, NY *300*, 329-332.

Boyle, S.N., Michaud, G.A., Schweitzer, B., Predki, P.F., and Koleske, A.J. (2007). A critical role for cortactin phosphorylation by Abl-family kinases in PDGF-induced dorsal-wave formation. Curr Biol *17*, 445-451.

Brat, D.J., Kaur, B., and Van Meir, E.G. (2003). Genetic modulation of hypoxia induced gene expression and angiogenesis: relevance to brain tumors. Front Biosci *8*, d100-116.

Brunton, V.G., Avizienyte, E., Fincham, V.J., Serrels, B., Metcalf, C.A., 3rd, Sawyer, T.K., and Frame, M.C. (2005). Identification of Src-specific phosphorylation site on focal adhesion kinase: dissection of the role of Src SH2 and catalytic functions and their consequences for tumor cell behavior. Cancer research *65*, 1335-1342.

Cano, A., Perez-Moreno, M.A., Rodrigo, I., Locascio, A., Blanco, M.J., del Barrio, M.G., Portillo, F., and Nieto, M.A. (2000). The transcription factor snail controls epithelial-mesenchymal transitions by repressing E-cadherin expression. Nat Cell Biol *2*, 76-83.

Carmeliet, P. (2003). Angiogenesis in health and disease. Nature medicine *9*, 653-660.

Carmeliet, P., Ferreira, V., Breier, G., Pollefeyt, S., Kieckens, L., Gertsenstein, M., Fahrig, M., Vandenhoeck, A., Harpal, K., Eberhardt, C*., et al.* (1996). Abnormal blood vessel development and lethality in embryos lacking a single VEGF allele. Nature *380*, 435-439.

Chen, T.H., Chang, T.C., Kang, J.O., Choudhary, B., Makita, T., Tran, C.M., Burch, J.B., Eid, H., and Sucov, H.M. (2002). Epicardial induction of fetal cardiomyocyte proliferation via a retinoic acid-inducible trophic factor. Dev Biol *250*, 198-207.

Cleaver, O., and Melton, D.A. (2003). Endothelial signaling during development. Nature medicine *9*, 661-668.

Compton, L.A., Potash, D.A., Mundell, N.A., and Barnett, J.V. (2006). Transforming growth factor-beta induces loss of epithelial character and smooth muscle cell differentiation in epicardial cells. Dev Dyn *235*, 82-93.

Crosby, J.R., Seifert, R.A., Soriano, P., and Bowen-Pope, D.F. (1998). Chimaeric analysis reveals role of Pdgf receptors in all muscle lineages. Nature genetics *18*, 385-388.

Cuevas, P., Gutierrez-Diaz, J.A., Reimers, D., Dujovny, M., Diaz, F.G., and Ausman, J.I. (1984). Pericyte endothelial gap junctions in human cerebral capillaries. Anat Embryol (Berl) *170*, 155-159.

Darland, D.C., Massingham, L.J., Smith, S.R., Piek, E., Saint-Geniez, M., and D'Amore, P.A. (2003). Pericyte production of cell-associated VEGF is differentiation-dependent and is associated with endothelial survival. Dev Biol *264*, 275-288.

Davis, G.E., and Senger, D.R. (2005). Endothelial extracellular matrix: biosynthesis, remodeling, and functions during vascular morphogenesis and neovessel stabilization. Circ Res *97*, 1093-1107.

Davis, S., Aldrich, T.H., Jones, P.F., Acheson, A., Compton, D.L., Jain, V., Ryan, T.E., Bruno, J., Radziejewski, C., Maisonpierre, P.C.*, et al.* (1996). Isolation of angiopoietin-1, a ligand for the TIE2 receptor, by secretion-trap expression cloning. Cell *87*, 1161-1169.

Dettman, R.W., Denetclaw, W., Jr., Ordahl, C.P., and Bristow, J. (1998). Common epicardial origin of coronary vascular smooth muscle, perivascular fibroblasts, and intermyocardial fibroblasts in the avian heart. Dev Biol *193*, 169-181.

Dettman, R.W., Pae, S.H., Morabito, C., and Bristow, J. (2003). Inhibition of alpha4-integrin stimulates epicardial-mesenchymal transformation and alters migration and cell fate of epicardially derived mesenchyme. Developmental biology *257*, 315-328.

Ding, K., Scortegagna, M., Seaman, R., Birch, D.G., and Garcia, J.A. (2005). Retinal disease in mice lacking hypoxia-inducible transcription factor-2alpha. Invest Ophthalmol Vis Sci *46*, 1010-1016.

Du, K.L., Ip, H.S., Li, J., Chen, M., Dandre, F., Yu, W., Lu, M.M., Owens, G.K., and Parmacek, M.S. (2003). Myocardin is a critical serum response factor cofactor in the transcriptional program regulating smooth muscle cell differentiation. Molecular and cellular biology *23*, 2425-2437.

Dumont, D.J., Gradwohl, G., Fong, G.H., Puri, M.C., Gertsenstein, M., Auerbach, A., and Breitman, M.L. (1994). Dominant-negative and targeted null mutations in the endothelial receptor tyrosine kinase, tek, reveal a critical role in vasculogenesis of the embryo. Genes & development *8*, 1897-1909.

Eklund, L., and Olsen, B.R. (2006). Tie receptors and their angiopoietin ligands are context-dependent regulators of vascular remodeling. Exp Cell Res *312*, 630-641.

Enge, M., Bjarnegard, M., Gerhardt, H., Gustafsson, E., Kalen, M., Asker, N., Hammes, H.P., Shani, M., Fassler, R., and Betsholtz, C. (2002). Endothelium-specific platelet-derived growth factor-B ablation mimics diabetic retinopathy. Embo J *21*, 4307-4316.

Erber, R., Thurnher, A., Katsen, A.D., Groth, G., Kerger, H., Hammes, H.P., Menger, M.D., Ullrich, A., and Vajkoczy, P. (2004). Combined inhibition of VEGF and PDGF signaling enforces tumor vessel regression by interfering with pericyte-mediated endothelial cell survival mechanisms. Faseb J *18*, 338-340.

Esner, M., Meilhac, S.M., Relaix, F., Nicolas, J.F., Cossu, G., and Buckingham, M.E. (2006). Smooth muscle of the dorsal aorta shares a common clonal origin with skeletal muscle of the myotome. Development *133*, 737-749.

Ferrara, N., Carver-Moore, K., Chen, H., Dowd, M., Lu, L., O'Shea, K.S., Powell-Braxton, L., Hillan, K.J., and Moore, M.W. (1996). Heterozygous embryonic lethality induced by targeted inactivation of the VEGF gene. Nature *380*, 439-442.

Fischer, A.N., Fuchs, E., Mikula, M., Huber, H., Beug, H., and Mikulits, W. (2007). PDGF essentially links TGF-beta signaling to nuclear beta-catenin accumulation in hepatocellular carcinoma progression. Oncogene *26*, 3395-3405.
Fong, G.H., Rossant, J., Gertsenstein, M., and Breitman, M.L. (1995). Role of the Flt-1 receptor tyrosine kinase in regulating the assembly of vascular endothelium. Nature *376*, 66-70.
Gee, M.S., Procopio, W.N., Makonnen, S., Feldman, M.D., Yeilding, N.M., and Lee, W.M. (2003). Tumor vessel development and maturation impose limits on the effectiveness of anti-vascular therapy. Am J Pathol *162*, 183-193.
Gerhardt, H., and Betsholtz, C. (2003). Endothelial-pericyte interactions in angiogenesis. Cell Tissue Res *314*, 15-23.
Gittenberger-de Groot, A.C., Vrancken Peeters, M.P., Mentink, M.M., Gourdie, R.G., and Poelmann, R.E. (1998). Epicardium-derived cells contribute a novel population to the myocardial wall and the atrioventricular cushions. Circulation research *82*, 1043-1052.
Grako, K.A., and Stallcup, W.B. (1995). Participation of the NG2 proteoglycan in rat aortic smooth muscle cell responses to platelet-derived growth factor. Experimental cell research *221*, 231-240.
Guadix, J.A., Carmona, R., Munoz-Chapuli, R., and Perez-Pomares, J.M. (2006). In vivo and in vitro analysis of the vasculogenic potential of avian proepicardial and epicardial cells. Dev Dyn *235*, 1014-1026.
Hellstrom, M., Gerhardt, H., Kalen, M., Li, X., Eriksson, U., Wolburg, H., and Betsholtz, C. (2001). Lack of pericytes leads to endothelial hyperplasia and abnormal vascular morphogenesis. J Cell Biol *153*, 543-553.
Hellstrom, M., Kalen, M., Lindahl, P., Abramsson, A., and Betsholtz, C. (1999). Role of PDGF-B and PDGFR-beta in recruitment of vascular smooth muscle cells and pericytes during embryonic blood vessel formation in the mouse. Development (Cambridge, England) *126*, 3047-3055.
Hellstrom M, K.M., Lindahl P, Abramsson A, and Betsholtz C (1999). Role of PDGF-B and PDGFRbeta in recruitment of vascular smooth muscle cells and pericytes during embryonic blood vessel formation in the mouse. Development (Cambridge, England) *126*, 3047-3055.
Hidai, H., Bardales, R., Goodwin, R., Quertermous, T., and Quertermous, E.E. (1998). Cloning of capsulin, a basic helix-loop-helix factor expressed in progenitor cells of the pericardium and the coronary arteries. Mech Dev *73*, 33-43.
Hirose, T., Karasawa, M., Sugitani, Y., Fujisawa, M., Akimoto, K., Ohno, S., and Noda, T. (2006). PAR3 is essential for cyst-mediated epicardial development by establishing apical cortical domains. Development (Cambridge, England) *133*, 1389-1398.

Hirota, K., and Semenza, G.L. (2006). Regulation of angiogenesis by hypoxia-inducible factor 1. Crit Rev Oncol Hematol *59*, 15-26.
Hirschi, K.K., Rohovsky, S.A., Beck, L.H., Smith, S.R., and D'Amore, P.A. (1999). Endothelial cells modulate the proliferation of mural cell precursors via platelet-derived growth factor-BB and heterotypic cell contact. Circ Res *84*, 298-305.
Hogan, B. (1994). Manipulating the mouse embryo : a laboratory manual, 2nd edn (Plainview, N.Y., Cold Spring Harbor Laboratory Press).
Hungerford, J.E., and Little, C.D. (1999). Developmental biology of the vascular smooth muscle cell: building a multilayered vessel wall. Journal of vascular research *36*, 2-27.
Hungerford, J.E., Owens, G.K., Argraves, W.S., and Little, C.D. (1996). Development of the aortic vessel wall as defined by vascular smooth muscle and extracellular matrix markers. Dev Biol *178*, 375-392.
Ishibe, S., Joly, D., Zhu, X., and Cantley, L.G. (2003). Phosphorylation-dependent paxillin-ERK association mediates hepatocyte growth factor-stimulated epithelial morphogenesis. Molecular cell *12*, 1275-1285.
Iwano, M., Plieth, D., Danoff, T.M., Xue, C., Okada, H., and Neilson, E.G. (2002). Evidence that fibroblasts derive from epithelium during tissue fibrosis. J Clin Invest *110*, 341-350.
Jain, R.K. (2003). Molecular regulation of vessel maturation. Nature medicine *9*, 685-693.
Jain, R.K., and Booth, M.F. (2003). What brings pericytes to tumor vessels? J Clin Invest *112*, 1134-1136.
Jechlinger, M., Sommer, A., Moriggl, R., Seither, P., Kraut, N., Capodiecci, P., Donovan, M., Cordon-Cardo, C., Beug, H., and Grunert, S. (2006). Autocrine PDGFR signaling promotes mammary cancer metastasis. J Clin Invest *116*, 1561-1570.
Jiang, X., Rowitch, D.H., Soriano, P., McMahon, A.P., and Sucov, H.M. (2000). Fate of the mammalian cardiac neural crest. Development *127*, 1607-1616.
Jo, N., Mailhos, C., Ju, M., Cheung, E., Bradley, J., Nishijima, K., Robinson, G.S., Adamis, A.P., and Shima, D.T. (2006). Inhibition of platelet-derived growth factor B signaling enhances the efficacy of anti-vascular endothelial growth factor therapy in multiple models of ocular neovascularization. Am J Pathol *168*, 2036-2053.
Kalluri, R. (2003). Basement membranes: structure, assembly and role in tumour angiogenesis. Nat Rev Cancer *3*, 422-433.
Kalman, F., Viragh, S., and Modis, L. (1995). Cell surface glycoconjugates and the extracellular matrix of the developing mouse embryo epicardium. Anatomy and embryology *191*, 451-464.

Kang, Y., and Massague, J. (2004). Epithelial-mesenchymal transitions: twist in development and metastasis. Cell *118*, 277-279.
Kattan, J., Dettman, R.W., and Bristow, J. (2004). Formation and remodeling of the coronary vascular bed in the embryonic avian heart. Dev Dyn *230*, 34-43.
Kim, K.E., Cho, C.H., Kim, H.Z., Baluk, P., McDonald, D.M., and Koh, G.Y. (2007). In vivo actions of angiopoietins on quiescent and remodeling blood and lymphatic vessels in mouse airways and skin. Arterioscler Thromb Vasc Biol *27*, 564-570.
Klinghoffer RA, M.-N.P., Faerman A, Shani M and Soriano P (2001). The Two PDGF Receptors Maintain Conserved Signaling In Vivo despite Divergent Embryological Functions. Molecular Cell *7*, 343-354.
Koblizek, T.I., Weiss, C., Yancopoulos, G.D., Deutsch, U., and Risau, W. (1998). Angiopoietin-1 induces sprouting angiogenesis in vitro. Curr Biol *8*, 529-532.
Komiyama, M., Ito, K., and Shimada, Y. (1987). Origin and development of the epicardium in the mouse embryo. Anat Embryol (Berl) *176*, 183-189.
Landerholm, T.E., Dong, X.R., Lu, J., Belaguli, N.S., Schwartz, R.J., and Majesky, M.W. (1999). A role for serum response factor in coronary smooth muscle differentiation from proepicardial cells. Development (Cambridge, England) *126*, 2053-2062.
Lau, H.K. (1999). Regulation of proteolytic enzymes and inhibitors in two smooth muscle cell phenotypes. Cardiovasc Res *43*, 1049-1059.
Lavine, K.J., Yu, K., White, A.C., Zhang, X., Smith, C., Partanen, J., and Ornitz, D.M. (2005). Endocardial and epicardial derived FGF signals regulate myocardial proliferation and differentiation in vivo. Dev Cell *8*, 85-95.
Lepilina, A., Coon, A.N., Kikuchi, K., Holdway, J.E., Roberts, R.W., Burns, C.G., and Poss, K.D. (2006). A dynamic epicardial injury response supports progenitor cell activity during zebrafish heart regeneration. Cell *127*, 607-619.
Leveen, P., Pekny, M., Gebre-Medhin, S., Swolin, B., Larsson, E., and Betsholtz, C. (1994). Mice deficient for PDGF B show renal, cardiovascular, and hematological abnormalities. Genes Dev *8*, 1875-1887.
Li, L., Liu, Z., Mercer, B., Overbeek, P., and Olson, E.N. (1997). Evidence for serum response factor-mediated regulatory networks governing SM22alpha transcription in smooth, skeletal, and cardiac muscle cells. Developmental biology *187*, 311-321.
Li, S., Wang, D.Z., Wang, Z., Richardson, J.A., and Olson, E.N. (2003). The serum response factor coactivator myocardin is required for vascular smooth muscle development. Proceedings of the National Academy of Sciences of the United States of America *100*, 9366-9370.
Li, W.E., Waldo, K., Linask, K.L., Chen, T., Wessels, A., Parmacek, M.S., Kirby, M.L., and Lo, C.W. (2002). An essential role for connexin43 gap junctions in mouse coronary artery development. Development *129*, 2031-2042.

Lie-Venema, H., Eralp, I., Maas, S., Gittenberger-De Groot, A.C., Poelmann, R.E., and DeRuiter, M.C. (2005). Myocardial heterogeneity in permissiveness for epicardium-derived cells and endothelial precursor cells along the developing heart tube at the onset of coronary vascularization. Anat Rec A Discov Mol Cell Evol Biol *282*, 120-129.

Lie-Venema, H., Gittenberger-de Groot, A.C., van Empel, L.J., Boot, M.J., Kerkdijk, H., de Kant, E., and DeRuiter, M.C. (2003). Ets-1 and Ets-2 transcription factors are essential for normal coronary and myocardial development in chicken embryos. Circulation research *92*, 749-756.

Lindahl, P., Hellstrom, M., Kalen, M., Karlsson, L., Pekny, M., Pekna, M., Soriano, P., and Betsholtz, C. (1998). Paracrine PDGF-B/PDGF-Rbeta signaling controls mesangial cell development in kidney glomeruli. Development *125*, 3313-3322.

Lindahl, P., Johansson, B.R., Leveen, P., and Betsholtz, C. (1997). Pericyte loss and microaneurysm formation in PDGF-B-deficient mice. Science *277*, 242-245.

Lindblom, P., Gerhardt, H., Liebner, S., Abramsson, A., Enge, M., Hellstrom, M., Backstrom, G., Fredriksson, S., Landegren, U., Nystrom, H.C.*, et al.* (2003). Endothelial PDGF-B retention is required for proper investment of pericytes in the microvessel wall. Genes Dev *17*, 1835-1840.

Lu, J., Landerholm, T.E., Wei, J.S., Dong, X.R., Wu, S.P., Liu, X., Nagata, K., Inagaki, M., and Majesky, M.W. (2001). Coronary smooth muscle differentiation from proepicardial cells requires rhoA-mediated actin reorganization and p160 rho-kinase activity. Dev Biol *240*, 404-418.

Lu, J., Richardson, J.A., and Olson, E.N. (1998). Capsulin: a novel bHLH transcription factor expressed in epicardial progenitors and mesenchyme of visceral organs. Mech Dev *73*, 23-32.

Manabe, I., and Owens, G.K. (2001). Recruitment of serum response factor and hyperacetylation of histones at smooth muscle-specific regulatory regions during differentiation of a novel P19-derived in vitro smooth muscle differentiation system. Circulation research *88*, 1127-1134.

McIlroy, M., O'Rourke, M., McKeown, S.R., Hirst, D.G., and Robson, T. (2006). Pericytes influence endothelial cell growth characteristics: role of plasminogen activator inhibitor type 1 (PAI-1). Cardiovasc Res *69*, 207-217.

Merki, E., Zamora, M., Raya, A., Kawakami, Y., Wang, J., Zhang, X., Burch, J., Kubalak, S.W., Kaliman, P., Belmonte, J.C.*, et al.* (2005). Epicardial retinoid X receptor alpha is required for myocardial growth and coronary artery formation. Proc Natl Acad Sci U S A *102*, 18455-18460.

Miano, J.M., Cserjesi, P., Ligon, K.L., Periasamy, M., and Olson, E.N. (1994). Smooth muscle myosin heavy chain exclusively marks the smooth muscle lineage during mouse embryogenesis. Circ Res *75*, 803-812.

Mikawa, T., and Gourdie, R.G. (1996). Pericardial mesoderm generates a population of coronary smooth muscle cells migrating into the heart along with ingrowth of the epicardial organ. Dev Biol *174*, 221-232.
Miki, H., Suetsugu, S., and Takenawa, T. (1998). WAVE, a novel WASP-family protein involved in actin reorganization induced by Rac. The EMBO journal *17*, 6932-6941.
Miki, H., Yamaguchi, H., Suetsugu, S., and Takenawa, T. (2000). IRSp53 is an essential intermediate between Rac and WAVE in the regulation of membrane ruffling. Nature *408*, 732-735.
Molin, D.G., Bartram, U., Van der Heiden, K., Van Iperen, L., Speer, C.P., Hierck, B.P., Poelmann, R.E., and Gittenberger-de-Groot, A.C. (2003). Expression patterns of Tgfbeta1-3 associate with myocardialisation of the outflow tract and the development of the epicardium and the fibrous heart skeleton. Dev Dyn *227*, 431-444.
Moore, A.W., McInnes, L., Kreidberg, J., Hastie, N.D., and Schedl, A. (1999). YAC complementation shows a requirement for Wt1 in the development of epicardium, adrenal gland and throughout nephrogenesis. Development (Cambridge, England) *126*, 1845-1857.
Morabito, C.J., Dettman, R.W., Kattan, J., Collier, J.M., and Bristow, J. (2001). Positive and negative regulation of epicardial-mesenchymal transformation during avian heart development. Dev Biol *234*, 204-215.
Nystrom, H.C., Lindblom, P., Wickman, A., Andersson, I., Norlin, J., Faldt, J., Lindahl, P., Skott, O., Bjarnegard, M., Fitzgerald, S.M.*, et al.* (2006). Platelet-derived growth factor B retention is essential for development of normal structure and function of conduit vessels and capillaries. Cardiovasc Res *71*, 557-565.
Orlidge, A., and D'Amore, P.A. (1987). Inhibition of capillary endothelial cell growth by pericytes and smooth muscle cells. J Cell Biol *105*, 1455-1462.
Ostman, A., and Heldin, C.H. (2007). PDGF Receptors as Targets in Tumor Treatment. Adv Cancer Res *97*, 247-274.
Owens, G.K. (1995). Regulation of differentiation of vascular smooth muscle cells. Physiological reviews *75*, 487-517.
Perez-Pomares, J.M., Carmona, R., Gonzalez-Iriarte, M., Atencia, G., Wessels, A., and Munoz-Chapuli, R. (2002). Origin of coronary endothelial cells from epicardial mesothelium in avian embryos. Int J Dev Biol *46*, 1005-1013.
Perez-Pomares, J.M., Macias, D., Garcia-Garrido, L., and Munoz-Chapuli, R. (1997). Contribution of the primitive epicardium to the subepicardial mesenchyme in hamster and chick embryos. Dev Dyn *210*, 96-105.
Perez-Pomares, J.M., Phelps, A., Sedmerova, M., and Wessels, A. (2003). Epicardial-like cells on the distal arterial end of the cardiac outflow tract do not derive from the proepicardium but are derivatives of the cephalic pericardium. Dev Dyn *227*, 56-68.

Poelmann, R.E., Gittenberger-de Groot, A.C., Mentink, M.M., Bokenkamp, R., and Hogers, B. (1993). Development of the cardiac coronary vascular endothelium, studied with antiendothelial antibodies, in chicken-quail chimeras. Circ Res *73*, 559-568.

Ponten, A., Folestad, E.B., Pietras, K., and Eriksson, U. (2005). Platelet-derived growth factor D induces cardiac fibrosis and proliferation of vascular smooth muscle cells in heart-specific transgenic mice. Circ Res *97*, 1036-1045.

Pouget, C., Gautier, R., Teillet, M.A., and Jaffredo, T. (2006). Somite-derived cells replace ventral aortic hemangioblasts and provide aortic smooth muscle cells of the trunk. Development *133*, 1013-1022.

Ramsauer, M., and D'Amore, P.A. (2007). Contextual role for angiopoietins and TGFbeta1 in blood vessel stabilization. J Cell Sci *120*, 1810-1817.

Richarte, A.M., Mead, H.B., and Tallquist, M.D. (2007). Cooperation between the PDGF receptors in cardiac neural crest cell migration. Developmental biology *306*, 785-796.

Risau, W. (1997). Mechanisms of angiogenesis. Nature *386*, 671-674.

Robb, L., Mifsud, L., Hartley, L., Biben, C., Copeland, N.G., Gilbert, D.J., Jenkins, N.A., and Harvey, R.P. (1998). epicardin: A novel basic helix-loop-helix transcription factor gene expressed in epicardium, branchial arch myoblasts, and mesenchyme of developing lung, gut, kidney, and gonads. Dev Dyn *213*, 105-113.

Sasaki, A.T., and Firtel, R.A. (2006). Regulation of chemotaxis by the orchestrated activation of Ras, PI3K, and TOR. European journal of cell biology *85*, 873-895.

Sato, T.N., Tozawa, Y., Deutsch, U., Wolburg-Buchholz, K., Fujiwara, Y., Gendron-Maguire, M., Gridley, T., Wolburg, H., Risau, W., and Qin, Y. (1995). Distinct roles of the receptor tyrosine kinases Tie-1 and Tie-2 in blood vessel formation. Nature *376*, 70-74.

Saunders, W.B., Bohnsack, B.L., Faske, J.B., Anthis, N.J., Bayless, K.J., Hirschi, K.K., and Davis, G.E. (2006). Coregulation of vascular tube stabilization by endothelial cell TIMP-2 and pericyte TIMP-3. J Cell Biol *175*, 179-191.

Savagner, P. (2001). Leaving the neighborhood: molecular mechanisms involved during epithelial-mesenchymal transition. Bioessays *23*, 912-923.

Savagner, P., Karavanova, I., Perantoni, A., Thiery, J.P., and Yamada, K.M. (1998). Slug mRNA is expressed by specific mesodermal derivatives during rodent organogenesis. Dev Dyn *213*, 182-187.

Sengbusch, J.K., He, W., Pinco, K.A., and Yang, J.T. (2002). Dual functions of [alpha]4[beta]1 integrin in epicardial development: initial migration and long-term attachment. The Journal of cell biology *157*, 873-882.

Seo, D.W., Li, H., Guedez, L., Wingfield, P.T., Diaz, T., Salloum, R., Wei, B.Y., and Stetler-Stevenson, W.G. (2003). TIMP-2 mediated inhibition of angiogenesis: an MMP-independent mechanism. Cell *114*, 171-180.
Shalaby, F., Rossant, J., Yamaguchi, T.P., Gertsenstein, M., Wu, X.F., Breitman, M.L., and Schuh, A.C. (1995). Failure of blood-island formation and vasculogenesis in Flk-1-deficient mice. Nature *376*, 62-66.
Shikama, N., Lutz, W., Kretzschmar, R., Sauter, N., Roth, J.F., Marino, S., Wittwer, J., Scheidweiler, A., and Eckner, R. (2003). Essential function of p300 acetyltransferase activity in heart, lung and small intestine formation. The EMBO journal *22*, 5175-5185.
Shinbrot, E., Peters, K.G., and Williams, L.T. (1994). Expression of the platelet-derived growth factor beta receptor during organogenesis and tissue differentiation in the mouse embryo. Dev Dyn *199*, 169-175.
Smart, N., Risebro, C.A., Melville, A.A., Moses, K., Schwartz, R.J., Chien, K.R., and Riley, P.R. (2007). Thymosin beta4 induces adult epicardial progenitor mobilization and neovascularization. Nature *445*, 177-182.
Somogyi, K., and Rorth, P. (2004). Cortactin modulates cell migration and ring canal morphogenesis during Drosophila oogenesis. Mechanisms of development *121*, 57-64.
Soriano, P. (1994a). Abnormal kidney development and hematological disorders in PDGF beta-receptor mutant mice. Genes and Development *8*, 1888-1896.
Soriano, P. (1994b). Abnormal kidney development and hematological disorders in PDGF beta-receptor mutant mice. Genes Dev *8*, 1888-1896.
Sossey-Alaoui, K., Li, X., Ranalli, T.A., and Cowell, J.K. (2005). WAVE3-mediated cell migration and lamellipodia formation are regulated downstream of phosphatidylinositol 3-kinase. The Journal of biological chemistry *280*, 21748-21755.
Stoeltzing, O., Ahmad, S.A., Liu, W., McCarty, M.F., Wey, J.S., Parikh, A.A., Fan, F., Reinmuth, N., Kawaguchi, M., Bucana, C.D*., et al.* (2003). Angiopoietin-1 inhibits vascular permeability, angiogenesis, and growth of hepatic colon cancer tumors. Cancer Res *63*, 3370-3377.
Streit, M., Velasco, P., Brown, L.F., Skobe, M., Richard, L., Riccardi, L., Lawler, J., and Detmar, M. (1999). Overexpression of thrombospondin-1 decreases angiogenesis and inhibits the growth of human cutaneous squamous cell carcinomas. Am J Pathol *155*, 441-452.
Strobeck, M., Kim, S., Zhang, J.C., Clendenin, C., Du, K.L., and Parmacek, M.S. (2001). Binding of serum response factor to CArG box sequences is necessary but not sufficient to restrict gene expression to arterial smooth muscle cells. The Journal of biological chemistry *276*, 16418-16424.
Sundberg, C., Kowanetz, M., Brown, L.F., Detmar, M., and Dvorak, H.F. (2002). Stable expression of angiopoietin-1 and other markers by cultured pericytes:

phenotypic similarities to a subpopulation of cells in maturing vessels during later stages of angiogenesis in vivo. Lab Invest *82*, 387-401.
Suri, C., Jones, P.F., Patan, S., Bartunkova, S., Maisonpierre, P.C., Davis, S., Sato, T.N., and Yancopoulos, G.D. (1996). Requisite role of angiopoietin-1, a ligand for the TIE2 receptor, during embryonic angiogenesis. Cell *87*, 1171-1180.
Suri, C., McClain, J., Thurston, G., McDonald, D.M., Zhou, H., Oldmixon, E.H., Sato, T.N., and Yancopoulos, G.D. (1998). Increased vascularization in mice overexpressing angiopoietin-1. Science *282*, 468-471.
Tallquist, M.D., French, W.J., and Soriano, P. (2003). Additive effects of PDGF receptor beta signaling pathways in vascular smooth muscle cell development. PLoS biology *1*, E52.
Tallquist, M.D., Klinghoffer, R.A., Heuchel, R., Mueting-Nelsen, P.F., Corrin, P.D., Heldin, C.H., Johnson, R.J., and Soriano, P. (2000). Retention of PDGFR-beta function in mice in the absence of phosphatidylinositol 3'-kinase and phospholipase Cgamma signaling pathways. Genes & development *14*, 3179-3190.
Tallquist, M.D., and Soriano, P. (2003). Cell autonomous requirement for PDGFRalpha in populations of cranial and cardiac neural crest cells. Development *130*, 507-518.
Tehrani, S., Tomasevic, N., Weed, S., Sakowicz, R., and Cooper, J.A. (2007). Src phosphorylation of cortactin enhances actin assembly. Proceedings of the National Academy of Sciences of the United States of America.
Tevosian, S.G., Deconinck, A.E., Tanaka, M., Schinke, M., Litovsky, S.H., Izumo, S., Fujiwara, Y., and Orkin, S.H. (2000). FOG-2, a cofactor for GATA transcription factors, is essential for heart morphogenesis and development of coronary vessels from epicardium. Cell *101*, 729-739.
Theisen, C.S., Wahl, J.K., 3rd, Johnson, K.R., and Wheelock, M.J. (2007). NHERF links the N-cadherin/catenin complex to the platelet-derived growth factor receptor to modulate the actin cytoskeleton and regulate cell motility. Molecular biology of the cell *18*, 1220-1232.
Thiery, J.P. (2003). Epithelial-mesenchymal transitions in development and pathologies. Current opinion in cell biology *15*, 740-746.
Thiery, J.P., and Sleeman, J.P. (2006). Complex networks orchestrate epithelial-mesenchymal transitions. Nature reviews *7*, 131-142.
Thorin, E., and Shreeve, S.M. (1998). Heterogeneity of vascular endothelial cells in normal and disease states. Pharmacol Ther *78*, 155-166.
Thurston, G., and Jean-Guillaume, D. (2003). Methods for visualizing intact blood vessels (Berlin, Springer Verlag).
Thurston, G., Wang, Q., Baffert, F., Rudge, J., Papadopoulos, N., Jean-Guillaume, D., Wiegand, S., Yancopoulos, G.D., and McDonald, D.M. (2005). Angiopoietin

1 causes vessel enlargement, without angiogenic sprouting, during a critical developmental period. Development *132*, 3317-3326.
Tidhar, A., Reichenstein, M., Cohen, D., Faerman, A., Copeland, N.G., Gilbert, D.J., Jenkins, N.A., and Shani, M. (2001). A novel transgenic marker for migrating limb muscle precursors and for vascular smooth muscle cells. Dev Dyn *220*, 60-73.
Uemura, A., Ogawa, M., Hirashima, M., Fujiwara, T., Koyama, S., Takagi, H., Honda, Y., Wiegand, S.J., Yancopoulos, G.D., and Nishikawa, S. (2002). Recombinant angiopoietin-1 restores higher-order architecture of growing blood vessels in mice in the absence of mural cells. J Clin Invest *110*, 1619-1628.
Van Den Akker, N.M., Lie-Venema, H., Maas, S., Eralp, I., DeRuiter, M.C., Poelmann, R.E., and Gittenberger-De Groot, A.C. (2005). Platelet-derived growth factors in the developing avian heart and maturating coronary vasculature. Dev Dyn *233*, 1579-1588.
Viragh, S., and Challice, C.E. (1981). The origin of the epicardium and the embryonic myocardial circulation in the mouse. Anat Rec *201*, 157-168.
Visconti, R.P., Richardson, C.D., and Sato, T.N. (2002). Orchestration of angiogenesis and arteriovenous contribution by angiopoietins and vascular endothelial growth factor (VEGF). Proc Natl Acad Sci U S A *99*, 8219-8224.
Vrancken Peeters, M.P., Gittenberger-de Groot, A.C., Mentink, M.M., and Poelmann, R.E. (1999). Smooth muscle cells and fibroblasts of the coronary arteries derive from epithelial-mesenchymal transformation of the epicardium. Anatomy and embryology *199*, 367-378.
Wada, A.M., Smith, T.K., Osler, M.E., Reese, D.E., and Bader, D.M. (2003). Epicardial/Mesothelial cell line retains vasculogenic potential of embryonic epicardium. Circ Res *92*, 525-531.
Wilm, B., Ipenberg, A., Hastie, N.D., Burch, J.B., and Bader, D.M. (2005). The serosal mesothelium is a major source of smooth muscle cells of the gut vasculature. Development *132*, 5317-5328.
Wisdom, R., Huynh, L., Hsia, D., and Kim, S. (2005). RAS and TGF-beta exert antagonistic effects on extracellular matrix gene expression and fibroblast transformation. Oncogene *24*, 7043-7054.
Witzenbichler, B., Maisonpierre, P.C., Jones, P., Yancopoulos, G.D., and Isner, J.M. (1998). Chemotactic properties of angiopoietin-1 and -2, ligands for the endothelial-specific receptor tyrosine kinase Tie2. J Biol Chem *273*, 18514-18521.
Woodcock-Mitchell, J., Mitchell, J.J., Low, R.B., Kieny, M., Sengel, P., Rubbia, L., Skalli, O., Jackson, B., and Gabbiani, G. (1988). Alpha-smooth muscle actin is transiently expressed in embryonic rat cardiac and skeletal muscles. Differentiation *39*, 161-166.

Xavier-Neto, J., Shapiro, M.D., Houghton, L., and Rosenthal, N. (2000). Sequential programs of retinoic acid synthesis in the myocardial and epicardial layers of the developing avian heart. Developmental biology *219*, 129-141.

Xian, X., Hakansson, J., Stahlberg, A., Lindblom, P., Betsholtz, C., Gerhardt, H., and Semb, H. (2006). Pericytes limit tumor cell metastasis. J Clin Invest *116*, 642-651.

Yan, C., Martinez-Quiles, N., Eden, S., Shibata, T., Takeshima, F., Shinkura, R., Fujiwara, Y., Bronson, R., Snapper, S.B., Kirschner, M.W*., et al.* (2003). WAVE2 deficiency reveals distinct roles in embryogenesis and Rac-mediated actin-based motility. The EMBO journal *22*, 3602-3612.

Yang, J.T., Rayburn, H., and Hynes, R.O. (1995). Cell adhesion events mediated by alpha 4 integrins are essential in placental and cardiac development. Development *121*, 549-560.

Yang, L., Lin, C., and Liu, Z.R. (2006). P68 RNA helicase mediates PDGF-induced epithelial mesenchymal transition by displacing Axin from beta-catenin. Cell *127*, 139-155.

Yoshida, T., Sinha, S., Dandre, F., Wamhoff, B.R., Hoofnagle, M.H., Kremer, B.E., Wang, D.Z., Olson, E.N., and Owens, G.K. (2003). Myocardin is a key regulator of CArG-dependent transcription of multiple smooth muscle marker genes. Circulation research *92*, 856-864.

Zeisberg, M., and Kalluri, R. (2004). The role of epithelial-to-mesenchymal transition in renal fibrosis. Journal of molecular medicine (Berlin, Germany) *82*, 175-181.

Zhang, Z.G., Zhang, L., Croll, S.D., and Chopp, M. (2002). Angiopoietin-1 reduces cerebral blood vessel leakage and ischemic lesion volume after focal cerebral embolic ischemia in mice. Neuroscience *113*, 683-687.